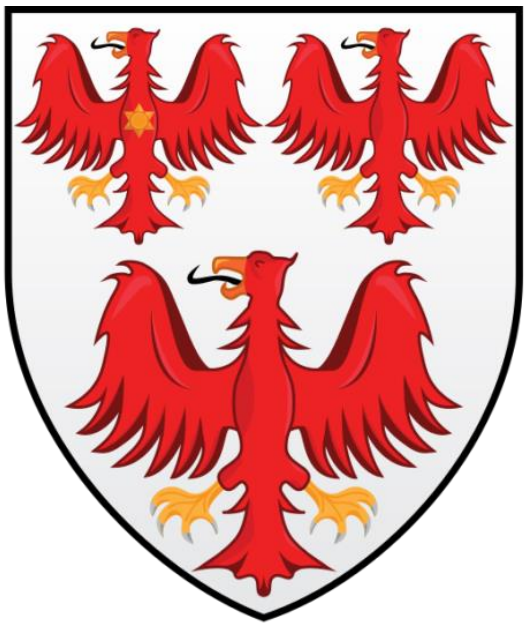
Synthesis of Si=E Containing Compounds Using Novel Silylene Precursors (E = O, N, C and Se)





Lu Ying
The Queen's College

Thesis submitted for the Degree of Doctor of Philosophy

March 2021

Acknowledgement

Almost five years ago I was just a fresh graduate from college, not knowing exactly what I should do. And now here I am, reaching the finish point of my DPhil study, the one moment that has never been thunk of when I was a little boy. Surely it is not possible for me to be here all by myself, therefore, I would like to express my greatest appreciations towards everyone who has been there for me during this journey.

First and foremost, I would like to thank my supervisor, Professor Simon Aldridge, for offering me such an opportunity to study in one of the most prestige institutions in the world, and his endless patience when guiding me through the most difficult time during the first years of my program. The completion of this thesis could not be possible without his supervision and encouragement.

Next, I would like to say thank you to all the past and present group members. They easy-going lab environment they have created makes me feel like being in a family. Special appreciation goes to all the current crew members, together we made through one of the gloomiest moments, during the pandemic of COVID-19.

Many thanks to Dr Ying Kai Loh and Dr Dinh Cao Huan Do, the collaborators of my bisboryloxysilylene project. Working with them has been an absolute pleasure. Although we hit the rock bottom during our first submission, eventually and surely, we did it. I would also like to thank Dr Andrey Protchenko, who mentored me during the first months of my program when I was all at sea, and countless times when he helped me through difficult situations.

Discussing and sharing ideas with brilliant minds here in Oxford has been the most enjoyable experience for my study. Here, I would like to thank Dr Christian Sindlinger, Dr Petra Vasko, Dr Matthiew Roy, Dr Alexa Caise, Dr Lilja Kristinsdottir, Dr Haoyu Niu, Dr Rob Mangan, Dr Ili Zulkifly, Ms. Xueer Zhou, Ms. Anna Booth and Mr. Xiongfei Zheng. Their ingenious ideas are like beacons at the darkest night, guiding me through the endless ocean of chemistry.

Big thanks to the crystallographers in the group, namely Dr Evgeny Kolychev, Dr Maria Ángeles-Fuentes, Dr Jamie Hicks, Ms. Caitilín McManus and Mr. Andreas Heilmann. Their round the clock work and selfless help are a crucial and indispensable part of this thesis. Special appreciation here gives to Kirsten Christensen, who offered her expertise in solving the modulated crystal structure of silahyponitrite.

Lastly, I would like to give my deepest appreciation to my dear mom and dad, for their everlasting support both mentally and financially. It is also them who were there when I was in the middle of some toughest moments, and when I was to make some most difficult life choices. Having them as my parents, I know I am truly the luckiest.

Abstract

This thesis examines the synthesis of novel acyclic silylenes with amido, boryl, gallyl and/or boryloxyl substituents, and their reactivities towards small molecules such as H_2, CO_2, H_2O, NH_3 *etc*. The silylene systems were also used as precursors for compounds featuring silicon-heteroatom double bonds, with a focus on the attempted synthesis of molecules featuring a Si=O moiety (silanones).

Chapter 2 discusses the reactions between the gallyl anion $[(DippNCH)_2Ga]^-$ and Si(II) precursors such as IDipp·$SiCl_2$ and (NTMSDipp)(I^iPrMe)SiCl. While an unexpected silyl anion formed when IDipp·$SiCl_2$ is used, a novel NHC stabilized silylene can be synthesized by metathesis between $[(DippNCH)_2Ga]^-$ and (NTMSDipp)(I^iPrMe)SiCl. The gallyl-substituted silylene reacts with N_2O, however, only a silyl migrated product can be isolated instead of the expected silanone. The reaction between Cy_2NSiBr_3 and $[(DippNCH)_2B]^-$, in attempt to install an amido substituent on a potential silylene system without a labile N-$SiMe_3$ moiety, results instead in a C–H activation product.

Chapter 3 reports the synthesis of a novel bisboryloxysilylene, together with its heavier Ge, Sn and Pb congeners (the latter in collaboration with Dr Ying Kai Loh). Structural parameters of these tetrylenes obtained by X-ray crystallography, including the E–O, O–B bond distances and O-E-O, E-O-B bond angles (E = Si, Ge, Sn or Pb) show a trend consistent with expected periodic trend for group 14 elements, resulting from relativistic effects and increasingly poor *s-p* mixing on descending group 14. Further investigation involves studies of the reactivity of the bisboryloxysilylene fowards small molecules possessing an E–H bond (E = H, N or O). Although no reaction is detected with H_2, the silylene is able to activate the polar E–H bonds in water, ammonia and *tert*-butyl amine. Such processes most likely occur through a three-molecule transition state as shown by DFT calculations.

Chapter 4 explores the possibilities of synthesizing Si=E (E = C, N, O or Se) containing compounds using the bisboryloxysilylene as the precursor. The reaction between the silylene and N_2O generates the first example of a silahyponitrite, which can be regarded as a masked silanone (by N_2O) as the bound N_2O can easily be substituted in reactions with CO_2 and Ph_3P=O. When the silylene is treated with an excess amount of selenium, a novel tetraselenosilolane can be isolated. Three out of the four selenium atoms in this compound can be removed by adding Ph_3P to generate a silaselenone. Attempts have been made to synthesize a Si=N or Si=C double bond. In the former case Me_3SiN_3 was used as the source of Me_3SiN. However, this reaction only gives a two-fold addition product, a silaazide. In the latter case Ph_3P=CH_2 was utilized to act as a :CH_2 transferring agent. The reaction proceeds instead via a [4+1] cycloaddition process, yielding a dearomatized silaheterocyclic compound.

List of Abbreviations

The following abbreviations will be employed throughout this thesis

Ad = admantyl
Ar = aryl
Cy = *cyclo*-hexyl
DFT = Density Functional Theory
Dipp = 2,6-di-*iso*-propylphenyl
DMAP = 4-dimethylaminopyridine
ESD = estimated standard deviation
Et = ethyl
Hex = hexyl
h = hour(s)
hν = photon
HOMO = highest occupied molecular orbital
IDipp = $(DippNCH)_2C$:
I^{i}PrMe = $(^i PrNC(CH_3)_2)_2C$:
^{i}Pr = *iso*-propyl
LA = Lewis acid
LB = Lewis base
LUMO = lowest unoccupied molecular orbital
Me = methyl
Mes = mesityl, 2,4,6-trimethylphenyl
NMR = nuclear magnetic resonance
Ph = phenyl
ppm = parts per million
R = aliphatic group (unless otherwise stated)
rt = room temperature
^{t}Bu = *tert*-butyl
Tf = trifluoromethanesulfonate
THF = tetrahydrofuran
Trip = 2,4,6-tri-*iso*-propylphenyl
X = halide (unless otherwise stated)
xs = excess

Table of Contents

Chapter 1: Introduction 1

1.1 Low Valent Silicon(II) Compounds: Disilenes 1
1.2 From Disilenes to Silylenes: Cyclic and Electronic Stabilization 9
1.3 Acyclic Silylenes: A Breakthrough in the 21 st Century 15
1.4 Acid/Base Free Silanones: a Holy Grail in Modern Silicon Chemistry 21
1.5 Project Aims 30
1.6 References 31

Chapter 2: Boryl and Gallyl Substituted Silylenes 35

2.1 Introduction: Anionic Group 13 Carbene Analogues 35
2.2 Synthesis of a Gallyl-substituted Silylene 39
2.3 Silyl Migration: DFT Calculations 46
2.4 Attempted Synthesis of a Gallyl-substituted Silanone 48
2.5 Attempted Synthesis of a Silylene with a Biscyclohexylamido Substituent 51
2.6 Conclusions 55
2.7 Experimental Details 56
2.8 References 60

Chapter 3: A Bisboryloxysilylene 63

3.1 Introduction: From N-heterocyclic Iminato (NHI) to N-heterocyclic Boryloxide (NHBO) 63
3.2 NHBO Ligands: A DFT Analysis 68
3.3 Synthesis of the NHBO Ligand and Bisboryloxysilylene 70
3.4 Structural Features of Bis(boryloxy)tetrylenes 75
3.5 Reactivity of a Bisboryloxysilylene: E–H Bond Activation (E = O or N) 78
3.6 Conclusions 86
3.7 Experimental Details 86
3.8 References 93

Chapter 4: Towards Si=E Double Bonds 96

4.1 Chemistry of Nitrous Oxide: Beyond Sex, Drugs and Rock & Roll 96
4.2 Synthesis of a Silahyponitrite 99
4.3 Reactivity of Silahyponitrite: Donor Exchange 102
4.4 Synthesis of Silaselenone 107
4.5 Attempted Formation of a Silicon-Heteroatom Double Bonds 110
4.6 Conclusions 115

4.7 Experimental Details 115
4.8 References 122
Chapter 5: Conclusions 125

Chapter 1: Introduction

1.1 Low Valent Silicon(II) Compounds: Disilenes

Silicon is the second most abundant element in Earth's crust, representing about 28% by mass. In synthetic chemistry, silicon has attracted much attention in recent years with a number of landmark systems having been reported.[1] The most common oxidation-state in silicon-containing compounds is silicon(IV). These are typically eight-electron species and, therefore relatively chemically inert, compared to silicon species in other oxidation states, due to the octet rule.[2] Silicon(II) species, on the other hand, have attracted much interest due to their enhanced reactivity and potential access

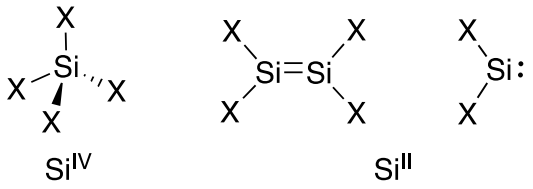
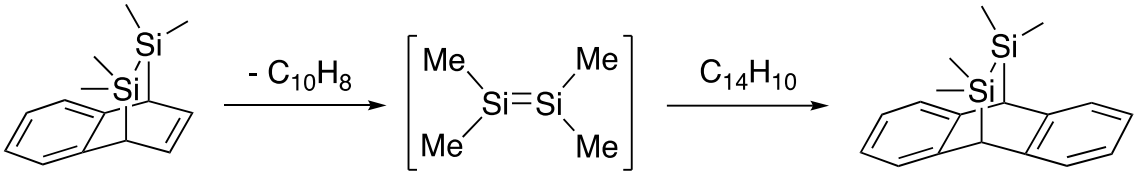


Figure 1. Selected examples of Si(IV) and Si(II) compounds

to 0/+2 or +2/+4 redox cycles (*Figure 1*). However, the isolation of Si(II) compounds (*e.g.* disilenes, $X_2Si{=}SiX_2$) has proved to be challenging. In the early 20th century, attempts were made to synthesize such compounds, but these typically led to the isolation of polymeric compounds featuring Si–Si single bonds.[3] Early *ab initio* studies suggested that, unlike its the carbon analogue, the parent disilene (Si_2H_4) has a relatively small singlet-triplet gap (0.8-46.4 kJ mol^{-1}, depending on the method), which leads to a strong tendency for dimerization into a four-membered ring, or isomerization into a silylsilylene ($HSi–SiH_3$).[4] Experimentally, the first observation of a transient

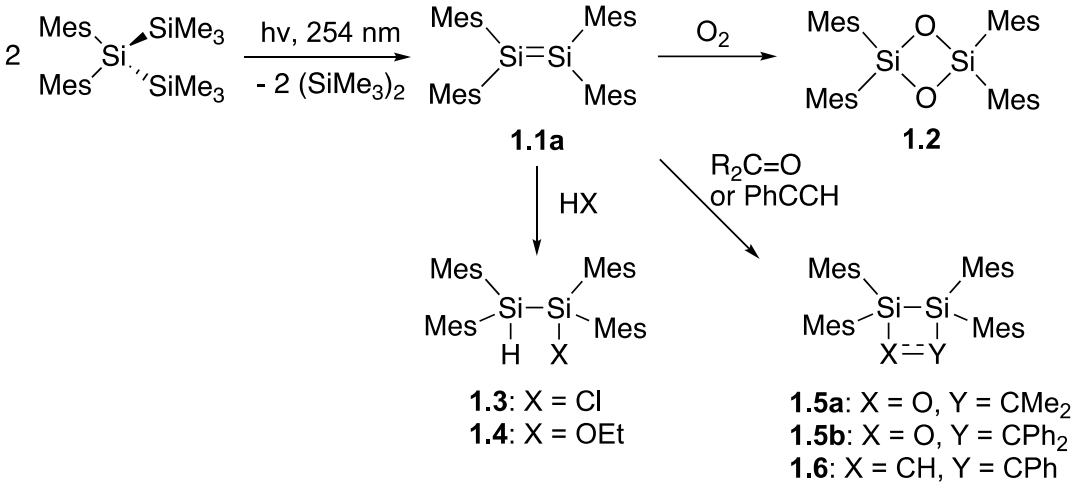
disilene was published in 1972 by Peddle.[5] In this report, the authors described the reaction between a Si_2Me_4 bridged naphthalene system and anthracene, in which the Si_2Me_4 unit was transferred to the middle ring of anthracene (potentially via dissociation of free Si_2Me_4) ultimately forming the thermodynamically more stable bridged anthracene (*Scheme 2*).[5] However, Si_2Me_4 has never been isolated in its free form. In part due to such findings, chemists in the 1970s believed that compounds with multiple bonds between silicon or heavier atoms were unstable (the so called "Double Bond Rule"), due to poor *pπ-pπ* overlap.[6]



Scheme 2. Disilene transfer from naphthalene to anceracene

The rule was challenged by the ground-breaking report of the isolation of the disilene Si_2Mes_4 (**1.1a**) by West in 1981 (*Scheme 3*). This compound was synthesized by irradiating silane $Mes_2Si(SiMe_3)_2$ with ultra-violet light. With the elimination of $(SiMe_3)_2$, **1.1a** was isolated as yellow solid which is stable at room temperature under an inert atmosphere. When exposed to air, **1.1a** rapidly reacts with oxygen forming the doubly oxygen bridged compound **1.2**. The stability of **1.1a** is believed to originate from the introduction of sterically demanding mesityl groups, which provide kinetic stabilization that prevents the Si=Si double bond from dimerization/oligomerization/isomerization. The UV-Vis spectrum of **1.1a** shows an absorption band at 420 nm, which was assigned to a π to π* transition.[7a] Such a result is consistent with theoretical calculations, which predict that disilenes should have a

smaller singlet-triplet gap than alkenes. As a consequence, **1.1a** is yellow in color, while alkenes are typically colorless, with a π to π* transition in the UV region.[8] A subsequent report revealed the solid-state structure of **1.1a**.[7b] The length of the Si=Si double bond in **1.1a** is 2.160 Å (ESD not available in the original paper), i.e. about 0.2 Å shorter than a typical Si–Si single bond (*cf.* 2.350-2.362 Å for Si–Si in $Si_2H_2Mes_4$[9]). The structure also showed a *trans*-bent geometry around the central Si=Si bond, with a 18° angle between the C-Si-C plane and the Si=Si vector. The different nature of the ground states (:CH_2 (triplet) vs :SiH_2 (singlet)) offers an explanation as to why the Si=Si double bond in **1.1a** has a non-planar nature, as opposed to the a planar geometry commonly seen in olefins. Singlet states necessarily dimerize via a two-way donor/accepter interaction, rather than an conventional (σ+π) double bond.[7b]



Scheme 3. Synthesis and reactivity of disilene **1.1a**

Since the first report of stable disilene **1.1a**, a number of isolable disilenes have been reported, which opened a doorway towards systematic reactivity studies of Si=Si bonds (**1.1b-l**, *Figure 4*).[10]As with a C=C double bond, Si=Si double bonds can undergo addition reactions with HX (X = Cl, **1.3** or OEt, **1.4**), as indicated in the original report

by West.[7a] Disilene **1.1a** also reacts with ketones and alkynes, forming the corresponding [2+2] cycloaddition products (**1.5a-b**, **1.6**) (*Scheme 3*).[11] More recently, the chemical community has started to focus on reactivity towards small molecules that are otherwise hard to activate (e.g. H_2, CO_2, CO *etc*.).[12]

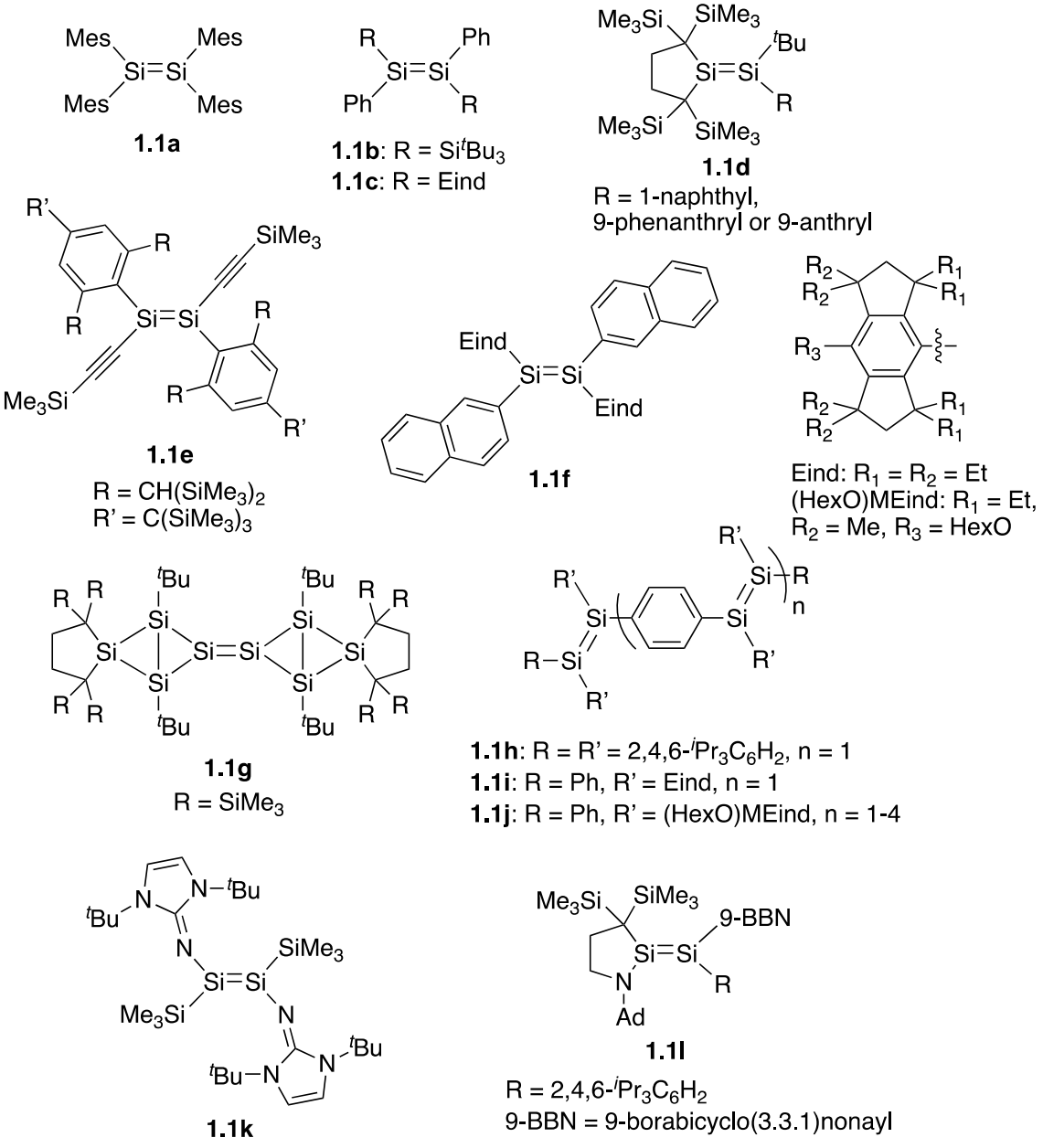
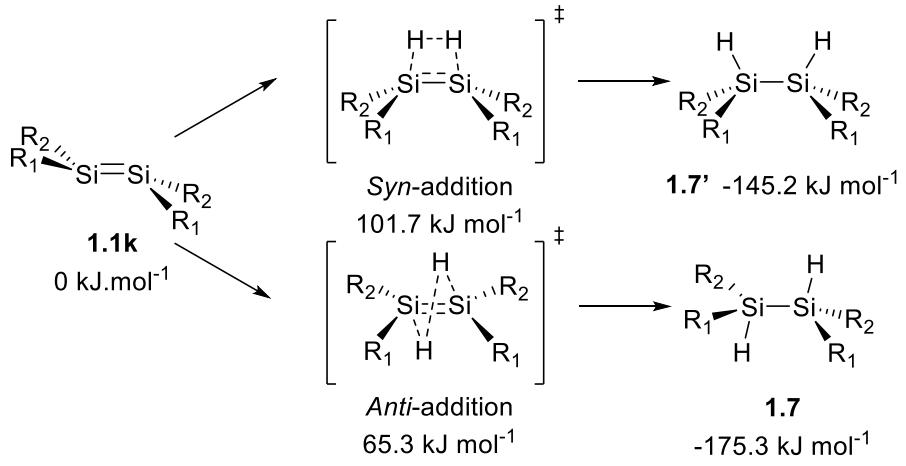


Figure 4. Selected examples of structurally characterized disilenes

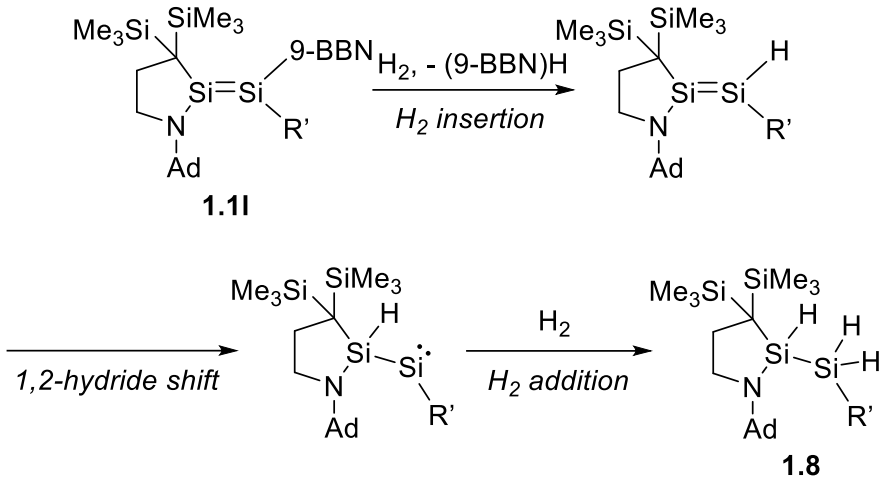
The H–H bond in a dihydrogen molecule is chemically robust, and thus not easy to activate via homolytic cleavage. The first example of dihydrogen activation by a main

group system was reported by Power in 2005, using a digermyne.[13] However, analogous H_2 activation using disilenes is rarely seen. In 2017 Inoue and Rieger reported the activation of dihydrogen using a disilene stabilized by N-hetercyclic iminato and silyl substituents (**1.1k**).[10i] Interestingly, this activation reaction gives exclusively the *anti*-addition product (**1.7**, *Scheme 5*).[14] Quantum chemical calculations show that the activation barrier for *anti*-addition (65.3 kJ mol^{-1}) is almost 50 kJ mol^{-1} lower than that of *syn*-addition (101.7 kJ mol^{-1}). The authors believe that the *trans*-bent nature of **1.1k** contributes to the unexpectedly high transition state energy for *syn*-addition: in order for the dihydrogen molecule to be activated from the same side of the Si=Si double bond, one of the silicon centers must planarize first and (due to the bulky substituents on both silicon centers), this process requires a considerable amount of energy (74.1 kJ mol^{-1}).[10i] Another case of H_2 activation (using disilene **1.1l**) was reported in 2018 by Iwamoto.[10j] In this case, instead of activation by the Si=Si double bond, the first H–H bond activation event happens when an H_2 molecule inserts to the Si–B bond in **1.1l**.



Scheme 5 Syn- vs anti-addition of H_2

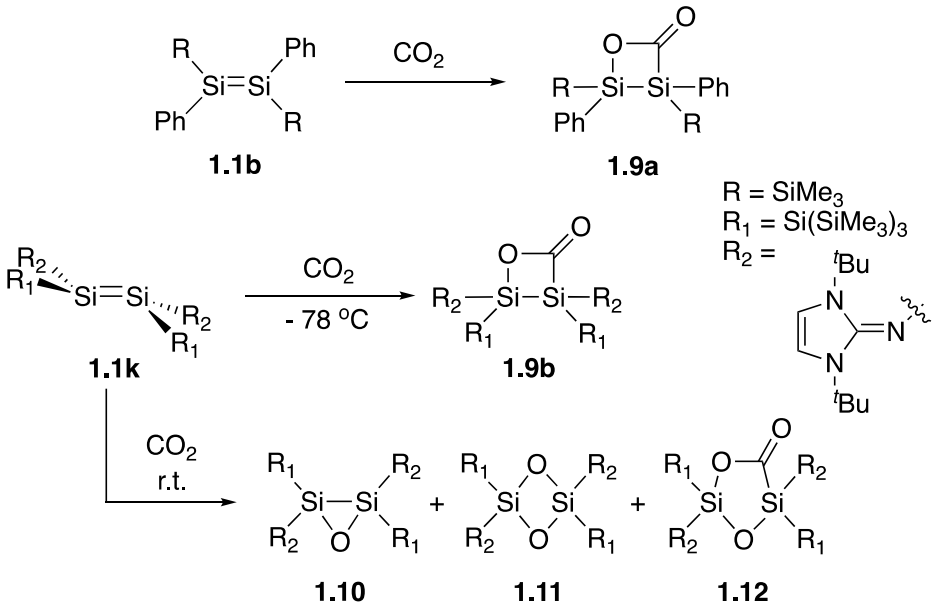
According to computational results, a silylene intermediate is then generated via a 1,2-hydride shift, which activates a second molecule of H_2 in a concerted fashion, forming



Scheme 6. "Double" dihydrogen activation of disilene **1.1l**

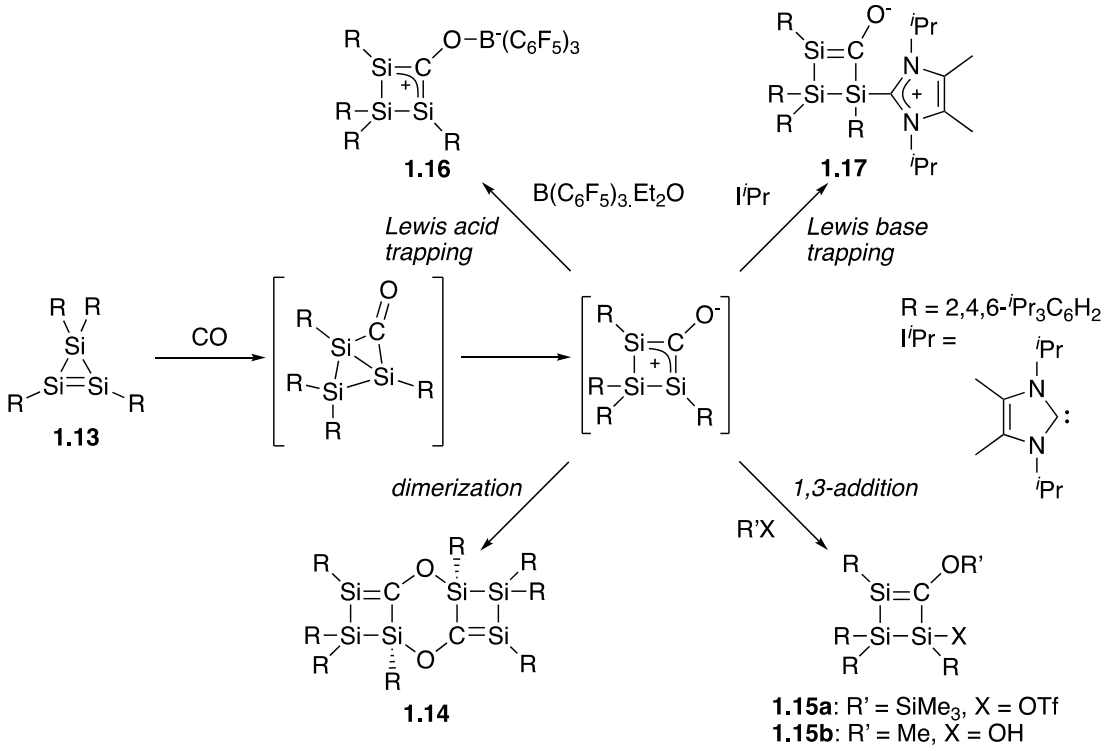
the "double" hydrogen activation product **1.8** (*Scheme 6*).[10j]

Disilenes also show reactivity towards carbon dioxide. In their reactions with CO_2, the activation products differ from case to case. A report in 2002 by Wiberg shows a [2+2] cycloaddition (**1.9a**) between disilene **1.1b** and CO_2.[10a] Another report in 2018 by Inoue and Rieger reveals temperature dependence of the mode of CO_2 activation by disilene **1.1k**. At -78 °C, the activation product is the [2+2] cycloaddition product (**1.9b**); at ambient temperature, a mixture of disilaoxirane (**1.10**), dioxadisiletane (**1.11**) and **1.12**



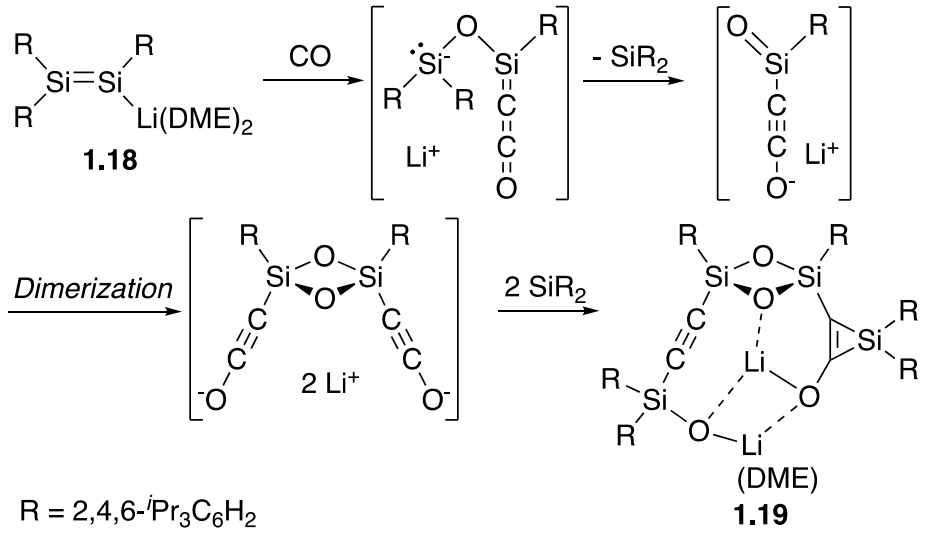
Scheme 7. CO_2 activation of disilenes **1.1b** and **1.1k**

is obtained, with each component being independently identified by reacting **1.1k** with O_2 or N_2O (*Scheme 7*). Interestingly, the product **1.11** retains its stereochemistry from precursor **1.1k** when reacted with O_2, while product **1.10** rapidly isomerizes to give the thermally more stable *trans* isomer (with an energy gap of 24.3 kJ mol^{-1}).[15] As for CO, functionalized disilenes have shown great potential for CO binding and CO triple bond cleavage. In 2013, Sekiguchi and Scheschkewitz reported the carbonylation of a cyclotrisilene (**1.13**).[16a] The reaction between **1.13** and CO proceeds at ambient temperature forming a yellow precipitate, which is identified as the dimeric product **1.14**. The first step of the reaction presumably involves the binding of one molecule of CO across one of the Si=Si double bonds, generating a bicyclic intermediate. The carbonyl carbon then inserts into the Si–Si single bond, forming a monomeric intermediate, which could either be trapped by itself (dimerization, **1.14**), or by external



Scheme 8. CO binding of cyclotrisilene **1.13**

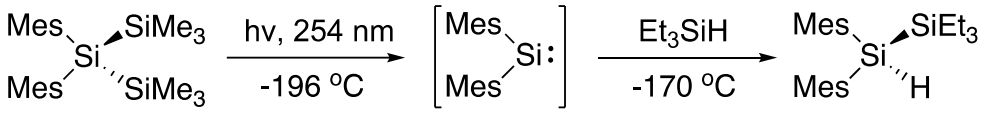
electrophiles (Me_3SiOTf or MeOH, **1.15a-b**),[16a] a Lewis acid ($B(C_6F_5)_3 \cdot Et_2O$, **1.16**) or a Lewis base (carbene, **1.17**) (*Scheme 8*).[16b] The same group reported another case of CO reduction in 2015, this time using a disilenide (**1.18**).[16c] **1.18** reacts with four equivalents of CO, with three of the CO bonds being cleaved completely. The activation product (**1.19**) shows a high degree of asymmetry, consistent with a complex reaction pathway. Computational studies reveal a potential reaction mechanism: firstly disilenide **1.18** reacts with two molecules of CO, forming a silakenylidene intermediate. Then an endogonic silylene elimination takes place, resulting in a molecule of the silylene $Trip_2Si$: and a silanone intermediate, which then dimerizes in head-to-tail fashion. The final step involves a two-fold reaction of $Trip_2Si$: with one molecule of silylene inserting into one of terminal alkynyl C–O bonds and another molecule undergoing [1+2] cyclization with the CC triple bond.[16c]



Scheme 9. CO binding of disilenide **1.18**

1.2 From Disilenes to Silylenes: Cyclic and Electronic Stabilization

As early as in 1981, in West's first report of disilene, the authors discovered that performing the same irradiation reaction at cryogenic temperatures in a hydrocarbon matrix, resulted in the formation of a blue compound. Slowly warming the matrix resulted in a color change from blue to yellow and disilene **1.1a** was formed. With an appropriate trapping agent such as Et_3SiH, the authors were able to isolate the formal Si–H bond activation product of the transient silylene Mes_2Si: (**1.20**), i.e. silane $Mes_2SiH(SiEt_3)$ (**1.21**) (*Scheme 10*). It is believed that the blue compound generated at low temperatures is the silylene **1.20** and that it dimerizes into disilene **1.1a** on warming.[7a] Despite the sterically demanding mesityl substituents on the silicon atoms, the overall bulkiness of **1.20** is not enough to prevent it from dimerizing. For this reason, chemists started to seek other types of stabilization in order to isolate a stable, divalent silylene.



1.20 **1.21**

Scheme 10. Formation of transient silylene **1.20**

In 1991, Arduengo reported an N-heterocyclic carbene (NHC, **1.22**, *Figure 11*) with

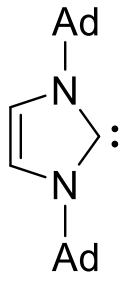
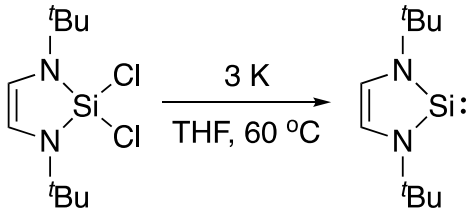


Figure 11. NHC **1.22**

remarkable thermal stability at room temperature.[17] In addition to kinetic stability provided by bulky adamantyl substituents, the carbene centre of NHC **1.22** is also stabilized by electronic factors: the endocyclic nitrogen atoms provide π donation to the carbon *p*π orbital as well as a σ-withdrawing effect due to the difference of electronegativity between nitrogen and carbon (3.04 for N and 2.55 for C, Pauling scale). The combination of these effects stabilizes the HOMO of NHC **1.22** (carbon-bound lone pair) and at the same time destabilizes the LUMO (carbon empty *p* orbital). As a result, the singlet-triplet gap of **1.22** is widened. A quantum chemical study by Apeloig and Schwarz also pointed out that the delocalization of the endocyclic π electrons also provides thermodynamic stabilization.[18] Inspired by this result, a similar N–C=C–N scaffold was used in attempt to synthesize an N-heterocyclic silylene (NHSi, **1.23**).[19] Such a compound was realized experimentally in 1993 by Dank and West, two years after the synthesis of Arduengo's NHC.[20a] Similar to NHC **1.22**, **1.23a** also



1.23a

Scheme 12. Synthesis of NHSi **1.23a**

possesses exceptional thermal stability: a toluene solution of **1.23a** does not show any decomposition after being heated at 150 °C for four months; in the solid-state **1.23a** only decomposes at its melting point, which is 220 °C. Unexpectedly, **1.23a** is relatively chemically inert compared to transient silylenes (as Si(II) species were expected to be highly reactive). It does not react with Et_3SiH, the agent used to trap silylene **1.20**, even

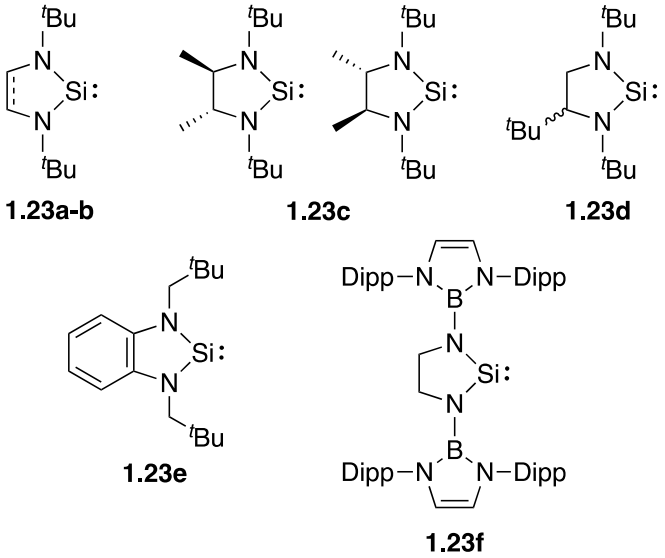
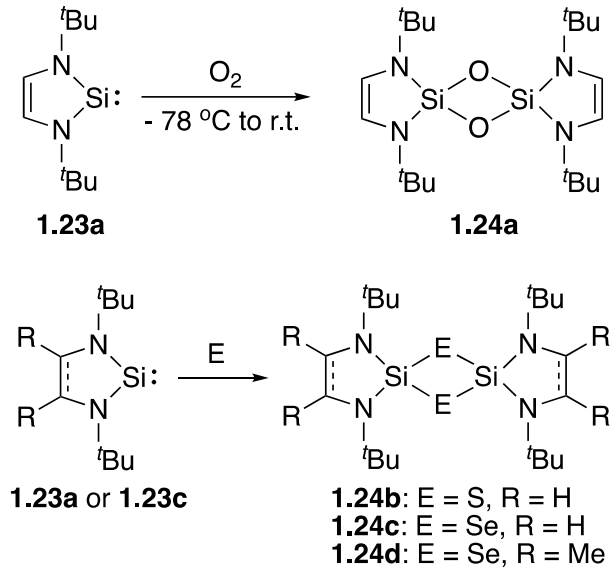


Figure 13. Selected examples of NHSis

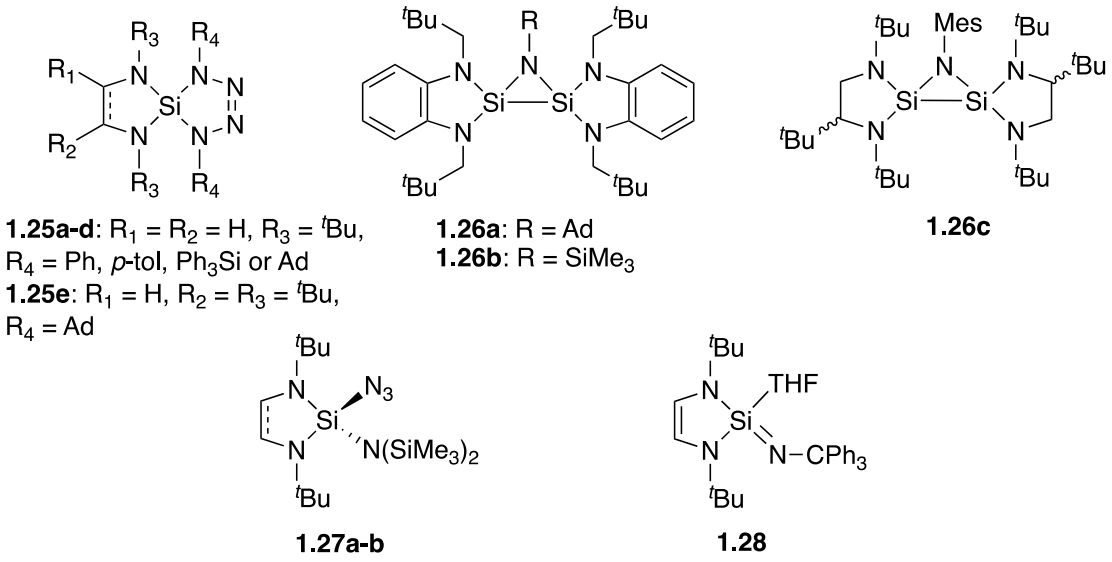
after prolonged heating at 110 °C. It also does not form Lewis acid-base adduct with coordinating solvents such as THF, pyridine or triethylamine. Kinetic stabilization provided by the sterically demanding N-bound *tert*-butyl groups, as well as electronic stabilization from the N–C=C–N backbone are thought to be the main contributors to the robustness of **1.23a**.[20a]

Following this first report of an NHSi, different nitrogen containing substituents have been used for synthesizing novel cyclic silylenes (*Figure 13*).[20] With a range of NHSis in hand, chemists then probed the reactivity of this new class of compounds. Although chemically robust, NHSis do show reactivity towards certain classes of small molecule. Reaction with elemental chalcogens leads to the formation of compounds with Si(μ-E)$_2$Si (E = O, S, or Se) four-membered rings (**1.24a-d**). The formation of compounds of type **1.24** is likely the result of head-to-tail dimerization of two Si=E containing molecules (*Scheme 14*).[21] The reactions between NHSis and covalent azides are



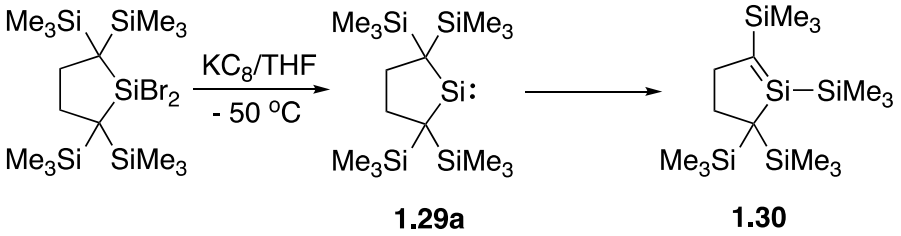
Scheme 14. Reactivities of NHSis with chalcogens

typically dependent on the azide substituents. When PhN_3, *p*-$TolN_3$, Ph_3SiN_3 or AdN_3 are used, a silatetrazoline (**1.25**) is isolated in most cases, presumably the product of a [2+3] cycloadditon between the azide and a silaimine (Si=N containing compound), which is itself generated as the intermediate when NHSi reacts with the first molecule of azide.[20d,22b-e] However, when AdN_3 or Me_3SiN_3 is added to two equivalents of **1.23e**, an azadisilacyclopropane (**1.26**) is isolated instead.[22c] Whatismore, the azadisilacyclopropane **1.26c** is the only product of the reaction between **1.23d** and $MesN_3$.[20d] When Me_3SiN_3 is used, in most of the cases, azidosilanes (**1.27**) are isolated.[22a,d-e] Silaimine **1.28** has been synthesized by reacting NHSi **1.23a** with Ph_3CN_3 in THF, and its solid-state structure shown to feature one molecule of THF coordinated to the silicon centre. Repeating the same reaction in a non-coordinating solvent generates the corresponding silatetrazoline.[21a]



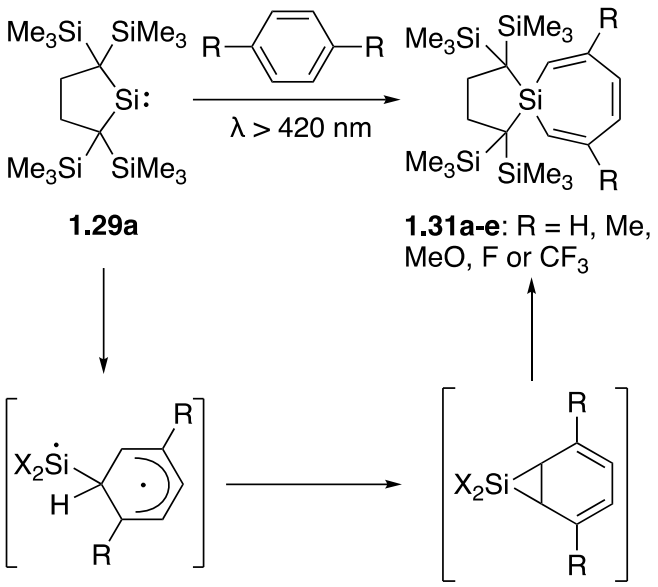
Scheme 15. Products of azide reaction with disilenes

Within a cyclic framework, silylenes can be stabilized even without an endocyclic π system. In 1999, Kira reported the synthesis of a cyclic bisalkylsilylene (**1.29a**), by reduction of the Si(IV) precursor by KC_8 at -50 °C.[22a] Without nitrogen atoms to act as π donors, the main contributor to the π interaction with the empty silicon *p* orbital is the C–$SiMe_3$ σ bond through hyperconjugation. A result of this weaker interaction is the



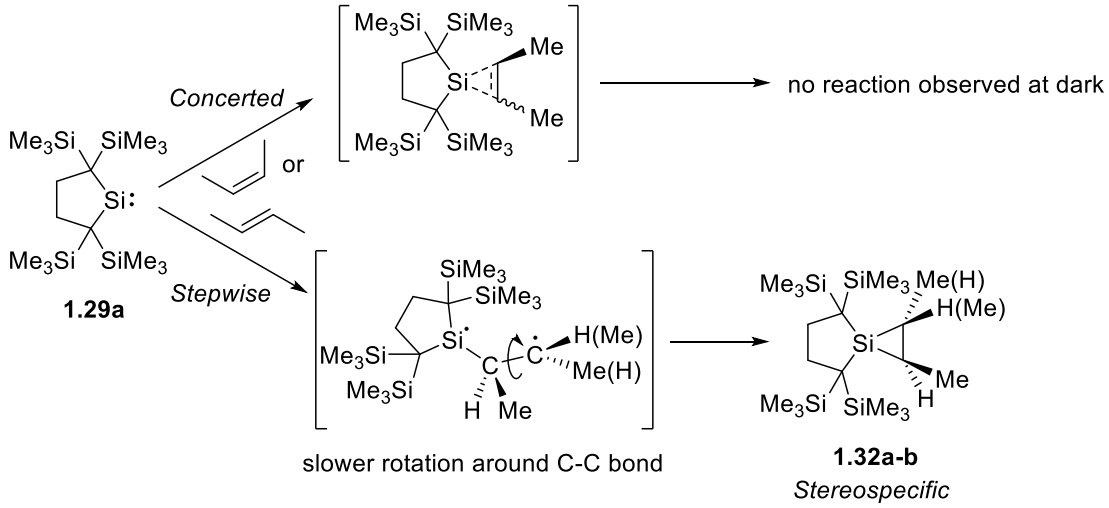
Scheme 16. Synthesis and isomerization of **1.29a**

reduced thermal stability of **1.29a**. In hexane solution **1.29a** gradually isomerizes into a silyl migrated species **1.30** (*Scheme 16*).[23] On the other hand, less endocyclic π donation means a more accessible LUMO for **1.29a**. On irradiation with visible light (λ > 420 nm), silylene **1.29a** reacts quantitatively with various *para*-substituted benzenes, forming silepins (**1.31**) through a C–C bond insertion.[24] The reaction



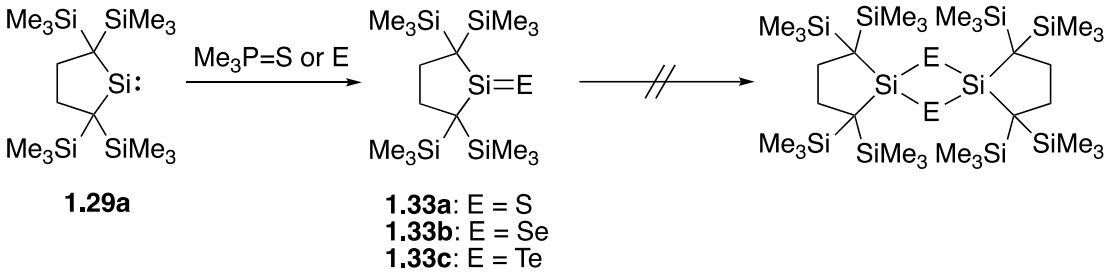
Scheme 17. Photolytic C–C bond insertion by silylene **1.29a**

presumably proceeds through a radical interaction between the triplet excited state of **1.29a** and the phenyl ring, forming a silyl substituted phenyl biradical as the first intermediate. The biradical then cyclizes into a bicyclic intermediate, which subsequently ring opens to give the product silepin (*Scheme 17*).[24] Under similar irradiation conditions, **1.29a** also reacts with alkenes forming silacyclopropane **1.32**. The reactions between **1.29a** and *cis*- or *trans*-2-butene show stereospecificity. Here the authors believe that such reactions go through a stepwise addition via a biradical



Scheme 18. Olefin activations by silylene **1.29a**

intermediate rather than a concerted one-step process, as no reaction is observed at dark. The stereospecificity is ensured in the biradical process because the rate constant of cycloaddtion is determined to be at least 10 times higher than that for rotation around the C–C bond.[25] Compared with NHSis, the four $SiMe_3$ groups in silylene **1.27a** provide extra steric protection, as the reaction between **1.27a** and Me_3P=S, Se or Te generates monomeric species with Si=E (E = S, Se or Te) double bonds (**1.33**) in contrast to the dimeric compounds commonly obtained from reactions between NHSis and elemental chalcogens (*Scheme 19*).[26]



1.29a

1.33a: E = S
1.33b: E = Se
1.33c: E = Te

Scheme 19. Formation of Si=E double bonds

1.3 Acyclic Silylenes: A Breakthrough in the 21st Century

For decades, silylene chemistry had been limited to cyclic systems or acyclic systems with coordination number 3 or more at the silicon center. Up to the early 2010s, two-coordinate acyclic silylenes had only been observed at low temperatures: Mes_2Si (**1.20**) only survives at temperatures lower than -170 °C;[7a] $\{(Me_3Si)_2N\}_2Si$ (reported in 2003) has been spectroscopically identified but decomposes in solution above 0 °C.[27] In 2012, two back-to-back reports of two-coordinate acyclic silylenes finally put an end to this decades-long pursuit: an amidoborylsilylene (**1.34a**) was reported by Jones, Kaltsoyannis, Mountford and Aldridge,[28a] and a bisthiolatosilylene (**1.34b**) by

Tuononen and Power.[28b] Since then, a handful of other novel silylenes have emerged (**1.34**), featuring a variety of different substituents attached to the silicon center (*Figure 20*).[28]

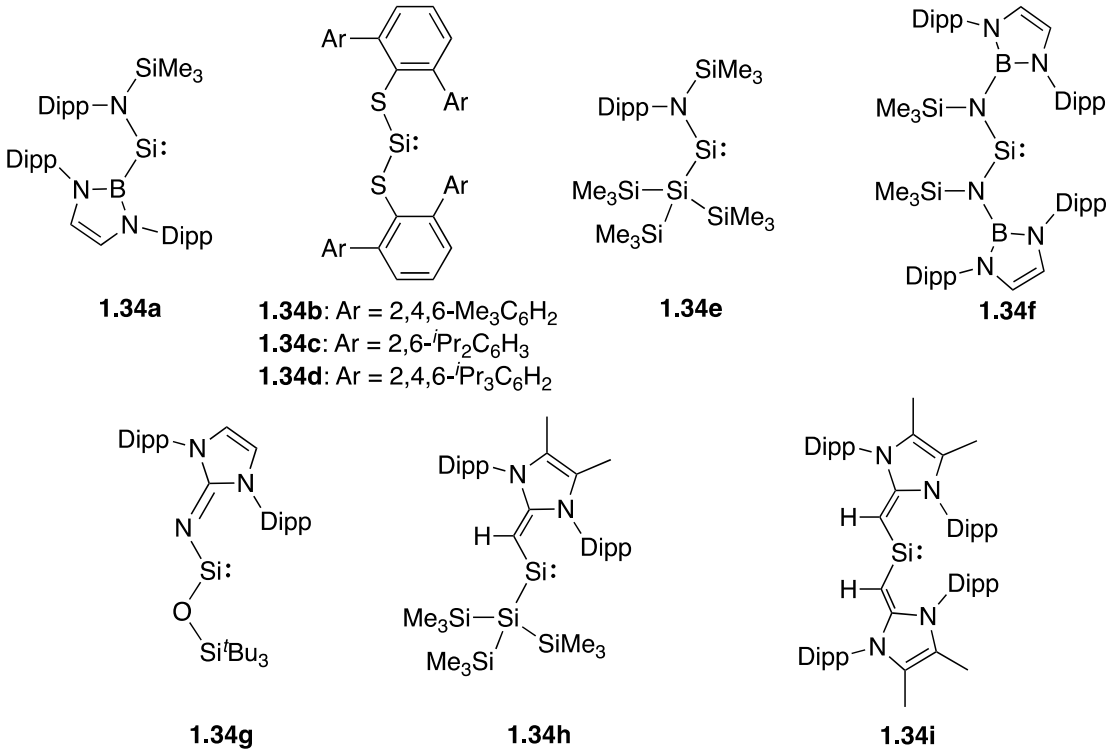


Figure 20. Structurally characterized two-coordinate acyclic silylenes

The syntheses of acyclic silylene systems so far are surprisingly facile. For symmetric systems, the synthetic pathway involves either direct salt metathesis between the metallated ligand and $SiBr_4$ followed by reduction (**1.34b-d**)[28b,d] or metathesis with a silicon(II) precursor, such as IDipp·$SiCl_2$ (**1.34f**)[28e] or Me_2IDipp·$SiBr_2$ (**1.34i**).[28h] For the unsymmetrical systems (**1.34a,e,h**), a one pot reaction between $LSiBr_3$ (L = amido or vinyl ligand) and two equivalents of metallated ligand is utilized in which half of the ligand acts as a reductant.[28a,c,g] Interestingly, one exception is **1.34g**, which is the decomposition product of the corresponding silanone.[28f] In fact acyclic systems appear to provide more flexibility in the choice of silicon-bound substituents as it is not always

synthetically trivial to build up a cyclic framework from complex building blocks. This tunability gives the acyclic systems an opportunity to better balance thermal stability and reactivity: silylenes **1.34** all contain at least one π-donating substituents (N, S, O or an extended π framework) which provides electronic stability (all silylenes of type **1.34** are stable at ambient temperature in solution and in solid-state). An additional σ-donating substituent (i.e. boryl in **1.34a**, silyl in **1.34e,h**) can boost the reactivity (by destabilizing the HOMO) to a degree that cyclic systems have never reached.[28] The reactivities of such acyclic systems are revealed to some degree by their structural and electronic features, namely the angle at silicon and the calculated HOMO-LUMO gaps. Among structurally characterized acyclic silylenes, **1.34a**, **1.34e** and **1.34f** bear the widest bite angles (109.7(1) for **1.34a**,[28a] 116.91(5) for **1.34e**,[28c] 110.94(5) for **1.34f**[28e]), indicating a significant component of *p*-orbital character in the silicon-bound lone pair. Correspondingly, these silylene systems have the smallest calculated HOMO-LUMO gaps (2.04 eV for **1.34a**,[28a] 1.99 eV for **1.34e**,[28c] 2.55 eV for **1.34f**[28e]). Bulky substituents as well as strong σ-donors (boryl, silyl *etc*.) tend to lead to wide angles: steric crowding naturally pushes silicon-bound ligands away from each other; σ-donor ligands destabilize the silicon-bound lone pair, and as a result narrow the HOMO-LUMO gap. In fact, **1.34a** and **1.34e** are able to activate dihydrogen rapidly at ambient temperature, these being the first reported examples of H_2 activation at a silicon center.[28a,c] Silylene **1.34f** shows no such reactivity towards dihydrogen, presumably due to limited access to the overly crowded silicon center.[28e] Silylenes bearing exclusively π-donor ligands show much narrower angles at silicon and comparatively larger

HOMO-LUMO gaps. Bisthiolatosilylenes **1.34b-d** feature S-Si-S angles close to 90°, i.e. essentially that between two 3*p* orbitals (90.52(2)° for **1.34b**,[28b] 85.08(5)° for **1.34c** and 84.8(1)° for **1.34d**[28d]), which implies little to no *p*-orbital character in the silicon-bound lone pair. Not surprisingly, the HOMO-LUMO gap for **1.34b** is calculated to be 4.26 eV, i.e. more than double that calculated for **1.34a** and **1.34e**. Despite having strong σ-donor substituents (iminato or silyl), the HOMO-LUMO gaps for silylenes **1.34g** and **1.34h** are as large as 4.33 eV[28f] and 4.79 eV[28g] respectively, presumably due to the overwhelming π-stabilizing effect from the siloxy or vinyl ligands (iminato groups are also strong π-donors). Although they have wider HOMO-LUMO gaps than

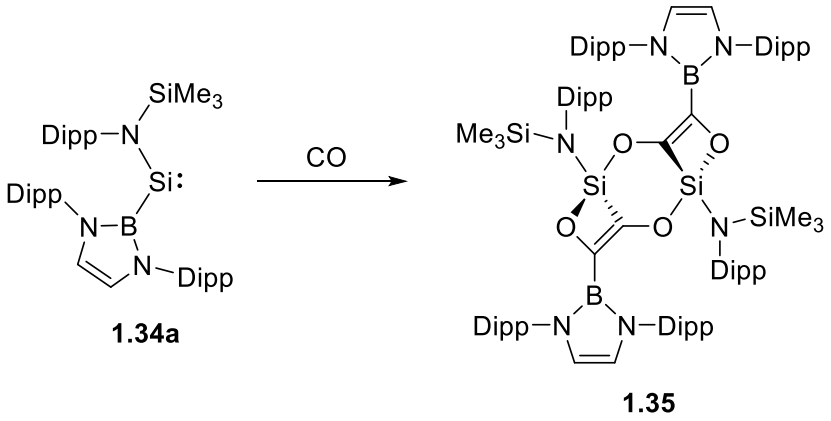
Silylene	∠L-Si-L' (°)	HOMO-LUMO gap (eV)
1.34a	109.7(1)	2.04
1.34b	90.519(19)	4.26
1.34c	85.08(5)	(Not reported)
1.34d	84.8(1)	(Not reported)
1.34e	116.91(5)	1.99
1.34f	110.94(5)	2.55
1.34g	103.56(8)	4.33
1.34h	101.59(7)	4.79
1.34i	100.5(8)	3.55

Table 21. Measured angles at silicon and calculated HOMO-LUMO gaps for acyclic silylenes **1.34**

bisthiolatosilylenes **1.34b-d**, the angles at silicon for silylenes **1.34g** and **1.34h** are on the other hand wider (103.56(8)° for **1.34g**,[28f] 101.59(7)° for **1.34h**[28g]), presumably due

to steric repulsion from the silyl group (**1.34h**) or electronic repulsion from nitrogen and oxygen atoms (**1.34g**).

In addition to H_2 activation, acyclic systems also show reactivity towards other small molecules (CO, NH_3, C_2H_4 *etc.*).[29] To the best of my knowledge, the only reactivity between an isolable silylene and CO reported to date is the reductive coupling of CO by **1.34a** (*Scheme 22*).[30*]

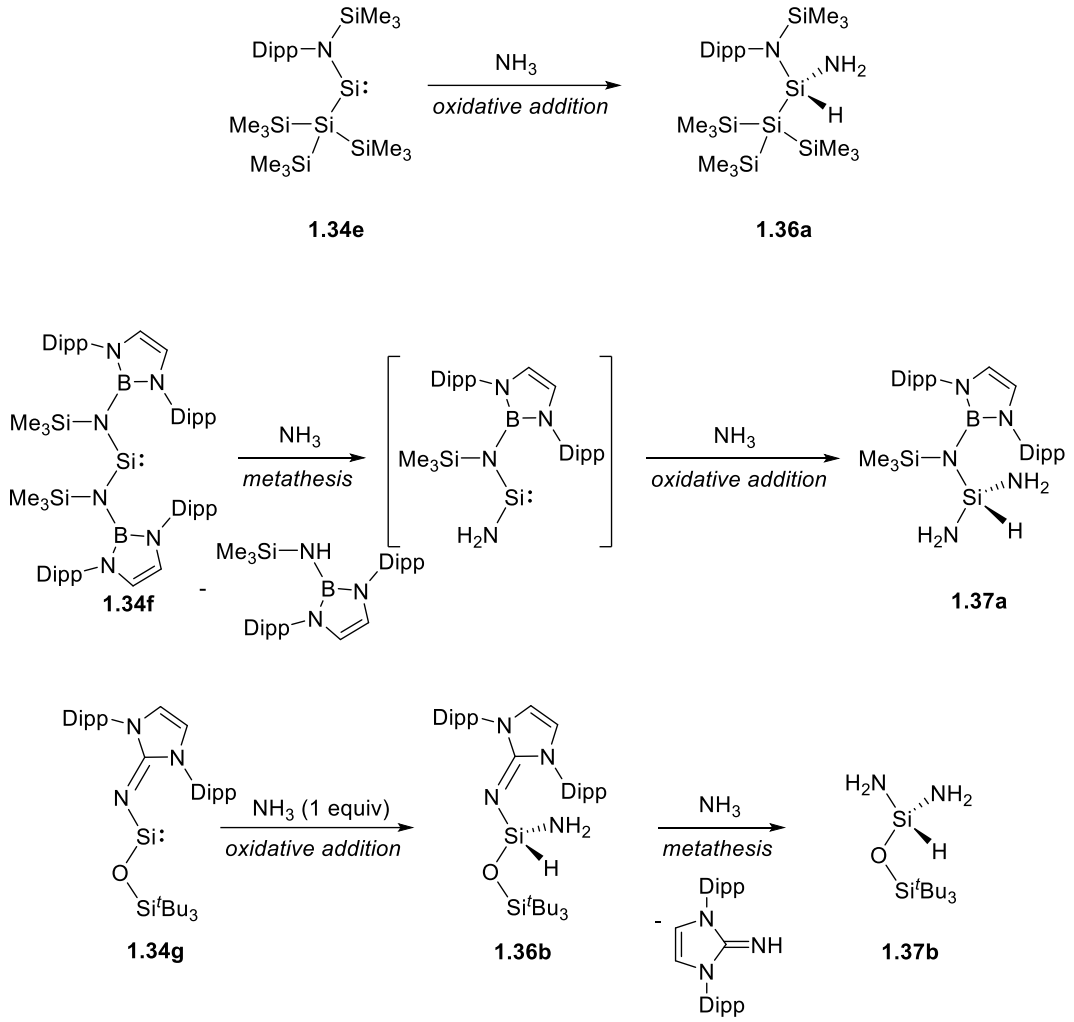


1.34a **1.35**

Scheme 22. CO coupling by silylene **1.34a**

Ammonia activation by acyclic silylenes follows two modes. The reaction between **1.34e** and ammonia forms exclusively the formal oxidative addition product.[32] The reaction between **1.34f** and NH_3 first takes place via σ-bond metathesis, eliminating one amido ligand. A second molecule of NH_3 then oxidatively adds to the silylene intermediate forming the two-fold ammonia activation product **1.37a**.[28e] With silylene **1.34g**, the formal oxidative addition product **1.36b** can be isolated when a stochiometric

[*] During the editing of this thesis two examples of silylene CO complexes were reported, see Ref. 31.

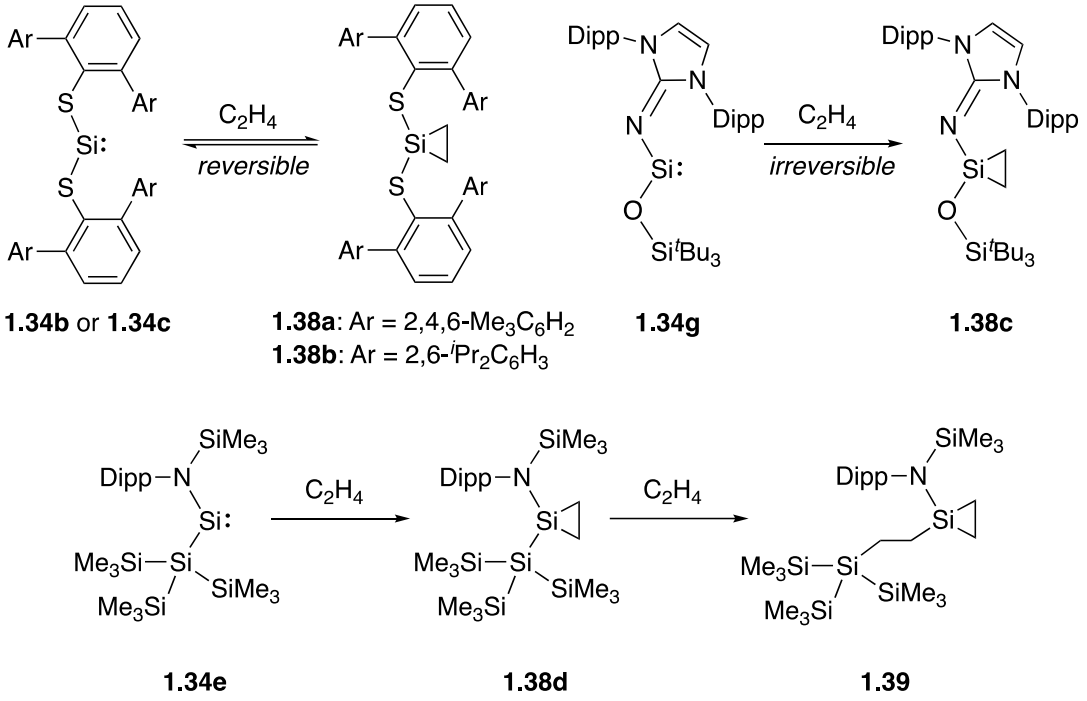


Scheme 23. Ammonia activation by silylenes **1.34e-g**

amount of ammonia is used. However, **1.36b** can react with excess ammonia via σ-bond metathesis, generating a complex mixture containing a similar "double" NH_3 activated compound, **1.37b**.[33]

Some acyclic silylene systems also show ethylene binding capabilities. Silylenes **1.34b,c,e,g** react with C_2H_4 at ambient temperature, forming the corresponding [1+2] cycloaddition products, i.e. silaranes **1.38**.[28f,33,34] Interestingly, these three silylenes behave differently: **1.34b** and **c** react with C_2H_4 in a reversible fashion[34] while the reaction between **1.34e** and **g** and C_2H_4 shows no sign of reversibility;[28f] at 60 °C, silarane **1.38d** reacts with one more equivalent of C_2H_4, forming a formal migratory

insertion product, **1.39**.[35]



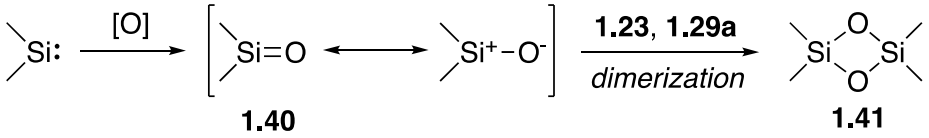
Scheme 24. Ethylene binding by silylenes **1.34b,c,e,g**

1.4 Acid/Base Free Silanones: a Holy Grail in Modern Silicon Chemistry

Carbonyl-containing compounds are one of the most common classes of organic molecule, not only in nature, but also in the chemical industry. The stability of the C=O double bond comes from the small difference of electronegativity between carbon and oxygen atoms (2.55 for carbon, 3.44 for oxygen, Pauling scale) as well as good overlap between carbon and oxygen 2*p* orbitals (due to their similar size), which results in a small difference in bond strength of C–O σ and π bonds (391.6 kJ mol^{-1} for the σ bond, 398.7 kJ mol^{-1} for the π bond, calculated at the B3LYP/TZ(d,p) level).[36] However, up to the beginning of my DPhil program, the heavier congeners of carbonyls, compounds containing Si=O double bond (also as known as silanones) featuring a neutral three-

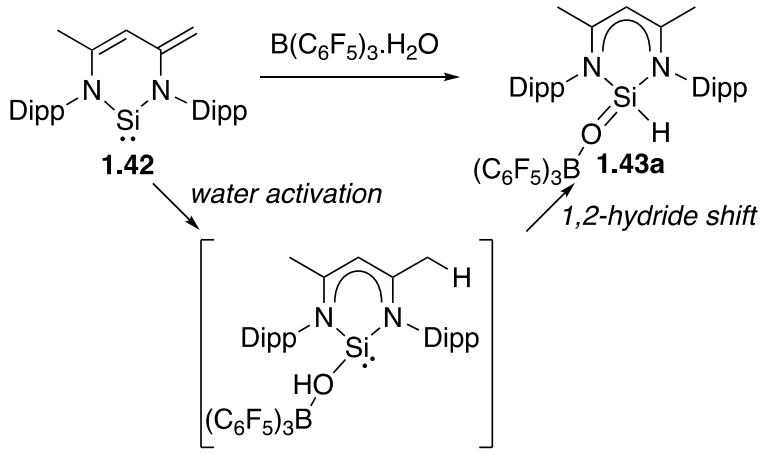
coordinate silicon center had remained elusive for more than 100 years. As early as in 1901 Kipping reported the isolation of a compound with the empirical formula "Ph_2SiO", however the physical properties of this compound (boiling point > 280 °C at 10 mmHg) do not resemble those of benzophenone, the carbon analogue of this compound, and the compound Ph_2SiO was ever then believed to have a oligomeric structure.[37a] Because of the pioneering works of Kipping, for a long time the isolation of compounds with a true Si=O double bond has been known as "Kipping's dream".[37] The different behavior of carbonyls and silanones at a molecular level originates from the differences between carbon and silicon themselves. In contrast to the strong C=O double bond, the Si=O bond is highly polarized due to the large difference between the electronegativity of silicon and oxygen (1.90 for silicon, 3.44 for oxygen, Pauling scale). In fact, the Si–O π bond is only half as strong as the Si–O σ bond (500.8 kJ mol^{-1} for the σ bond, 244.8 kJ mol^{-1} for the π bond, calculated at the B3LYP/TZ(d,p) level).[36] A theoretical study on compounds of the types $H_2E{=}O$ and $Me_2E{=}O$ (E = C or Si) also reveals the different nature of C=O and Si=O double bonds: a natural atomic charge (NPA) calculation shows that in silanones the oxygen is more negatively charged (-0.53 for $H_2C{=}O$, -0.57 for $Me_2C{=}O$, -1.12 for $H_2Si{=}O$, -1.16 for $Me_2Si{=}O$). In addition, the NPA bond orders for silanones are closer to those of single bonds (0.84 for $H_2Si{=}O$, 0.79 for $Me_2Si{=}O$).[38] Realistically speaking, the Si=O double bond should perhaps be better described as a zwitterionic Si^{+}–O^{-} single bond. Thanks to the recent development of silylene chemistry, chemists now have a new synthetic pathway for making silanones: direct oxygenation of silylenes using various oxygen atom sources (O_2, CO_2, N_2O,

R_3NO *etc*.).[39] However, early studies showed that the reactions between NHSis (e.g. **1.23**) or bisalkylsilylense (e.g. **1.29a**) and oxygen sources result in the isolation of head-to-tail dimerization products (**1.41**) of the putative silanones (**1.40**), presumably due to the polarization of the Si=O double bond.[19c,40]

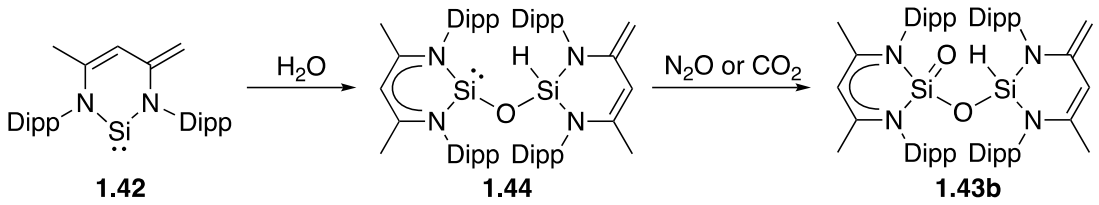


Scheme 25. Head-to-tail dimerization of silanones

To circumvent the problem of dimerization, chemists postulated the ideas of: (i) introducing a Lewis acid and/or a Lewis base to reduce the propensity for dimerization and/or (ii) increasing the steric protection around the silicon center. The first example of a Lewis acid and Lewis base stabilized silanone (a sila-aldehyde, to be consistent with the carbon analogue, **1.43a**) was reported by Driess in 2007.[41a] **1.43a** is synthesized by the reaction between a β-diketiminate-stabilized silylene (**1.42**) and $B(C_6F_5)_3 \cdot H_2O$. The reaction is believed to proceed *via* an intermediate formed *via* water activation, followed by a 1,2-hydride shift from oxygen to silicon (*Scheme 26*). The solid-state structure of **1.43a** shows a Si=O bond length of 1.552(2) Å, i.e. significantly

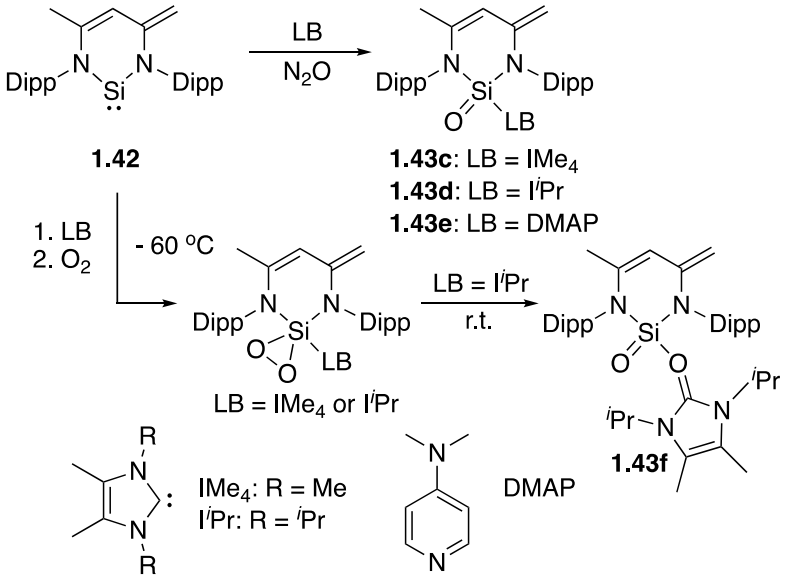


Scheme 26. Synthesis of sila-aldehyde **1.43a**



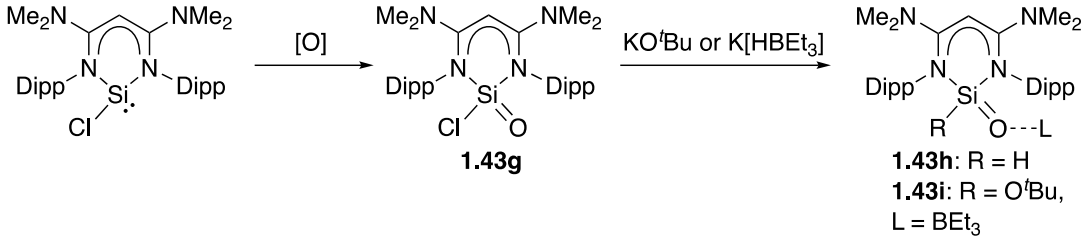
Scheme 27. Synthesis of silanoic acid **1.43b**

shorter than a common Si–O single bond (*cf.* 1.643(1) Å for Si–O in **1.34g**[28f]). Here the stabilization of $B(C_6F_5)_3$ is crucial since the reaction between **1.42** and water alone does not generate a Si=O containing species, but rather a mixed-valence disiloxane **1.44**.[41a] Interestingly enough, further reaction between **1.44** and N_2O or CO_2 generates another base-stabilized silanone (silanoic ester, **1.43b**, *Scheme 27*).[41b] By using different bases (IMe_4,[41c-d] I^iPr[41d,f] or DMAP[41e]), the same group reported a number of novel silanones (**1.43**), thanks to the stabilization of the Si–O unit by a Lewis acid and/or Lewis base. By using a different β-diketiminate scaffold, our group isolated the first example of Lewis base-stabilized sila-acylchloride (**1.43g**), which can then undergo electrophilic substitution forming a sila-aldehyde (**1.43h**) or a silanoic ester (**1.43i**).[41g] Although not exactly analogous to Kipping's picture of a neutral three-coordinate



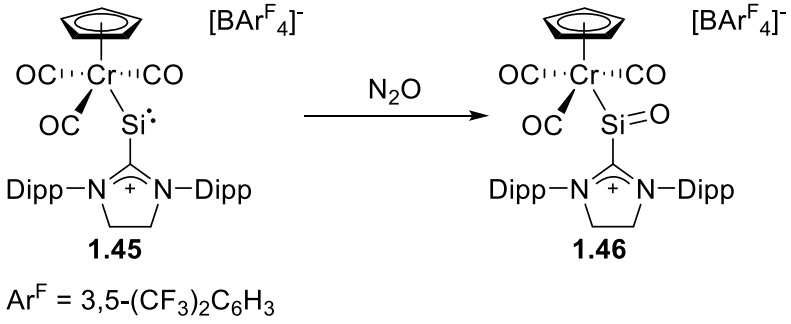
Scheme 28. Lewis base stabilized silanones

silanone, $R_2Si=O$, the successful isolation of Lewis base stabilized silanones at least shows that a Si=O double bond can exist with the help of sufficiently strong σ-donors. In 2014, Filippou reported the first cationic three-coordinate "silanone" **1.46**, by



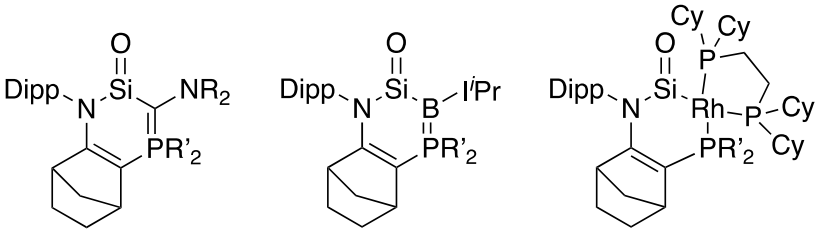
Scheme 29. Synthesis and reactivities of sila-acylchloride **1.43g**

oxygenation of the metallasilylene precursor **1.45** using N_2O.[42] The electronic stabilization of **1.46** mainly comes from the cyclopentadienyl chromium fragment, and similar transition metal moieties have been used to stabilize other highly unsaturated silicon centers.[43] It also provides steric protection (along with the NHC ligand) that the "silanone" needs to prevent dimerization. The Si=O distance in **1.46** is 1.523(3) Å, slightly shorter than that in **1.43a** (1.552(2) Å)[41a], presumably due to the cationic nature of **1.46**. If Filippou's cationic "silanone" is just a stone's throw away from realizing "Kipping's dream", then the isolation of "a fairly stable crystalline silanone" signalled the fact that the 100-year-long dream had finally come true. In 2017 Kato reported landmark compounds in the form of the neutral three-coordinate silanones **1.47a-b** (*Figure 31*).[44a] Again, the syntheses of **1.47a-b** involve direct oxygenation of the



Scheme 30. Synthesis of cationic silanone **1.46**

corresponding silylenes by N_2O at -40 °C. Both compounds are stable at low temperature but dimerize to give a Si(μ-O)$_2$Si four-membered ring upon warming to room temperature (half-life in THF for **1.47a**: 0.5 hours; **1.47b**: 5 hours). The difference in the half-lives of **1.47a** and **1.47b** is most likely due to the size of N-bound substituents. In **1.47a-b** strong σ-donation to the Si–O moiety mainly comes from the ylidic carbon atom, as quantum chemical calculations demonstrate that the HOMO of **1.47a** features π character delocalized across the Si-C-P moiety.[44a] By using a similar ligand system, the same group reported the isolation of two other silanones with a phosphonium bora-ylide (**1.47c**)[44b] or rhodium(I) (**1.47d**)[44d] substituent instead of the carbo-ylide (*Figure 31*). The increasing σ-donating ability from carbo-ylide to bora-ylide to rhodium(I) leads to gradual increase in the thermal stability of the silanone. **1.47c** slowly decomposes in a benzene solution with an estimated half-life of 4 days, which is significantly longer than those of **1.47a** and **1.47b** (0.5 hours and 5 hours respectively), while **1.47d** is indefinitely stable at ambient temperature and shows no sign of decomposition in a benzene solution at 60 °C for one week. A similar trend is also



1.47a: R = ^{i}Pr
1.47b: R = Cy

1.47c

1.47d

PR'$_2$ =

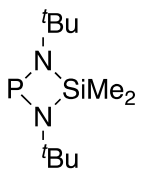
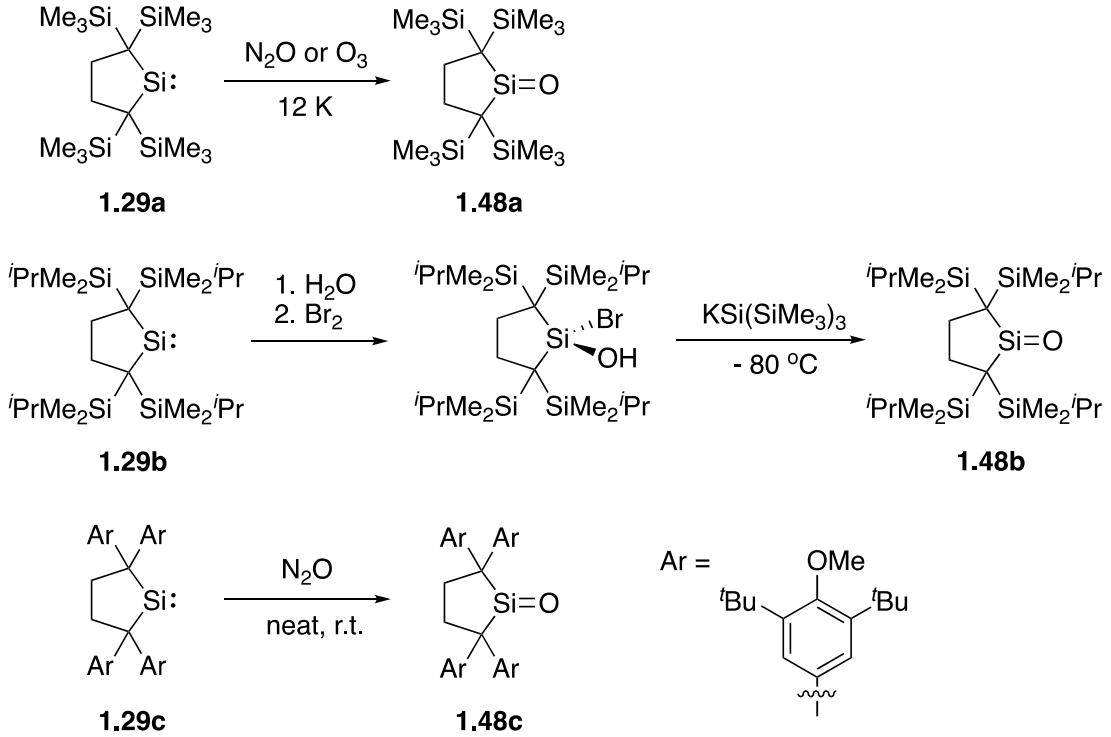


Figure 31. Kato's silanones **1.47**

revealed by the calculated natural bond orbital (NBO) charges of the silicon atoms in **1.47a** (+2.14), **1.47c** (+1.94) and **1.47d** (+1.69), where the formal positive charge on the silicon center decreases with increasing σ-donating ability of the C, B or Rh substituents. As a result this decreases the polarity of the Si=O bond in the same order.[44a-b,d]

The term "ketone" represents the compounds RR'C=O where both R and R' are alkyl or aryl groups. So, an "unperturbed silanone" should have carbon-based ligands at the silicon centre. In 2015, Apeloig and Schreiner first observed such a silanone (**1.48a**) at 12 K in an argon matrix, which was generated by reacting Kira's bisalkylsilylene (**1.29a**) with oxygen transfer agents (N_2O or O_3).[45a] The same year Ishida and Iwamoto reported a similar compound, **1.48b** featuring increased steric profile of the pendant silyl groups (one of the Me groups is substituted by an ^{i}Pr group). With increased steric protection,



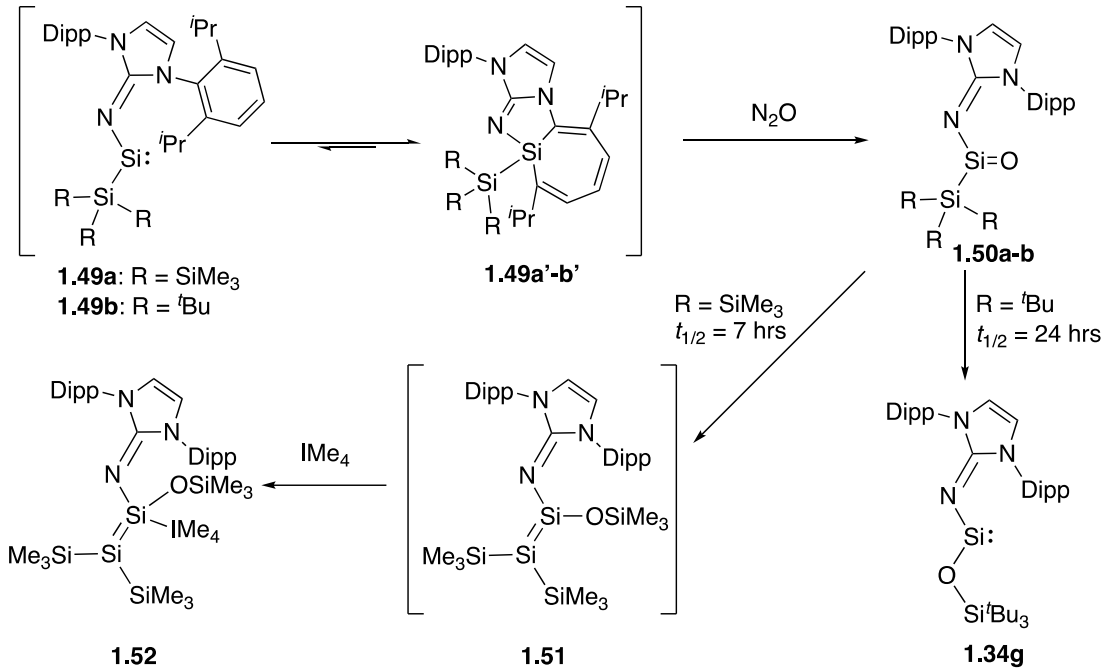
Scheme 32. Syntheses of bisalkylsilanones **1.48**

silanone **1.48b** is stable in toluene to up to -80 °C, at which temperature it was characterized by NMR spectroscopy.[45b] The first ambient temperature stable unperturbed silanone (**1.48c**) was reported by Iwamoto in 2019, featuring four 3,5-ditertbutyl-4-methoxyphenyl side groups to further increase steric protection.[44c] **1.48c** can be obtained by reaction between N_2O and silylene **1.29c** in the solid-state in quantitative yield. In the solid-state, **1.48c** is stable at 25 °C, but it slowly dimerizes in benzene solution at 60 °C over the course of a day. As an example, the combination of steric protection and strongly σ-donating alkyl substituents has made the isolation of **1.48c** possible at ambient temperature. Moreover, such stability has made the structural characterization of **1.48c** possible by X-ray crystallography. In the structure of **1.48c**, the Si=O distance is 1.518(2) Å, which is shorter than those measured for **1.47a-d** (1.527(3) to 1.5432(12) Å).[44a-b,d] The distance between silicon and oxygen atoms from neighboring molecules is 10.336(2) Å, consistent with the absence of significant intermolecular interactions.

The recent development of acyclic silylenes has opened new opportunities for the isolation of stable silanones: as stated in section 1.3, the synthetic accessibility of acyclic systems enables chemists to choose from a much wider spectrum of silicon-bound substituents with more suitable electronic and/or steric profiles. In 2017, Inoue and Rieger reported an acyclic silylene (**1.49a**)-silepin (**1.49a'**) equilibrium (*Scheme 33*). **1.49a** can be generated at low temperatures, but inserts into one of the Dipp aromatic C–C bonds when temperature is elevated to 25 °C. Though existing as silepin in solution at ambient temperature, **1.49a'** still undergoes silylene-like reactivity: the

reactions between **1.49a'** and H_2, CO_2, C_2H_4 or $B(C_6F_5)_3$ give products consistent with those one would expect from reactions proceeding via **1.49a**.[46] As a silylene, **1.49a** is a convenient silanone precursor: the N-heterocyclic iminato and the silyl substituents are considered to be good σ-donors, and also sterically crowded. In a follow-up report by the same group, direct oxygen-transfer from N_2O to **1.49a** at -78 °C to ambient temperature produced the acyclic silanone **1.50a**, which is structurally characterized as its acetonitrile adduct. **1.50a** slowly decomposes in a benzene solution at ambient temperature with a half-life of 7 hours. Interestingly, the decomposition pathway of **1.50a** does not go through a head-to-tail dimerization, but rather a silyl migration into an intermediary disilene (**1.51**) (with further decompositions), which is trapped by IMe_4 and characterized structurally as the carbene adduct (**1.52**). By changing the $Si(SiMe_3)_3$ substituent into Si^tBu_3, the authors synthesized a similar silepin **1.49b'**. The reaction between **1.49b'** and N_2O also produced the desired silanone **1.50b** with improved thermal stability (indefinitely stable in solid-state at ambient temperature, with a half-life of 24 hours in benzene). As such, **1.50b** could be structurally characterized in its free form. The Si=O distance in **1.50b** is 1.537(3) Å, slightly longer than that measured for **1.48c** (1.518(2) Å)[44c] but within the range defined by **1.47a-d** (1.527(3) to 1.5432(12) Å)[44a-b,d]. Remarkably, the decomposition of **1.50b** also does not involve dimerization: at ambient temperature, **1.50b** slowly transforms into an iminosiloxysilylene **1.34g** via a silyl migration in quantitative yield.[28f] The spontaneous transformation from **1.50b** to **1.34g** with the change of oxidation state of silicon from +4 (usually regarded as the more stable oxidation state) to +2 is likely due to the oxophilicity of silicon, which

thermodynamically favors the formation of a Si–O σ bond via the cleavage of a Si–O π bond.



Scheme 33. Syntheses of silanones **1.50a-b**

1.5 Project Aims

The purposes of this thesis mainly focus on establishing an acyclic silylene system, which is suitable for silanone synthesis. Chapter 2 discusses the study of a gallyl-substituted silylene and its reactivity towards oxygen-transferring agents. Chapter 3 covers the synthesis of a novel acyclic bisboryloxysilylene and its reactivity towards small molecules containing polar E–H bonds. Chapter 4 explores the synthesis of Si=E (E = O, Se, C or N) containing compounds using this bisboryloxysilylene as the common precursor.

1.6 References

1. For reviews on main group chemistry: (a) P. P. Power, *Nature*, **2010**, *463*, 171-177; (b) R. L. Melen, *Science*, **2019**, *363*, 479-484.
2. I. Langmuir, *J. Am. Chem. Soc*. **1919**, *41*, 868-934.
3. (a) F. S. Kipping, *J. Chem. Soc., Trans*. **1924**, *125*, 2291-2297; (b) F. S. Kipping, *Proc. R. Soc. A*, **1937**, *159*, 139-148.
4. For calculations on disilene: (a) R. Daudel, R. E. Kari, R. A. Poirier, J. D. Goddard, I. G. Csizmadia, *J. Mol. Struct*. **1978**, *50*, 115-121; (b) R. A. Poirier, J. D. Goddard, *Chem. Phys. Lett*. **1981**, *80*, 37-41; (c) H. J. Köhler, H. Lischka, *J. Am. Chem. Soc*. **1982**, *104*, 5884-5889.
5. D. N. Roark, G. J. D. Peddle, *J. Am. Chem. Soc*. **1972**, *94*, 5837-5841.
6. L. E. Gusel'Nikov, N. S. Nametkin, *Chem. Rev*. **1979**, *79*, 529-577.
7. (a) R. West, M. Fink, J. Michl, *Science*, **1981**, *214*, 1343-1344; (b) M. J. Fink, M. J. Michalczyk, K. J. Haller, R. West, J. Michl, *J. Chem. Soc., Chem. Commun*. **1983**, 1010-1011.
8. For review on disilenes: R. West, *Angew. Chem. Int. Ed. Engl*. **1987**, *26*, 1201-1211.
9. S. G. Baxter, K. Mislow, J. F. Blount, *Tetrahedron*, **1980**, *36*, 605-616.
10. Selected examples of disilenes: (a) N. Wiberg, W. Niedermayer, K. Polborn, P. Mayer, *Chem. Eur. J*. **2002**, *8*, 2730-2739; (b) I. Bejan, D. Scheschkewitz, *Angew. Chem. Int. Ed*. **2007**, *46*, 5783-5786; (c) A. Fukazawa, Y. Li, S. Yamaguchi, H. Tsuji, K. Tamao, *J. Am. Chem. Soc*. **2007**, *129*, 14164-14165; (d) T. Iwamoto, M. Kobayashi, K. Uchiyama, S. Sasaki, S. Nagendran, H. Isobe, M. Kira, *J. Am. Chem. Soc*. **2009**, *131*, 3156-3157; (e) T. Sato, Y. Mizuhata, N. Tokitoh, *Chem. Commun*. **2010**, *46*, 4402-4404; (f) M. Kobayashi, T. Matsuo, T. Fukunaga, D. Hashizume, H. Fueno, K. Tanaka, K. Tamao, *J. Am. Chem. Soc*. **2010**, *132*, 15162-15163. (g) T. Iwamoto, N. Akasaka, S. Ishida, *Nat. Commun*. **2014**, *5*, 5353; (h) L. Li, T. Matsuo, D. Hashizume, H. Fueno, K. Tanaka, K. Tamao, *J. Am. Chem. Soc*. **2015**, *137*, 15026-15035; (i) D. Wendel, T. Szilvási, C. Jandl, S. Inoue, B. Reiger, *J. Am. Chem. Soc*. **2017**, *139*, 9156-9159; (j) T. Kosai, T. Iwamoto, *J. Am. Chem. Soc*. **2017**, *139*, 18146-18149.
11. M. J. Fink, D. J. DeYoung, R. West, J. Michl, *J. Am. Chem. Soc*. **1983**, *105*, 1070-1701.
12. For review on reactivities of disilenes: F. Hanusch, L. Groll, S. Inoue, *Chem. Sci*. **2021**, *12*, 2001-2015.
13. G. H. Spikes, J. C. Fettinger, P. P. Power, *J. Am. Chem. Soc*. **2005**, *127*, 12232-12233.
14. For Woodward-Hoffmann Rule: (a) R. B. Woodward, R. Hoffmann, *J. Am. Chem. Soc*. **1965**, *87*, 395-397; (b) R. B. Woodward, R. Hoffmann, *Angew. Chem. Int. Ed*. **1969**, *8*, 781-853.
15. D. Wendel, T. Szilvási, D. Henschel, P. J. Altmann, C. Jandl, S. Inoue, B. Rieger, *Angew. Chem. Int. Ed*. **2018**, *57*, 14575-14579.
16. For CO reduction by disilenes: (a) M. J. Cowley, Y. Ohmori, V. Huch, M. Ichinohe,

A. Sekiguchi, D. Scheschkewitz, *Angew. Chem. Int. Ed*. **2013**, *52*, 13247-13250; (b) M. J. Cowley, V. Huch, D. Scheschkewitz, *Chem. Eur. J*. **2014**, *20*, 9221-9224; (c) M. Majumdar, I. Omlor, C. B. Yildiz, A. Azizoglu, V. Huch, D. Scheschkewitz, *Angew. Chem. Int. Ed*. **2015**, *54*, 8746-8750.

17. A. J. Arduengo, III, R. L. Harlow, M. Kline, *J. Am. Chem. Soc*. **1991**, *113*, 361-363.
18. C. Heinemann, T. Müller, Y. Apeloig, H. Schwarz, *J. Am. Chem. Soc*. **1996**, *118*, 2023-2038.
19. For reviews on NHSi's: (a) M. Haaf, T. A. Schmedake, R. West, *Acc. Chem. Res*. **2000**, *33*, 704-714; (b) N. J. Hill, R. West, *J. Organomet. Chem*. **2004**, *689*, 4165-4183; (c) M. Asay, C. Jones, M. Driess, *Chem. Rev*. **2011**, *111*, 354-396.
20. Selected examples of NHSi: (a) M. Denk, R. Lennon, R. Hayashi, R. West, A. V. Belyakov, H. P. Verne, A. Haaland, M. Wagner, N. Metzler, *J. Am. Chem. Soc*. **1994**, *116*, 2691-2692; (b) B. Gehrhus, P. B. Hitchcock, M. F. Lappert, J. Heinicke, R. Boese, D. Bläser, *J. Organomet. Chem*. **1996**, *521*, 211-220; (c) W. Li, N. J. Hill, A. C. Tomasik, G. Bikzhanova, R. West, *Organometallics*, **2006**, *25*, 3802-3805; (d) A. C. Tomasik, A. Mitra, R. West, *Organometallics*, **2009**, *28*, 378-381; (e) L. Zhu, J. Zhang, C. Cui, *Inorg. Chem*. **2019**, *58*, 12007-12010.
21. For reactivities of NHSi with chalcogens: (a) M. Haaf, A. Schmiedl, T. A. Schmedake, D. R. Powell, A. J. Millevolte, M. Denk, R. West, *J. Am. Chem. Soc*. **1998**, *120*, 12714-12719; (b) A. Mitra, J. P. Wojcik, D. Lecoanet, T. Müller, R. West, *Angew. Chem. Int. Ed*. **2009**, *48*, 4069-4072.
22. For reactivities of NHSi with azides: (a) M. Denk, R. K. Hayashi, R. West, *J. Am. Chem. Soc*. **1994**, *116*, 10813-10814; (b) R. West, M. Denk, *Pure Appl. Chem*. **1996**, *68*, 785-788; (c) B. Gehrhus, M. F. Lappert, *Polyhedron*, **1998**, *17*, 999-1000; (d) B. Gehrhus, P. Hitchcock, M. Lappert, *Z. Anorg. Allg. Chem*. **2001**, *627*, 1048-1054; (e) N. J. Hill, D. F. Moser, I. A. Guzei, R. West, *Organometallics*, **2005**, *24*, 3346-3349.
23. M. Kira, S. Ishida, T. Iwamoto, C. Kabuto, *J. Am. Chem. Soc*. **1999**, *121*, 9722-9723.
24. M. Kira, S. Ishida, T. Iwamoto, C. Kabuto, *J. Am. Chem. Soc*. **2002**, *124*, 3830-3831.
25. M. Kira, S. Ishida, T. Iwamoto, A. de Meijere, M. Fujitsuka, O. Ito, *Angew. Chem. Int. Ed*. **2004**, *43*, 4510-4512.
26. T. Iwamoto, K. Sato, S. Ishida, C. Kabuto, M. Kira, *J. Am. Chem. Soc*. **2006**, *128*, 16914-16920.
27. G-H. Lee, R. West, T. Müller, *J. Am. Chem. Soc*. **2003**, *125*, 8114-8115.
28. Selected examples of two-coordinate acyclic silylenes: (a) A. V. Protchenko, K. H. Birjkumar, D. Dange, A. D. Schwarz, D. Vidovic, C. Jones, N. Kaltsoyannis, P. Mountford, S. Aldridge, *J. Am. Chem. Soc*. **2012**, *134*, 6500-6503; (b) B. D. Rekken, T. M. Brown, J. C. Fettinger, H. M. Tuononen, P. P. Power, *J. Am. Chem. Soc*. **2012**, *137*, 6504-6507; (c) A. V. Protchenko, A. D. Schwarz, M. P. Blake, C. Jones, N. Kaltsoyannis, P. Mountford, S. Aldridge, *Angew. Chem. Int. Ed*. **2013**, *52*, 568-571; (d) B. D. Rekken, T. M. Brown, J. C. Fettinger, F. Lips, H. M. Tuononen, R. H. Herber, P. P. Power, *J. Am. Chem. Soc*. **2013**, *135*, 10134-10148; (e) T. J.

Headington, J. A. B. Abdalla, R. Tirfoin, S. Aldridge, C. Jones, *Chem. Comm*. **2016**, *52*, 1717-1720; (f) D. Wendel, D. Reiter, A. Porzelt, P. J. Altmann, S. Inoue, B. Rieger, *J. Am. Chem. Soc*. **2017**, *139*, 17193-17198; (g) M. M. D. Roy, M. J. Ferguson, R. McDonald, Y. Zhou, E. Rivard, *Chem. Sci.* **2019**, *10*, 6476-6481. (h) M. M. D. Roy, S. R. Baird, L. Miao, M. J. Ferguson, Y. Zhou, E. Rivard, *unpublished results*.

29. For reviews on acyclic silylenes: (a) S. Fujimori, S. Inoue, *Eur. J. Inorg. Chem*. **2020**, 3131-3142; (b) C. Shan, S. Yao, M. Driess, *Chem. Soc. Rev*. **2020**, *49*, 6733-6754.
30. A. V. Protchenko, P. Vasko, D. C. H. Do, J. Hicks, M. Á. Fuentes, C. Jones, S. Aldridge, *Angew. Chem. Int. Ed*. **2019**, *58*, 1808-1812.
31. For silylene CO complexes: (a) C. Ganesamoorthy, J. Schoening, C. Wölper, L. Song, P. R. Schreiner, S. Schulz, *Nat. Chem*. **2020**, *12*, 608-614; (b) D. Reiter, R. Holzner, A. Porzelt, P. Frisch, S. Inoue, *Nat. Chem*. **2020**, *12*, 1131-1135.
32. A. V. Protchenko, J. I. Bates, L. M. A. Saleh, M. P. Blake, A. D. Schwarz, E. L. Kolychev, A. L. Thompson, C. Jones, P. Mountford, S. Aldridge, *J. Am. Chem. Soc*. **2016**, *138*, 4555-4564.
33. D. Reiter, P. Frisch, D. Wendel, F. M. Hörmann, S. Inoue, *Dalton Trans*. **2020**, *49*, 7060-7068.
34. F. Lips, J. C. Fettinger, A. Mansikkamäki, H. M. Tuononen, P. P. Power, *J. Am. Chem. Soc*. **2014**, *136*, 634-637.
35. D. Wendel, W. Eisenreich, C. Jandl, A. Pöthig, B. Rieger, *Organometallics*, **2016**, *35*, 1-4.
36. H. Suzuki, N. Tokitoh, R. Okazaki, S. Nagase, M. Goto, *J. Am. Chem. Soc*. **1998**, *120*, 11096-11105.
37. For Kipping's dream: (a) F. Kipping, L. Lloyd, *J. Chem. Soc., Trans*. **1901**, *79*, 449-459; (b) R. Robinson, F. Kipping, *J. Chem. Soc., Trans*. **1908**, *93*, 439-456.
38. J. Kapp, M. Remko, P. Von Ragué Schleyer, *J. Am. Chem. Soc*. **1996**, *118*, 5745-5751.
39. For reviews on silanones: (a) Y. Xiong, S. Yao, M. Driess, *Angew. Chem. Int. Ed*. **2013**, *52*, 4302-4311; (b) Y. K. Loh, S. Aldridge, *Angew. Chem. Int. Ed*. **2020**. DOI: 10.1002/anie.202008174.
40. (a) T. Iwamoto, H. Masuda, S. ishida, C. Kabuto, M. Kira, *J. Am. Chem. Soc*. **2003**, *125*, 9300-9301; (b) T. Iwamoto, H. Masuda, S. ishida, C. Kabuto, M. Kira, *J. Organomet. Chem*. **2004**, *689*, 1337-1341.
41. Selected examples of β-diketiminate-stabilized silanones: (a) S. Yao, M. Brym, C. van Wüllen, M. Driess, *Angew. Chem. Int. Ed*. **2007**, *46*, 4159-4162; (b) S. Yao, Y. Xiong, M. Brym, M. Driess, *J. Am. Chem. Soc*. **2007**, *129*, 7268-7269; (c) Y. Xiong, S. Yao, M. Driess, *J. Am. Chem. Soc*. **2009**, *131*, 7562-7563; (d) S. Yao, Y. Xiong, M. Driess, *Chem. Eur. J*. **2010**, *16*, 1281-1288; (e) Y. Xiong, S. Yao, R. Müller, M. Kaupp, M. Driess, *J. Am. Chem. Soc*. **2010**, *132*, 6912-6913; (f) Y. Xiong, S. Yao, R. Müller, M Kaupp, M. Driess, *Nat. Chem*. **2010**, *2*, 577-580; (g) D. C. H. Do, A. V. Protchenko, M. Á. Fuentes, J. Hicks, E. L. Kolychev, P. Vasko, S. Aldridge, *Angew. Chem. Int. Ed*. **2018**, *57*, 13907-13911.

42. A. C. Filippou, B. Baars, O. Chernov, Y. N. Lebedev, G. Schnakenburg, *Angew. Chem. Int. Ed*. **2014**, *53*, 8820-8822.
43. For transition metal stabilized unsaturated silicon complexes: (a) A. C. Filippou, O. Chernov, K. W. Stumpf, G. Schnakenburg, *Angew. Chem. Int. Ed*. **2010**, *49*, 3296-3300; (b) A. C. Filippou, O. Chernov, G. Schnakenburg, *Angew. Chem. Int. Ed*. **2011**, *50*, 1122-1126.
44. For neutral three-coordinate silanones: (a) I. Alvarado-Beltran, A. Rosas-Sánchez, A. Baceiredo, N. Saffon-Merceron, V. Branchadell, T. Kato, *Angew. Chem. Int. Ed*. **2017**, *56*, 10481-10485; (b) A. Rosas-Sánchez, I. Alvarado-Beltran, A. Baceiredo, N. Saffon-Merceron, S. Massou, D. Hashizume, V. Branchadell, T. Kato, *Angew. Chem. Int. Ed*. **2017**, *56*, 15916-15920; (c) R. Kobayashi, S. Ishida, T. Iwamoto, *Angew. Chem. Int. Ed*. **2019**, *58*, 9425-9428; (d) S. Takahashi, K. Nakaya, M. Frutos, A. Baceiredo, N. Saffon-Merceron, S. Massou, N. Nakata, D. Hashizume, V. Branchadell, T. Kato, *Angew. Chem. Int. Ed*. **2020**, *59*, 15937-15941.
45. For transient bisalkylsilanones: (a) M. M. Linden, H. P. Reisenauer, D. Gerbig, M. Karni, A. Schäfer, T. Müller, Y. Apeloig, P. R. Schreiner, *Angew. Chem. Int. Ed*. **2015**, *54*, 12404-12409; (b) S. Ishida, T. Abe, F. Hirakawa, T. Kosai, K. Sato, M. Kira, T. Iwamoto, *Chem. Eur. J*. **2015**, *21*, 15100-15103.
46. D. Wendel, A. Porzelt, F. A. D. Herz, D. Sarkar, C. Jandl, S. Inoue, B. Rieger, *J. Am. Chem. Soc*. **2017**, *139*, 8134-8137.

Chapter 2: Boryl and Gallyl Subtituted Silylenes

2.1 Introduction: Anionic Group 13 Carbene Analogues

N-heterocyclic carbenes (NHCs) are cyclic singlet carbenes in which the carbon centre is directly attached to two α-nitrogen atoms. With a lone pair and an empty *p* orbital on the carbon atom, NHCs are regarded as good σ donors with relatively limited π accepting capabilities. The α-nitrogen atoms provide a σ electron withdrawing effect, due to the fact nitrogen is more electronegative than carbon, and a π donating effect due to the presence of nitrogen lone pairs that are in the plane of the carbon empty *p* orbital (*Figure 1*). Such effects widen the energy gap between the carbon-bound lone pair and empty *p* orbital, boosting the stability of NHCs and making them experimentally isolable. For the reasons above, NHCs have been utilized in stabilizing a large number

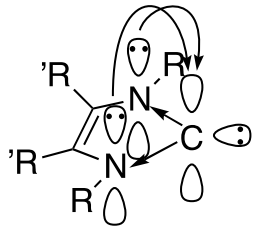
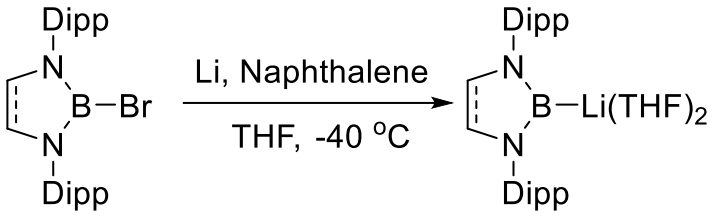


Figure 1 N-heterocyclic Carbene with σ withdrawing and π donating effects

of highly reactive main group systems.[1] The boron analogues of NHCs, on the other hand, are much scarcer due to their anionic nature which significantly increases the HOMO energy, leading to a reduced HOMO-LUMO gap. The first example of an N-heterocyclic boryl anion was synthesized by Yamashita and Nozaki in 2006 via the



Scheme 2 Synthesis of boryllithium

reduction of the corresponding bromoborane precursor using lithium naphthalenide.[2a] Its reactivity towards various electrophiles unveils its nucleophilic nature. Being isoelectronic with an NHC, this boryllithium system is also an exceptional σ donor (but a very weak π acceptor). Over the past 15 years, a number of main group element boryl complexes have been reported using this boryllithium reagent as the boron-containing precursor (*Figure 3*).[3] In 2007, the first group 2 boryl complexes, borylmagnesium bromide and bisborylmagnesium were reported. The syntheses of these compounds are based around simple salt metathesis between boryllithium and magnesium dibromide. The borylmagnesium compound can be used to construct C–B bonds; reaction with benzaldehyde generats an acylborane, which was the first example of such a type of compound.[3a] In 2014, a landmark report featuring EX_2 (E = Ga, In or Tl) radicals was published. With a strong and sterically bulky donor ligand such as boryl, these radicals are thermally robust, in stark contrast to the majority of EX_2 radicals, which are usually short-lived intermediates that can only be trapped at cryogenic temperatures or which

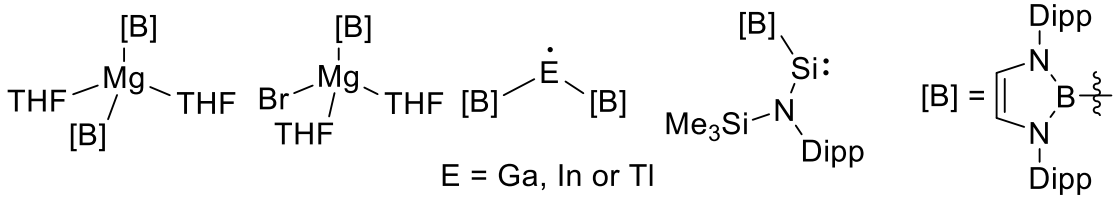
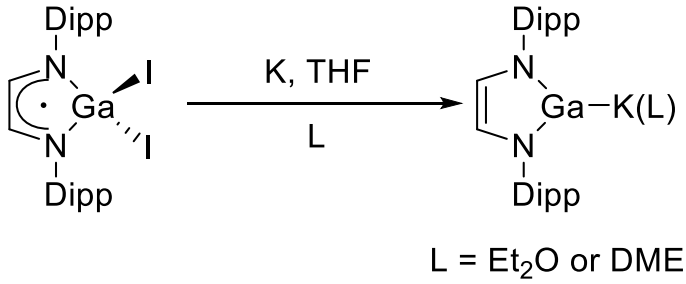


Figure 3 Selected examples of boryl main group complexes

dimerize to give systems of the type E_2X_4 via E–E bond formation.[3g] As for group 14 elements, the first acyclic two-coordinate silylene, stabilized by boryl and bulky amido substituents was also reported by our group. This compound also represented the first silylene system able to activate dihydrogen under ambient conditions, owing to its narrow HOMO-LUMO gap, presumably due to the strong σ donating ability from the boryl substituent directly attached to the silicon centre.[3i]

The corresponding gallium analogues, N-heterocyclic gallyl anions, are also well-known species that have been used to stabilize a number of main group systems.[4] Since the first synthesis reported by Schmidbaur,[5a] gallyl anions have attracted much attention



Scheme 4 Synthesis of gallyl potassium systems reported by Jones and co-workers

due to their stability and accessibility (with the Dipp substituents first reported by Jones, *Scheme 4*).[5b] Much like their boryl analogues, group 2,[4a-c] 13,[4d] 14[4e-g] and 15[4h] complexes featuring gallyl ligands have subsequently been isolated and structurally characterized. Due to poorer *s*/*p* mixing, gallyl anions typically possess a more stable HOMO (gallium-bound lone pair) when compared to boryl anions and are therefore considered weaker σ donors. The aluminum and indium analogues have only been reported very recently (*Figure 5*). The challenge of synthesizing these compounds is likely due to the low electronegativity of aluminum and indium (B: 2.04, Al: 1.61, Ga:

1.81, In: 1.78, Pauling scale), making Al(I) and In(I) species more prone to disproportionation. The first and only N-heterocyclic indyl anion to date was reported by Coles in 2018.[6] In the same year, Goicoechea and Aldridge reported the first example of an N-heterocyclic aluminyl anion, featuring a xanthene backbone, and a weak interaction between the xanthene oxygen and aluminum.[7a] Following this report, five other aluminyl anions have been reported.[7b-e]

As mentioned before, an acyclic silylene system has been reported featuring an anionic

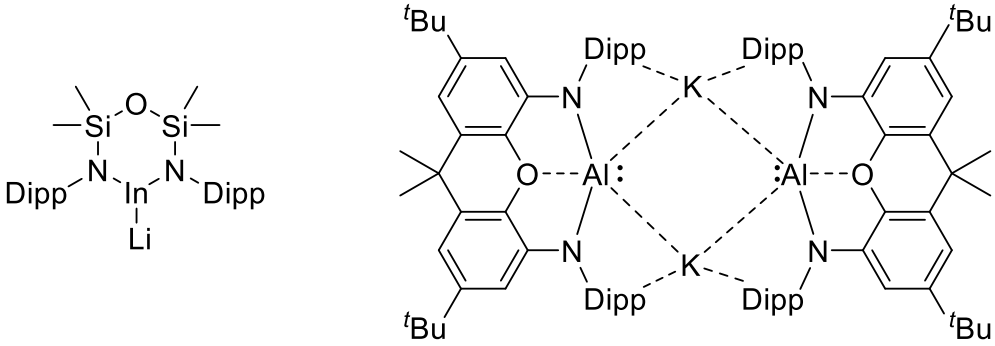
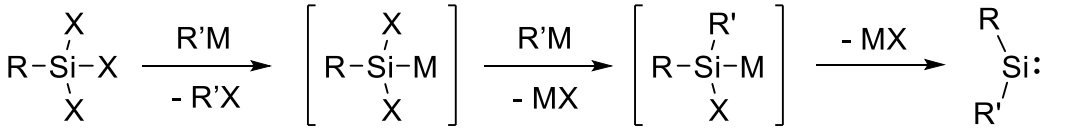


Figure 5 First examples of indyl and aluminyl anions

group 13 NHC analogue as one of the substituents, i.e. {(HCDippN)$_2$B}{Dipp(Me$_3$Si)N}Si (**1.34a**). However, the attempted synthesis of silanone using such silylene system has been proved to be unfeasible, as the reactions between the silylene and oxygen sources (i.e. N_2O or CO_2) result in a rearranged product via N-to-O substituent migration.[8] In this part of the project, the focus is on exploring the use of an N-heterocyclic gallyl ligand to synthesize novel acyclic silylenes and investigating their comparative structural and reaction chemistry (*cf.* related boryl-substituted systems)[3] including the possibility of generating a silanone from such a silylene system.

2.2 Synthesis of a Gallyl-substituted Silylene

To synthesize a gallyl-substituted silylene, a source of the gallyl ligand is required. In this case, the ligand selected was the potassium salt of an N-heterocyclic gallyl species ((HCDippN)$_2$GaK(C$_6$H$_6$), **2.1-K**). The synthesis of a *tert*-butyl analogue of this compound (^{t}Bu N-substituents instead of Dipp) was first reported in 1999 by Schmidbaur.[5a] The synthesis of the Dipp system was first disclosed in 2002 by Jones.[5b] There are multiple reasons why this ligand was chosen: (i) the synthesis of **2.1-K** is straightforward and it is easily isolable in reasonable quantities; (ii) it has a track record in stabilizing a number of main group/transition metal systems from across the Periodic Table; (iii) it is structurally similar to the boryl ligand, [(HCDippN)$_2$B], that has been used to stabilize an acyclic silylene system, making structural and electronic comparisons between the putative amidogallylsilylene and the reported amidoborylsilylene, {(HCDippN)$_2$B}{Dipp(Me$_3$Si)N}Si (**1.34a**)[3i] easier. It is important to notice that ligand **2.1** has already been used in attempt to synthesize a gallylsilylene using a "generic one-pot route", as reported by our group in 2013 (*Scheme 6*).[9] The one-pot methodology has been utilized in the synthesis of a number of acyclic silylenes.[3i,9,10] The underlying basis of this methodology is the use of two

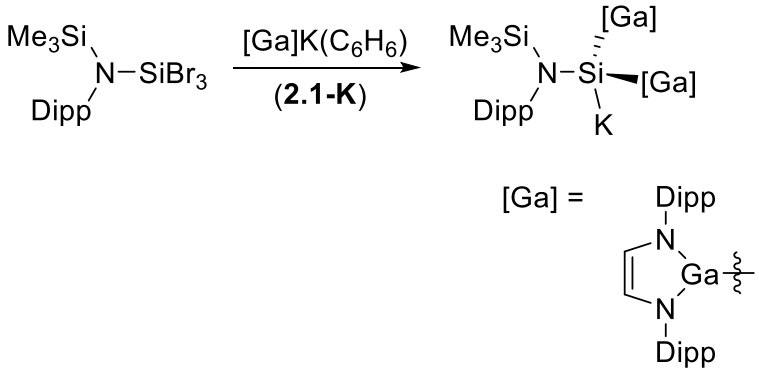


X = halide
M = group 1 metal

1.34a: R = DippN(SiMe$_3$), R' = (DippNCH)$_2$B
1.34e: R = DippN(SiMe$_3$), R' = (Me$_3$Si)$_3$Si
1.34h: R= (DippNCMe)$_2$C=CH, R' = (Me$_3$Si)$_3$Si

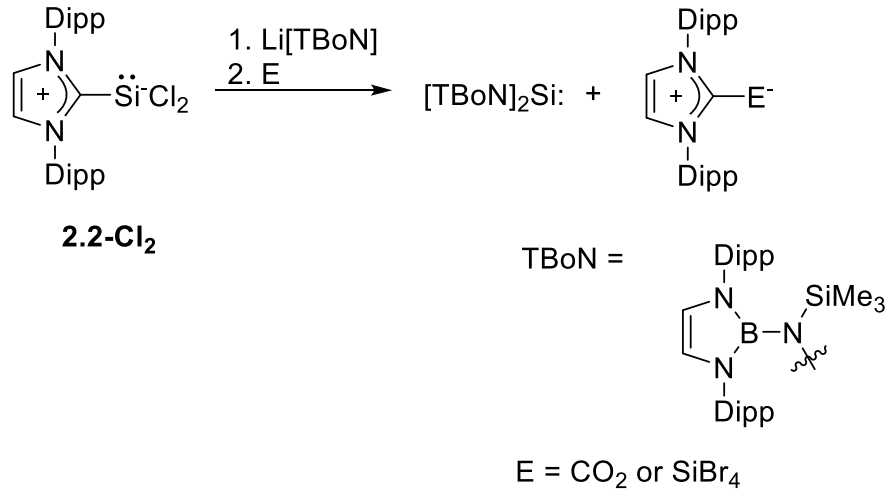
Scheme 6 A "generic one-pot route" for the synthesis of silylenes

equivalents of an anionic ligand to effect reduction as well as metathesis with the Si(IV) precursor (the anionic species necessarily has to be strongly reducing). As a result, half of the anionic ligand is used to substitute the halide on the silicon centre and the other half acts as a reductant to reduce Si(IV) to Si(II). To the best of my knowledge, this method has been successfully utilized to synthesize three different silylene systems.[3i,9,10] However, it fails to produce an acyclic silylene when using **2.1-K** as the anionic ligand: instead it substitutes twice at the Si(IV) centre and produces the bis(gallyl)amidosilyl anion, $[\{(HCDippN)_2Ga\}_2\{Dipp(Me_3Si)N\}Si]^-$ (*Scheme 7*).[9] This is thought to be due to the long Ga–Si distance which makes the steric protection around the silicon centre insufficient for the generation of a two-coordinate product, as well as the weaker reducing ability of the gallyl anion when compared to its gallyl counterpart. With this in mind, a different strategy must be followed. Instead of using a silicon (IV) precursor, a silicon (II) starting material needs to be employed. Candidates for this role include the NHC-stabilized silicon dichloride (IDipp·$SiCl_2$, **2.2-Cl_2**) first reported by Roesky and Stalke in 2009.[11] This compound can be regarded as an "$SiCl_2$" synthon. If the incoming nucleophile is sufficiently space-demanding, the stabilizing IDipp



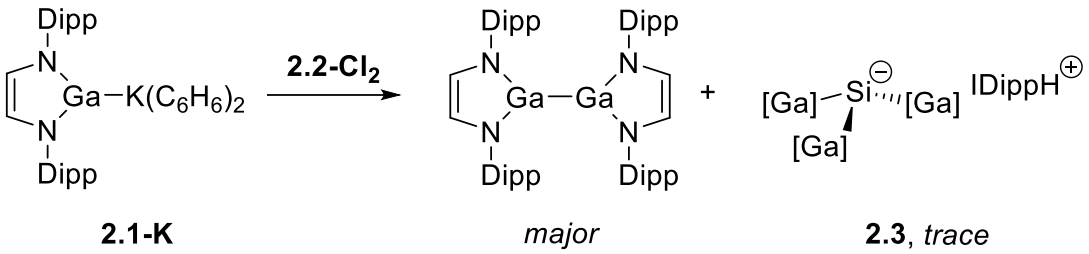
Scheme 7 Reaction between **2.1-K** and Si(IV) precursor

carbene donor is ejected from the silicon centre and can be sequestered by using $SiBr_4$ or CO_2, as illustrated in the synthesis of bisamidosilylene (**1.34f**) by Aldridge and Jones (*Scheme 8*).[12] With this in mind, attempts to synthesize a gallyl-substituted silylene were then made using this Si(II) precursor. In the first instances, equimolar amounts of **2.1-K** and **2.2-Cl₂** were mixed and dissolved in C_6D_6 in an NMR tube, in an attempt to synthesize the gallyl-subsitituted silicon(II) precursor {(HCDippN)$_2$Ga)}SiCl·IDipp.



Scheme 8 Synthesis of silylene using **2.2-Cl₂**

The solution turned dark red immediately with orange crystalline blocks being formed in the NMR tube. The ^{1}H NMR spectrum showed complete consumption of both starting materials with the appearance of signals consistent with literature reported Ga(II) dimer {(HCDippN)$_2$Ga}$_2$,[13] together with unidentifiable products. Attempts to isolate a tractable product from the mother liquor failed. However, the blocks formed in the reaction mixture were suitable for X-ray crystallography. Unexpectedly, the molecular structure of these showed that the compound formed (albeit in trace amounts only) was the three-fold substitution product [IDippH][{(HCDippN)$_2$Ga}$_3$Si] (**2.3**)



Scheme 9 Reaction between **2.1-K** and **2.2-Cl₂**

featuring a trisgallyl silanide anion with a protonated IDipp unit as the counterion (*Scheme 9*, *Figure 10*). The over-substitution implicit in the formation of **2.3** is presumably due to a lack of steric protection around the silicon centre in potential intermediates of the sorts $\{(HCDippN)_2Ga)\}SiCl\cdot IDipp$ and $\{(HCDippN)_2Ga)\}_2Si$. In **2.3**, the silicon atom sits in a trigonal pyramidal geometry (sum of angles 309.78(9)°), consistent with the presence of a silicon-bound lone pair projected in the opposite direction to the gallyl ligands. The average Si–Ga distance in **2.3** is 2.3718(9) Å, which is shorter than aforementioned bis(gallylamido)silyl anion (*cf*. 2.445(1) Å (mean) for

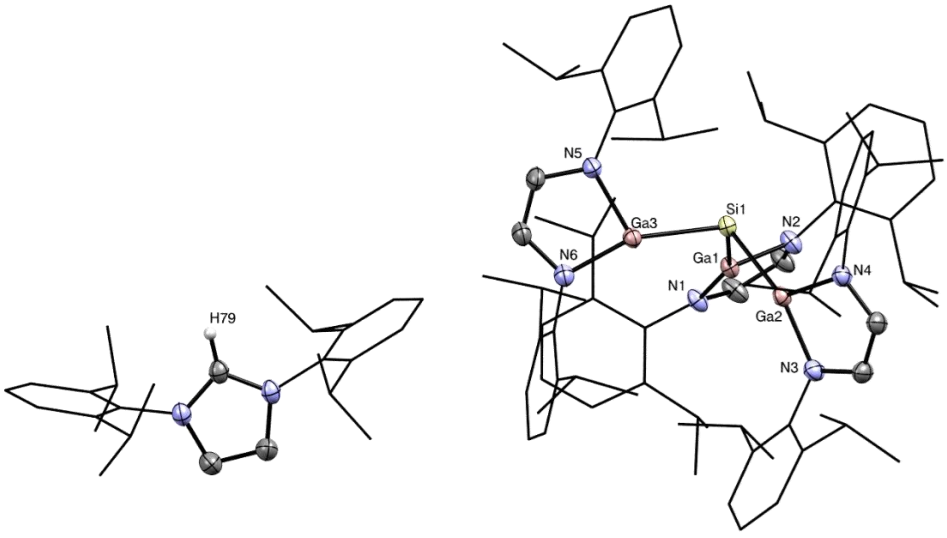
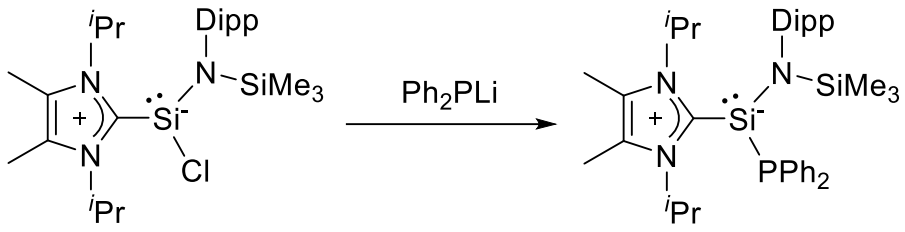


Figure 10 Molecular structure of **2.3** with ellipsoids set at the 50% probability level. For clarity, hydrogen atoms, except for H79, are omitted and the Dipp groups are simplified as wireframes. Selected bond lengths (Å) and bond angles: Si1–Ga1 2.3759(7), Si1–Ga2 2.3736(9), Si1–Ga3 2.366(1), Si1-Ga1-N1 155.40(6)°, Si1-Ga1-N2 114.33(6)°, Si1-Ga2-N3 147.78(6)°, Si1-Ga2-N4 121.62(6)°, Si1-Ga3-N5 113.80(6)°, Si1-Ga3-N6 158.93(6)°.

K[{(HCDippN)$_2$Ga}$_2${Dipp(Me$_3$Si)N}Si]).[9] Although all three gallium atoms sit in a trigonal planar environment (mean sum of angles around three gallium centers, 357.8(1)°), the N-Si-Ga angles are not distributed evenly (e.g. Si1-Ga1-N1 155.40(6)°, Si1-Ga1-N2 114.33(6)°), with the narrower angle being associated with the amido function aligned in the same direction as the silicon-bound lone pair. This is presumably due to the steric demands of three bulky gallyl ligands, which pushes all three to tilt upwards. Interestingly, although [IDippH]$^+$ is known to be deprotonated by various bases (e.g. *tert*-butoxides)[14], it coexists with the silyl anion in **2.3**, even though silyl anions are considered to be stronger bases than alkoxides. Whatismore, the C–H bond associated with the [IDippH]$^+$ proton is aligned in the opposite direction to the silicon-bound lone pair in the solid-state, indicating the absence of a secondary (H-bonding type) interaction between the proton and the silicon centre. The inability of the silyl anion in **2.3** to deprotonate (or even interact significantly with) [IDippH]$^+$ can presumably be explained by the steric crowding around the silicon centre due to the three gallyl substituents, making it a *de facto* weakly coordinating anion (WCA). Repeating the reaction using a different molar ratio of **2.1-K** and **2.2-Cl$_2$** produced a similar mixture of products. Due to the extremely low yield of **2.3**, meaningful spectroscopic/analytical data was unable to be obtained.

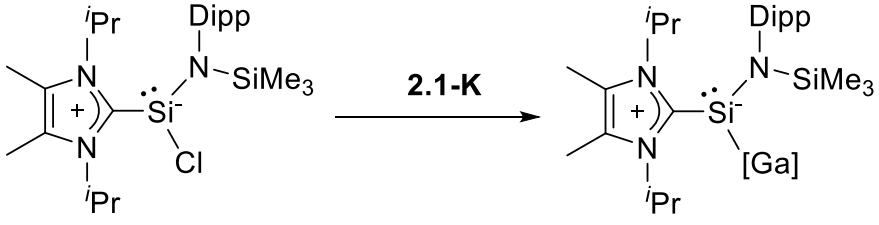
As the use of **2.2-Cl$_2$** did not produce the desired intermediate, another silicon(II) precursor, {Dipp(Me$_3$Si)N}SiCl·I^{i}PrMe (**2.2-Cl**) was used with the aim of generating an amido(gallyl)silylene directly. Compound **2.2-Cl** was first reported by Cui in 2011,[15]



2.2-Cl

Scheme 11 Synthesis of amidophosphidosilylene using **2.2-Cl**

and has been used in synthesizing a NHC stabilized amidophosphidosilylene, {Dipp(Me$_3$Si)N}(Ph$_2$P)Si·I^{i}PrMe (*Scheme 11*).[16] Following the literature procedure, **2.2-Cl** was successfully synthesized on a large scale. With that in hand, **2.2-Cl** and **2.1-K** were mixed in 1:1 molar ratio and dissolved in C_6D_6 in an NMR tube. At ambient temperature, no reaction took place. Upon heating the mixture to 80 ºC, full consumption of both starting materials was observed, as shown by the disappearance of the signals due to **2.2-Cl** and **2.1-K** in the ^{1}H NMR spectrum. In addition, a pattern of broad signals appeared, indicating the formation of a new compound. Repeating the reaction in toluene at larger scale produced a dark red precipitate after cooling the reaction mixture to ambient temperature, including crystals suitable for X-ray crystallography. The ^{1}H NMR spectrum showed eight distinct septets at 2.95, 3.37, 3.60, 3.81, 4.28, 5.38, 6.18 and 6.29 ppm, implying a highly unsymmetrical structure for the product. The broadness of the signals also implies hindered rotation at room



2.2-Cl **2.4**

Scheme 12 Synthesis of **2.4**

temperature. The $^{29}Si\{^{1}H\}$ NMR spectrum showed two singlets at 3.2 and -17.4 ppm, which correspond to a central silicon and a trimethylsilyl group, respectively. X-ray crystallography revealed the solid-state structure of the product, confirming that it is an NHC stabilized amidogallylsilylene $\{(HCDippN)_2Ga\}\{Dipp(Me_3Si)N\}Si{\cdot}I^{i}PrMe$ (**2.4**) (*Scheme 12*, *Figure 13*).

In **2.4**, the central silicon atom is found in a trigonal pyramidal geometry (sum of angles 321.55(12)º), consistent with the presence of a silicon-bound lone pair. The Si–Ga distance is 2.4498(5) Å, which is in close proximity of that in the bis(gallyl)amidosilyl anion (*cf.* 2.445(1) Å (mean) for $K[\{(HCDippN)_2Ga\}_2\{Dipp(Me_3Si)N\}Si]$).[9] Compared to the starting material **2.2-Cl**, the Si–N (1.784(1) Å, *cf.* 1.7861(15) Å for **2.2-Cl**)[15] distance is very similar, but the Si–C distance is somewhat shorter, despite the

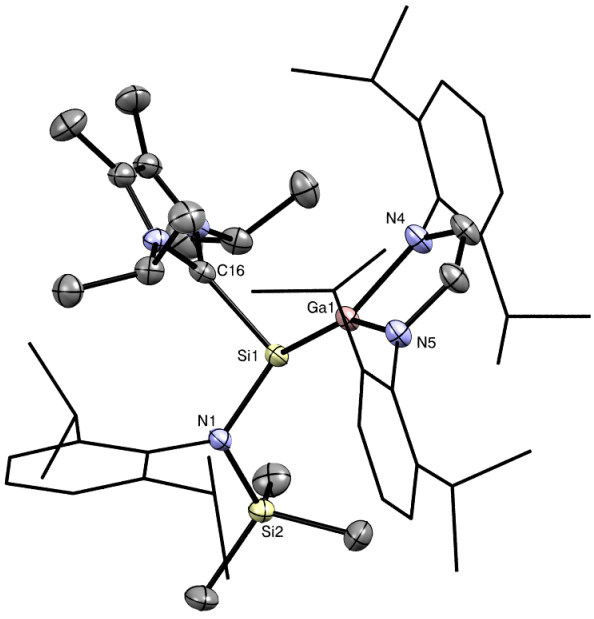


Figure 13 Molecular structure of **2.4** with ellipsoids set at the 50% probability level. For clarity, hydrogen atoms are omitted and the Dipp groups are simplified as wireframes. Selected bond lengths (Å) and bond angles: Si1–Ga1 2.4498(5), Si1–N1 1.784(1), Si1–C16 1.971(2), N1–Si2 1.762(1), Ga1-Si1-N1 119.02(5)°, N1-Si1-C16 104.27(6)°, Ga1-Si1-C16 98.26(5)°, Si1-Ga1-N4 113.39(4)°, Si1-Ga1-N5 156.37(4)°.

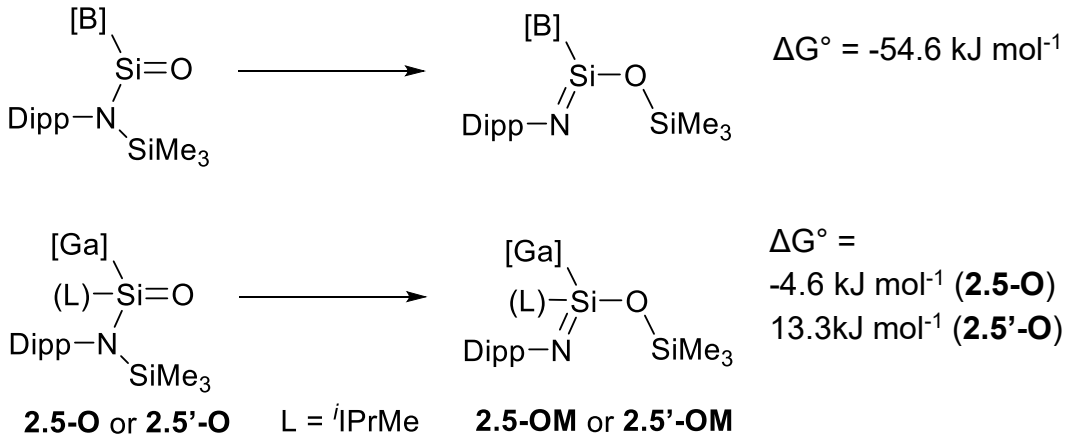
increase in steric bulk at silicon (1.971(2) Å, *cf*. 2.0023(19) Å for **2.2-Cl**)[15]. The gallium atom has an almost planar geometry (sum of angles 356.01(14)º), with a similar uneven distribution of the two N-Si-Ga angles (113.39(4)º and 156.37(4)º) to those found in **2.3**.

Significant attempts have been made to remove the NHC protecting group from **2.4**. Dissolving a sample of **2.4** in C_6D_6 in an NMR tube and back-filling with 1 bar of carbon dioxide resulted in complex mixture of products as shown by *in situ* ^{1}H NMR spectroscopy. When a spatially demanding Lewis acid was used (e.g. $B(C_6F_5)_3$, $B(C_6H_3(CF_3)_2)_3$ or BPh_3), the only identifiable products from the reaction mixture were the Ga(II) dimer $\{(HCDippN)_2Ga\}_2$, and the respective NHC-borane adduct, as indicated by the ^{1}H NMR spectrum. This is postulated to be due to the lack of steric protection after removal of the NHC from the silicon centre, which eventually leads to the cleavage of the Si–Ga bond forming the gallyl dimer.

2.3 Silyl Migration: DFT Calculations

In 2019 our group reported a reaction between an amidoborylsilylene (**1.34a**) and carbon dioxide or nitrous oxide. Here either CO_2 or N_2O acts as an oxygen atom transfer agent, and the underlying aim was to synthesize a Si=O double-bonded species (silanone). However, the product isolated from the reaction mixture is identified as resulting from silyl group migration (*Scheme 14*).[8] The reasons why this migration takes place can be thought of as being two-fold: (i) silicon has a high affinity for oxygen,

making the formation of a second Si–O σ bond energetically favorable, at the cost of breaking a Si–O π bond; (ii) silicon and oxygen have a large difference in terms of electronegativity (3.44 for O, 1.90 for Si on the Pauling scale), making the Si=O double bond highly polarized, with substantial formal negative charge on oxygen atom. As a result, the oxygen atom acts as a nucleophilic centre. To gain mechanistic insight into this silyl migration, quantum chemical calculations were utilized. Using the DFT method (M062X/6-31+g), the geometries of the putative amidoborylsilanone {[HCDippN)$_2$B]{Dipp(Me$_3$Si)N}Si=O, amidogallylsilanone with NHC ([(HCDippN)$_2$Ga]{Dipp(Me$_3$Si)N}(^{i}IPrMe)Si=O, **2.5-O**), and amidogallylsilanone without NHC ([(HCDippN)$_2$Ga]{Dipp(Me$_3$Si)N}Si=O, **2.5'-O**) and their corresponding silyl migrated species ([(HCDippN)$_2$B](OSiMe$_3$)Si=NSiMe$_3$, **2.5-OM** and **2.5'-OM**) were optimized, and their relative free energies compared (*Scheme 14*). Firstly, consistent with experimental observation, the amidoborylsilanone is found to be 54.6 kJ mol^{-1} higher in free energy compared to the silyl migrated species, showing that the migration is a highly exergonic process. The structurally similar gallyl species



Scheme 14 Silyl migration of amidoborylsilanone, **2.5-O** and **2.5'-O**

2.5'-O on the other hand, is 13.3 kJ mol^{-1} *lower* in energy than **2.5'-OM** in terms of free energy. With a coordinating NHC ligand, the free energy change is calculated to be -4.6 kJ mol^{-1}, which can be considered as effectively isoenergetic given the margin of error inherent in the DFT calculations.

2.4 Attempted Synthesis of a Gallyl-substituted Silanone

With the quantum chemical results in hand, attempts were made to synthesize the silanone **2.5-O**. In a J Young's NMR tube, a sample of **2.4** was dissolved in toluene-d_8 and charged with 1 bar of nitrous oxide. The colour of the solution slowly changed from red to light yellow over a course of 15 min. A ^{1}H NMR spectrum measured at this point indicated the complete consumption of **2.4**, and the appearance of a new set of signals (doublets at 0.54, 0.73, 1.09, 1.16, 1.22, 1.30 and 1.38 ppm; septets at 3.24, 3.54, 3.64 and 6.70 ppm). Repeating the same reaction on a larger scale in hexane solution resulted in the formation of single crystals suitable for X-ray crystallography. Despite the computational predictions, the compound isolated was actually the silyl migrated species {(HCDippN)$_2$Ga}(OSiMe$_3$)Si=NSiMe$_3$·I^{i}Pr **2.5-OM**, as revealed by its solid-state structure (*Figure 15*). Compared to the similar silyl-migrated boryl species {(HCDippN)$_2$B}(OSiMe$_3$)Si=NSiMe$_3$, the Si–O (1.645(3) Å, *cf.* 1.596(2) Å)[8] and Si–N distances (1.613(3) Å, *cf.* 1.579(1) Å)[8] in **2.5-OM** are slightly longer, likely due to the fact that the extra NHC ligand increases the steric demands (and indeed the coordination number) around the central silicon atom. The Si–Ga distance in **2.5-OM**

is slightly shorter than that in **2.4** (2.402(1) Å, *cf.* 2.4498(5) Å for **2.4**), while the Si–N distance is significantly shorter (1.613(3) Å, *cf.* 1.784(1) Å in **2.4**), showing a transition from single bond to double bond. The gallium atom in **2.5-OM** sits in a more planar (sum of angles 358.30(9)º, *cf.* 356.01(14)º for **2.4**) and more symmetrical geometry (132.69(9)º and 137.81(9)º for two N-Ga-Si angles, *cf.* 113.39(4)º and 156.37(4)º for **2.4**) compared to the gallium atom in **2.4**, presumably a result of reduced sterics around the silicon centre after the silyl migration.

Since only **2.5-OM** could be isolated and the ^{1}H NMR spectrum at room temperature is consistent with a single product, it is clear that no equilibrium exists at room temperature between **2.5-O** and **2.5-OM** despite their similar calculated energies. With this in mind, variable temperature ^{1}H NMR experiments were carried out to see if this

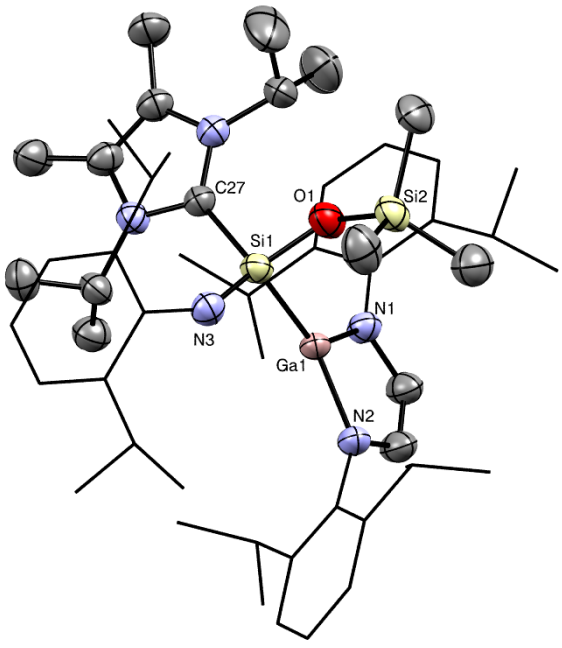


Figure 15 Molecular structure of **2.5-OM** with ellipsoids set at the 50% probability level. For clarity, hydrogen atoms are omitted and the Dipp groups are simplified as wireframes. Selected bond lengths (Å) and bond angles: Si1–Ga1 2.402(1), Si1–N3 1.613(3), Si1–C27 1.961(3), Si1–O1 1.645(3), O1–Si2 1.648(3), Ga1-Si1-O1 99.8(1)°, Ga1-Si1-N3 115.8(1)°, C27-Si1-N3 112.3(1)°, Si1-O1-Si2 144.9(2)°, Si1-Ga1-N1 132.69(9)°, Si1-Ga1-N2 137.81(9)°.

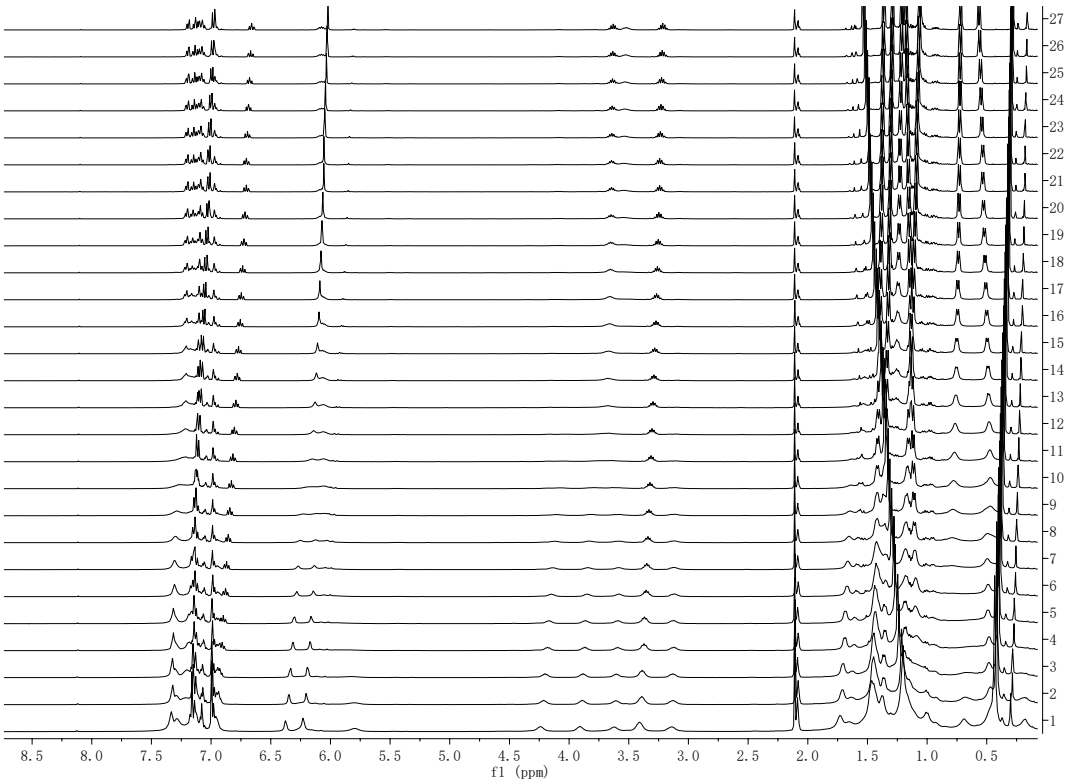
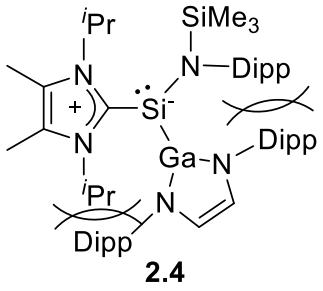


Figure 16 Various temperature NMR spectra of **2.5-OM** from -80 ºC (bottom) to +50 ºC (top)

situation changes as a function of temperature. A sample of **2.5-OM** was dissolved in toluene-d_8 and ^{1}H NMR spectra were obtained at temperatures ranging from -80 ºC to +50 ºC (*Figure 16*). Again, no sign of equilibrium between two species is detected, since no spectrum in this series shows signals for two different species. However, the low temperature spectra did show hindered rotation of **2.5-OM**: at temperatures below -35 ºC, six septets at 3.13, 3.39, 3.61, 3.88, 4.20 and 5.83 ppm, and two singlets at 6.19 and 6.33 ppm are observed, showing a lowering of symmetry at low temperatures. When warming up above -35 ºC, the six septets merge into four septets at 3.22, 3.53, 3.63 and 6.08 ppm; the two singlets merge into one at 6.03 ppm. In addition, at temperatures below 0 ºC, the aliphatic region of the spectra (0-2 ppm) shows only broad signals, while above this temperature regime, the signals become well-resolved. One

thing worth noting is that even at high temperature (+50 ºC), **2.5-OM** is still highly asymmetric as there are seven doublets at 0.56, 0.72, 1.06, 1.17, 1.21, 1.29 and 1.36 ppm for 8 different methyl groups in **2.5-OM**. This is consistent with the ^{1}H NMR spectrum obtained from **2.4**, which also shows high degree of asymmetry. Such observations are presumably due to the hindered rotation of Si–N and Si–Ga bonds at low temperatures, which originates from the sterically demanding Dipp substituents on both gallyl and amido moieties (*Figure 17*).



2.4

Figure 17 Sterically demanding Dipp groups in **2.4**

2.5 Attempted Synthesis of a Silylene with a Biscyclohexylamido Substituent

Since silylene **2.4** fails to generate the desired silanone when reacting with nitrous oxide, due to the migration of the silyl group to the silicon-bound oxygen, attempts have been made to synthesize silylenes without the labile N–Si bond. With this in mind, an amido group with two cyclohexyl substituents was selected, as the cyclohexyl groups also provide some degree of steric protection. The commercially available secondary amine Cy_2NH was treated with 1.1 equivalent of ^{n}BuLi in THF and stirred at -78 ºC. The mixture was then warmed up to ambient temperature and 1.1 equivalent of $SiBr_4$ added.

A white crystalline solid was obtained after work up. The ^{1}H NMR spectrum of the product was consistent with a new species with cyclohexyl substituents (multiplets at 0.83-0.93, 1.03-1.14, 1.40-1.44, 1.57-1.73 and 3.13-3.20 ppm). More informatively, X-ray crystallographic analysis confirmed that the solid-state structure is that of Cy_2NSiBr_3 (**2.6**) (*Figure 18*). In **2.6**, the Si–N distance is significantly shorter than a similar (but sterically bulkier) system reported by Jones (1.677(2) Å, *cf*. 1.724(3) for $(Ar^*SiMe_3N)SiBr_3$, Ar*=2,6-diphenylmethyl-4-isopropylphenyl)[17]. The nitrogen atom in **6** is in a trigonal planar geometry (sum of angles 359.7(6)º), an indication of steric protection around it.

With **2.6** successfully isolated, a one-pot reduction methodology was used in attempt to synthesize a novel silylene, in a similar manner to that used for boryl- and silyl-silylenes featuring the $N(Dipp)SiMe_3$ substituent. The use of **2.1-K** as reductant/substituent

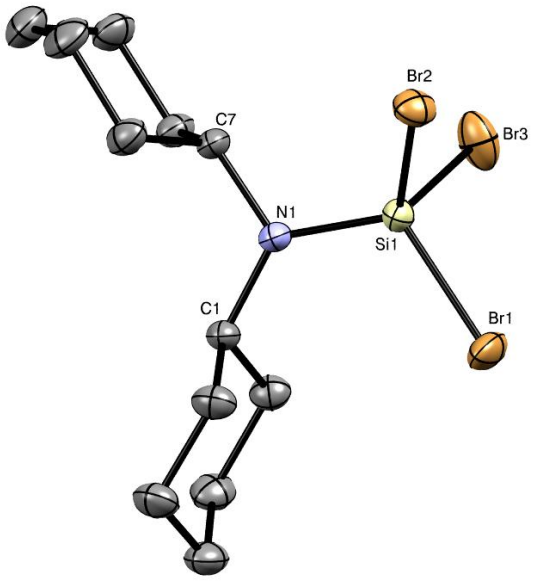


Figure 18 Molecular structure of **2.6** with ellipsoids set at the 50% probability level. For clarity, hydrogen atoms are omitted. Selected bond lengths (Å) and bond angles: Si1–N1 1.677(2), Si1–Br1 2.1899(7), Si1–Br2 2.2149(7), Si1–Br3 2.2145(7), N1–C1 1.483(3), N1–C7 1.482(3), Si1-N1-C1 128.8(2)°, Si1-N1-C7 116.5(2)°, C1-N1-C7 116.5(2)°.

proves to be unreliable since over-substitution takes place (as mentioned in section 2.2), and so the boryllithium reagent $\{(HCDippN)_2B\}Li(THF)_2$ was tested instead. When a 2:1 mixture of boryllithium and **2.6** was dissolved in C_6D_6, the colour of the solution changed briefly to red but quickly turned to yellow in a matter of seconds, with the precipitation of a white solid. The ^1H NMR spectrum of the mixture showed complete consumption of both starting materials, with the formation of $(HCDippN)_2BBr$ as the only easily identifiable product. Among the solids precipitated from solution, one solid was suitable for X-ray crystallography, which revealed its solid-state structure to be that of a boryl substituted disilane (**2.7**) (*Figure 19*). Certain structural parameters for **2.7** closely resemble the corresponding literature reported values for the amido(boryl)silylene (**1.34a**). Thus, the Si–B (2.022(2) Å, *cf*. 2.066(1) Å for **1.34a**)[3i] and Si–N distances (1.720(1) Å and 1.715(1) Å, *cf*. 1.731(1) Å for **1.34a**)[3i] distances

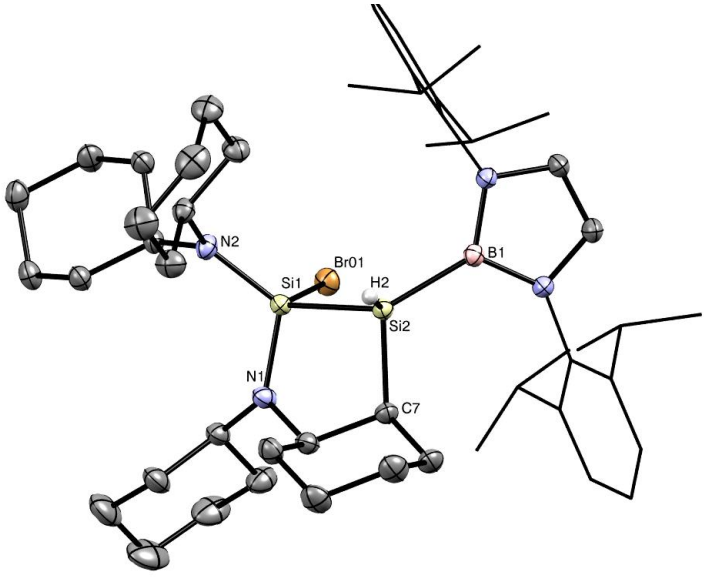
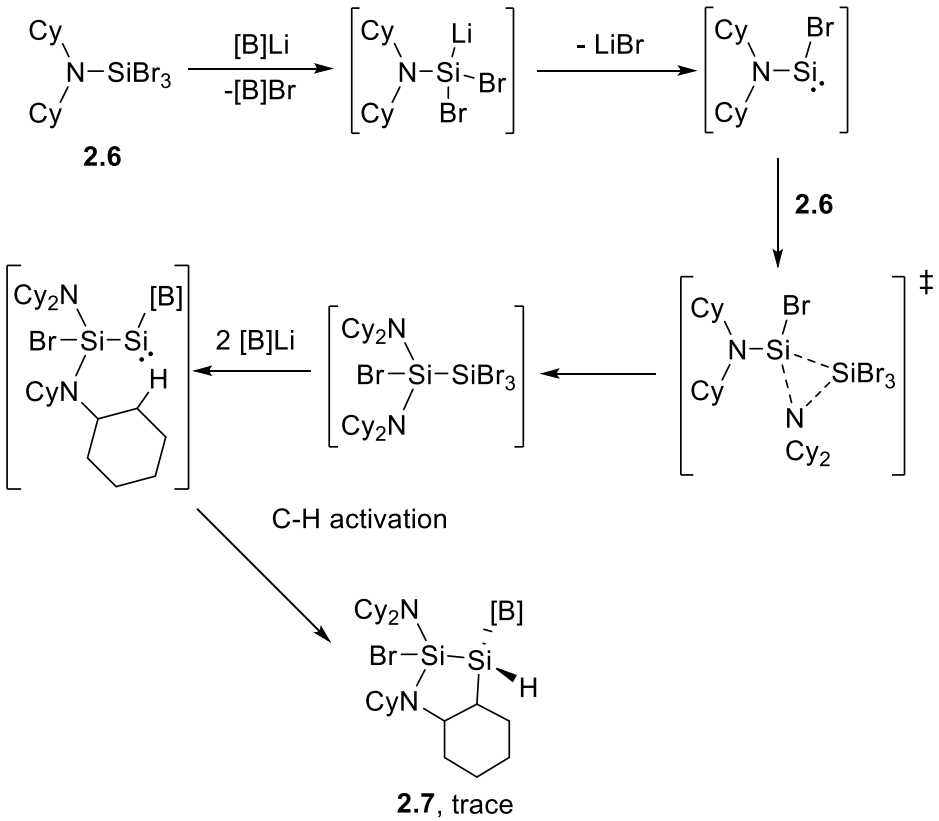


Figure 19 Molecular structure of **2.7** with ellipsoids set at the 50% probability level. For clarity, hydrogen atoms, except for H2, are omitted and the Dipp groups are simplified as wireframes. Selected bond lengths (Å) and bond angles: Si1–Si2 2.3344(5), Si1–N1 1.720(1), Si1–N2 1.715(1), Si1–Br01 2.2874(5), Si2–B1 2.2022(2), Si2–C7 1.917(2), N1-Si1-N2 117.70(6)°, Si2-Si1-N1 94.96(5)°, Si2-Si1-C7 88.63(5)°, B1-Si2-C7 114.18(6)°, B1-Si2-Si1 117.39(5)°.

are similar for the two systems. The Si–Si distance is also consistent with the length of a typical Si–Si single bond (2.3344(5) Å, *cf*. 2.363(1) Å for {Dipp(Me$_3$Si)N}SiBr$_2$–Si{N(SiMe$_3$)Dipp}Br$_2$)[9]. Due to the complexity of the structure of **2.7**, one can only postulate a plausible mechanism for its formation (*Scheme 20*). On possibility is that first one molecule of boryllithium reduces a molecule of **2.6**, generating Cy$_2$NSiBr$_2$K. This silyl anion then eliminates KBr intramolecularly, forming the transient silylene Cy$_2$N(Br)Si. Due to insufficient steric protection at the divalent silicon centre, it reacts with a further molecule of **2.6**, forming (Cy$_2$N)$_2$Si(Br)SiBr$_3$ via insertion of the silylene fragment into the Si–N single bond of **2.6**. This disilane then reacts with two more equivalents of borylllthium, generating the silylene (Cy$_2$N)$_2$BrSiSi{B(NDippCH)$_2$} in a fashion similar to that leading to the formation of {(HCDippN)$_2$B}{Dipp(Me$_3$Si)N}Si



Scheme 20 Proposed mechanism of the formation of **2.7**

from {Dipp(Me$_3$Si)N}SiBr$_3$. Finally, this silylene activates a C–H bonds from one of the cyclohexyl substituents, forming **2.7**; intramolecular C–H bond activation is precedented for acyclic silylenes of this sort.[3i]

2.6 Conclusions

The reaction between **2.2-Cl$_2$** with **2.1-K** failed to generate the target gallyl-substituted silicon species, while using **2.2-Cl** as the silicon(II) precursor successfully produced the desired amidogallylsilylene (**2.4**), albeit with retention of the stabilizing NHC base. Spectroscopic data for **2.4** showed a high degree of asymmetry as well as hindered rotation an ambient temperature. Upon reacting with nitrous oxide, a silyl migrated species (**2.5-OM**) was isolated despite the fact that quantum chemical calculations suggested the potential existence of a chemical equilibrium between the non-migrated **2.5-O** and **2.5-OM** with a calculated energy difference of -4.6 kJ mol^{-1} (i.e. very close to zero, implying an approximately isoenergetic process). In similar fashion to **2.4**, **2.5-OM** also showed hindered rotation around Si–N and Si–Ga bonds at low temperatures. To prevent the unintended silyl migration, an amido ligand without a labile Si–N bond was used in attempt to synthesize an acyclic silylene. However due to lack of steric protection afforded by the two cyclohexyl substituents, the reaction between **2.6** and boryllithium generated mainly bromoborane (HCDippN)$_2$BBr, with a trace amount of the disilane **2.7** isolated as single crystals.

2.7 Experimental details

General considerations

All manipulations were carried out under an inert atmosphere of argon or dinitrogen using standard Schlenk line technique or dry glovebox technique. Solvents were degassed by sparging with argon and dried by passing through a column of appropriate drying agent. NMR samples were prepared under dinitrogen in 5 mm Wilmad 507-PP tubes fitted with J-Young Teflon valve. NMR spectra were measured in benzene-d_6 or toluene-d_8, which were dried over CaH_2, distilled and stored over activated 3 Å molecular sieves. Unless otherwise stated, all NMR spectra were measured on Bruker Avance III HD nanobay 400 MHz or Bruker Avance 500 MHz equipped with a ^{13}C detect cryoprobe at ambient temperature. ^{1}H and ^{13}C resonances were referenced internally with residual protio solvent (^{1}H) or solvent (^{13}C) resonances and were reported relative to tetramethylsilane (δ = 0 ppm). ^{29}Si resonances were referenced externally to tetramethylsilane. Assignments were confirmed using two-dimensional ^{1}H-^{1}H and ^{1}H-^{13}C correlation NMR experiments. Chemical shifts were quoted in δ (ppm) and coupling constants in Hz. Compounds **2.1-K**,[5b] **2.2-Cl$_2$**[11] and **2.2-Cl**[15] were synthesized according to literature procedures. {(HCDippN)$_2$B}Li(THF)$_2$ was synthesized by Dr. Andrey V. Protchenko. All other reagents were purchased from Sigma Aldrich or Alfa Aesar and stored under an inert atmosphere (argon or nitrogen) prior to use.

All calculations were performed on DFT level using Gaussian09 (Revision A.02) program.[18] Geometry optimizations were performed on M062X[19]/6-31G(d)[20] level of theory; Frequency calculations were performed to verify the nature of stationary points (zero imaginary frequencies for a minimum; one imaginary frequency for transition state). Intrinsic reaction coordinates calculations were performed on optimized transition state to verify the nature of transition states.

Synthesis of [IDippH][{(HCDippN)$_2$Ga}$_3$Si] (**2.3**)

In an NMR tube equipped with a J-Young valve, **2.2-Cl$_2$** (15 mg, 0.031 mmol) and **2.1-K** (15 mg, 0.031 mmol) were mixed and dissolved in C_6D_6 (0.4 mL). Immediately the colour of the solution changed from yellow orange to dark red, with orange blocks suitable for X-ray crystallography precipitating out of the mother liquor. The orange crystals of **2.3** were picked by hand and subjected to X-ray analysis. Due to the extremely low yield of **2.3**, spectroscopic and analytic data was impossible to acquire.

Synthesis of {(HCDippN)$_2$Ga}$_2${Dipp(Me$_3$Si)N}Si·I^{i}PrMe (**2.4**)

A sample of **2.1-K** (140 mg, 0.25 mmol) and **2.2-Cl** (109 mg, 0.22 mmol) was dissolved in toluene (5 mL) in a sealed tube. The mixture was stirred at 80 ºC overnight. Upon cooling to room temperature, dark red crystals suitable for X-ray diffraction formed. The mixture was allowed to stand for several hours, allowing complete precipitation of the product. The mother liquor was then decanted off, and crystals of the product washed with a minimum amount of cold hexane and dried in vacuo, yielding **2.4** (129 mg, 0.14 mmol, 65%). ^{1}H NMR (C_6D_6, 400 MHz, 298 K): δ = 0.15 (d, 3H, *J* = 6.8 Hz,

CH(CH_3)$_2$), 0.24 (d, 3H, J = 7.0 Hz, CH(CH_3)$_2$), 0.30-0.39 (overlapping br s, 15H, Si(CH_3)$_3$ and CH_3C=CCH_3), 0.60 (br, 3H, CH(CH_3)$_2$), 1.10 (d, 3H, J = 6.8 Hz, CH(CH_3)$_2$) 1.14-1.24 (overlapping br, 15H, CH(CH_3)$_2$), 1.69-1.78 (overlapping br, 6H, CH(CH_3)$_2$), 2.95 (sept, 1H, J = 6.7 Hz, CH(CH$_3$)$_2$), 3.38 (br, 1H, CH(CH$_3$)$_2$), 3.60-3.82 (overlapping br, 3H, CH(CH$_3$)$_2$) 4.28 (br, 2H, CH(CH$_3$)$_2$), 5.38 (br, 1H, CH(CH$_3$)$_2$), 6.17 (br, 1H, CH=CH), 6.28 (br, 1H, CH=CH), 6.79-6.97 (m, 4H, Ar-H), 7.30-7.41 (m, 5H, Ar-H); ^{13}C NMR (C$_6$D$_6$, 101 MHz, 298 K): δ = 1.4, 3.0, 9.8, 10.0, 19.2, 20.0, 21.0, 21.4, 22.6, 23.4, 23.9, 24.8, 25.6, 25.9, 26.7, 27.5, 27.5, 28.3, 28.5, 53.0, 55.5, 122.9, 123.6, 123.8, 123.9, 124.0, 125.4, 128.5, 136.9, 144.5, 146.3, 147.8, 148.0, 150.5, 163.4, 164.9; ^{29}Si{^{1}H} NMR (C$_6$D$_6$, 99 MHz, 298 K): δ = 3.2 (s, central Si) -17.4 (s, SiMe$_3$).

Synthesis of {(HCDippN)$_2$Ga}(OSiMe$_3$)Si=NSiMe$_3$·I^{i}PrMe (**2.5-OM**)

A sample of **2.4** (100 mg, 0.11 mmol) was dissolved in toluene in an NMR tube with a J-Young valve. The tube was evacuated and recharged with N_2O (1 bar). The tube was hand shaken for 30 min, during which time the colour of the solution turned from deep red to bright yellow. Volatiles were removed in vacuo yielding **2.5-OM** (101 mg, 0.11 mmol, 100%) as a bright yellow powder. Single crystals suitable for X-ray diffraction were obtained by slowly evaporating a hexane solution of the product at ambient temperature under reduced pressure. ^{1}H NMR (toluene-d_8, 400 MHz, 323 K): δ = 0.28 (s, 9H, Si(CH_3)$_3$), 0.56 (d, 6H, J = 6.9 Hz, CH(CH_3)$_2$), 0.72 (d, 6H, J = 6.7 Hz, CH(CH_3)$_2$), 1.06 (d, 12H, J = 6.7 Hz, CH(CH_3)$_2$), 1.18 (d, 6H, J = 7.1 Hz, CH(CH_3)$_2$), 1.21 (d, 6H, J = 6.8 Hz, CH(CH_3)$_2$), 1.29 (d, 6H, J = 6.8 Hz, CH(CH_3)$_2$), 1.36 (d, 6H, J

= 6.9 Hz, C*H*(CH_3)$_2$), 1.54 (s, 6H, C*H*$_3$C=CC*H*$_3$), 3.21 (sept, 2H, *J* = 6.8 Hz, C*H*(CH_3)$_2$), 3.52 (br sept, 2H, C*H*(CH_3)$_2$), 3.63 (sept, 2H, *J* = 6.8 Hz, C*H*(CH_3)$_2$), 6.02 (s, 2H, C*H*=C*H*), 6.08 (sept, 2H, *J* = 7.0 Hz, C*H*(CH_3)$_2$), 6.66 (t, 1H, Ar-*H*), 7.05-7.20 (m, 8H, Ar-*H*); ^{13}C NMR (C_6D_6, 101 MHz, 298 K): δ = 2.7, 10.0, 14.3, 20.8, 21.4, 23.0, 23.6, 24.2, 24.6, 24.9, 25.5, 26.0, 28.5, 28.7, 29.1, 31.9, 50.8, 144.7, 122.5, 123.3, 123.9, 125.3, 126.6, 139.7, 144.8, 145.5, 148.0, 148.8, 152.7; ^{29}Si{^{1}H} NMR (C_6D_6, 80 MHz, 298 K): δ = 10.7.

Synthesis of Cy_2NSiBr_3 (**2.6**)

In a Schlenk tube Cy_2NH (1.0 mL, 5.0 mmol) was dissolved in THF (20 mL). The solution was cooled to -78 ºC and *n*BuLi (3.8 mL of a 1.6 M solution in hexane, 6.1 mmol) was added. The mixture was allowed to warm to ambient temperature with constant stirring over a period of 30 min, and then cooled again to 0 ºC. $SiBr_4$ (0.75 mL, 6.0 mmol) was then added to the mixture which was stirred at ambient temperature overnight. The solvent was removed *in vacuo* and the residue was extracted into hexane (3 x 10 mL). **2.6** was obtained as a white crystalline material by concentrating the hexane solution and recrystallization at -30 ºC (1.5 g, 3.4 mmol, 68%). Crude **2.6** was used without further purification. ^{1}H NMR (C_6D_6, 400 MHz, 298 K): δ = 0.88 (qt, 2H, C*H*$_2$), 1.08 (qt, 4H. C*H*$_2$), 1.42(br, 2H, C*H*$_2$), 1.57-1.73 (m, 12H, C*H*$_2$), 3.17 (tt, 2H, SiC*H*).

Reduction of Cy_2NSiBr_3 (**2.6**): isolation of **2.7**

In an NMR tube with J-Young valve, **2.6** and {(HCDippN)$_2$B}Li(THF)$_2$ were dissolved

in C_6D_6. The solution turned red briefly then yellow in a course of few seconds, with large quantity of white precipitate forming. One single crystal of **2.7** was picked by hand and subjected to X-ray crystallography analysis. Due to the extremely low yield of **2.7**, spectroscopic and analytic data were impossible to acquire.

2.8 References

1. For reviews on NHC stabilized main group systems: (a) C. Fliedel, G. Schnee, T. Avilés, S. Dagorne, *Coord. Chem. Rev*. **2014**, *275*, 63-86; (b) V. Nesterov, D. Reiter, P. Bag, P. Frisch, R. Holzner, A. Porzelt, S. Inoue, *Chem. Rev*. **2018**, *118*, 9678-9842.
2. (a) Y. Segawa, M. Yamashita, K. Nozaki, *Science*, **2006**, *314*, 113-115; (b) Y. Segawa, Y. Suzuki, M. Yamashita, K. Nozaki, *J. Am. Chem. Soc*. **2008**, *130*, 16069-16079.
3. Selected boryl-main group systems: for group 2 elements: (a) M. Yamashita, Y. Suzuki, Y. Segawa, K. Nozaki, *J. Am. Chem. Soc*. **2007**, *129*, 9570-9571; (b) T. Arnold, H. Braunschweig, W. C. Ewing, T. Kramer, J. Mies, J. K. Schuster, *Chem. Commun*. **2015**, *51*, 737-740; (c) J. K. Schuster, D. K. Roy, C. Lenczyk, J. Mies, H. Braunschweig, *Inorg. Chem*. **2019**, *58*, 2652-2658; for group 13 elements: (d) K. Nozaki, Y. Aramaki, M. Yamashita, S-H Ueng, M. Malacria, E. Lacôte, D. P. Curran, *J. Am. Chem. Soc*. **2010**, *132*, 11449-11451; (e) N. Dettenrieder, H. M. Dietrich, C. Schädle, C. Maichle-Mössmer, K. W. Törnroos, R. Anwander, *Angew. Chem. Int. Ed*. **2012**, *51*, 4461-4465; (f) N. Dettenrieder, C. Schädle, C. Maichle-Mössmer, P. Sirsch, R. Anwander, *J. Am. Chem. Soc*. **2014**, *136*, 886-889; (g) A. V. Protchenko, D. Dange, J. R. Harmer, C. Y. Tang, A. D. Schwarz, M. J. Kelly, N. Phillips, R. Tirfoin, K. H. Birjkumar, C. Jones, N. Kaltsoyannis, P. Mountford, S. Aldridge, *Nat. Chem*. **2014**, *6*, 315-319; (h) A. V. Protchenko, D. Dange, M. P. Blake, A. D. Schwarz, C. Jones, P. Mountford, S. Aldridge, *J. Am. Chem. Soc*. **2014**, *136*, 10902-10905; for group 14 elements: (i) A. V. Protchenko, K. H. Birjkumar, D. Dange, A. D. Schwarz, D. Vidovic, C. Jones, N. Kaltsoyannis, P. Mountford, S. Aldridge, *J. Am. Chem. Soc*. **2012**, *134*, 6500-6503; (j) A. V. Protchenko, D. Dange, A. D. Schwarz, C. Y. Tang, N. Phillips, P. Mountford, C. Jones, S. Aldridge, *Chem. Commun*. **2014**, *50*, 3841-3844; (k) A. V. Protchenko, J. I. Bates, L. M. A. Saleh, M. P. Blake, A. D. Schwarz, E. L. Kolychev, A. L. Thompson, C. Jones, P. Mountford, S. Aldridge, *J. Am. Chem. Soc*. **2016**, *138*, 4555-4564; (l) M. Usher, A. V. Protchenko, A. Rit, J. Campos, E. L. Kolychev, R. Tirfoin, S. Aldridge, *Chem. Eur. J*. **2016**, *22*, 11685-11698; (m) A. Rit, J. Campos, H. Niu, S. Aldridge, *Nat. Chem*. **2016**, *8*, 1022-1026; (n) M. Kaaz, J. Bender, D. Förster, W. Frey, M. Nieger, D.

Gudat, *Dalton Trans*. **2014**, *43*, 680-689; (o) D. Dange, A. Davey, J. A. B. Abdalla, S. Aldridge, C. Jones, *Chem. Commun*. **2015**, *51*, 7128-7131; (p) C. Helling, G. E. Cutsail III, H. Weinert, C. Wölper, S. Schulz, *Angew. Chem. Int. Ed*. **2020**, *59*, 7561-7568.

4. Selected gallyl-substituted main group systems: for group 2 elements: (a) C. Jones, D. P. Mills, J. A. Platts, R. P. Rose, *Inorg. Chem*. **2006**, *45*, 3146-3148; (b) I. L. Fedushkin, A. N. Lukoyanov, A. N. Tishkina, G. K. Fukin, K. A. Lyssenko, M. Hummert, *Chem. Eur. J*. **2010**, *16*, 7563-7571; (c) O. Bonello, C. Jones, A. Stasch, W. D. Woodul, *Organometallics*, **2010**, *29*, 4914-4922; for group 13 elements: (d) R. J. Baker, C. Jones, M. Kloth, J. A. Platts, *Angew. Chem. Int. Ed*. **2003**, *42*, 2660-2663; for group 14 elements: (e) S. P. Green, C. Jones, K-A Lippert, D. P. Mills, A. Stasch, *Inorg. Chem*. **2006**, *45*, 7242-7251; (f) P. A. Pupar, M. C. Jennings, K. M. Baines, *Can. J. Chem*. **2007**, *85*, 141-147; (g) A. V. Protchenko, A. D. Schwarz, M. P. Blake, C. Jones, N. Kaltsoyannis, P. Mountford, S. Aldridge, *Angew. Chem. Int. Ed*. **2013**, *52*, 568-571; for group 15 elements: (h) R. J. Baker, C. Jones, D. P. Mills, D. M. Murphy, E. Hey-Hawkins, R. Wolf, *Dalton Trans*. **2006**, 64-72.
5. (a) E. S. Schmidt, A. Jockisch, H. Schmidbaur, *J. Am. Chem. Soc*. **1999**, *121*, 9758-9759; (b) R. J. Baker, R. D. Farley, C. Jones, M. Kloth, D. M. Murphy, *J. Chem. Soc. Dalton Trans*. **2002**, 3844-3850.
6. R. J. Schwamm, M. D. Anker, M. Lein, M. P. Coles, C. M. Fitchett, *Angew. Chem. Int. Ed*. **2018**, *57*, 5885-5887.
7. (a) J. Hicks, P. Vasko, J. M. Goicoechea, S. Aldridge, *Nature*, **2018**, *557*, 92-95; (b) R. J. Schwamm, M. D. Anker, M. Lein, M. P. Coles, *Angew. Chem. Int. Ed*. **2019**, *58*, 1489-1493; (c) R. J. Schwamm, M. P. Coles, M. S. Hill, M. F. Mahon, C. L. McMullin, N. A. Rajabi, A. S. S. Wilson, *Angew. Chem. Int. Ed*. **2020**, *59*, 3928-3932; (d) S. Kurumada, S. Takamori, M. Yamashita, *Nat. Chem*. **2020**, *12*, 36-39; (e) K. Koshino, R. Kinjo, *J. Am. Chem. Soc*. **2020**, *142*, 9057-9062.
8. A. V. Protchenko, P. Vasko, D. C. H. Do, J. Hicks, M. Á. Fuentes, C. Jones, S. Aldridge, *Angew. Chem. Int. Ed*. **2019**, *58*, 1808-1812.
9. A. V. Protchenko, A. D. Schwarz, M. P. Blake, C. Jones, N. Kaltsoyannis, P. Mountford, S. Aldridge, *Angew. Chem. Int. Ed*. **2013**, *52*, 568-571.
10. M. M. D. Roy, M. J. Ferguson, R. McDonald, Y. Zhou, E. Rivard, *Chem. Sci*. **2019**, *10*, 6476-6481.
11. R. S. Ghadwal, H. W. Roesky, S. Merkel, J. Henn, D. Stalke, *Angew. Chem. Int. Ed*. **2009**, *48*, 5683-5686.
12. T. J. Hadlington, J. A. B. Abdalla, R. Tirfoin, S. Aldridge, C. Jones. *Chem. Commun*. **2016**, *52*, 1717-1720.
13. T. Pott, P. Jutzi, W. W. Schoeller, A. Stammler, H-G Stammler, *Organometallics*, **2001**, *20*, 5492-5494.
14. A. J. Arduengo III, R. Krafczyk, R. Schmutzler, *Tetrahedron*, **1999**, *55*, 14523-14534.
15. H. Cui, C. Cui, *Dalton Trans*. **2011**, *40*, 11937.

16. H. Cui, J. Zhang, Y. Tao, C. Cui, *Inorg. Chem*. **2016**, *55*, 46-50.
17. T. J. Hadlington, J. Li, C. Jones, *Can. J. Chem*. **2014**, *92*, 427-433.
18. Gaussian 09, Revision A.02, M. J. Frisch, G. W. Trucks, H. B. Schlegel, G. E. Scuseria, M. A. Robb, J. R. Cheeseman, G. Scalmani, V. Barone, B. Mennucci, G. A. Petersson, H. Nakatsuji, M. Caricato, X. Li, H. P. Hratchian, A. F. Izmaylov, J. Bloino, G. Zheng, J. L. Sonnenberg, M. Hada, M. Ehara, K. Toyota, R. Fukuda, J. Hasegawa, M. Ishida, T. Nakajima, Y. Honda, O. Kitao, H. Nakai, T. Vreven, J. A. Montgomery, Jr., J. E. Peralta, F. Ogliaro, M. Bearpark, J. J. Heyd, E. Brothers, K. N. Kudin, V. N. Staroverov, R. Kobayashi, J. Normand, K. Raghavachari, A. Rendell, J. C. Burant, S. S. Iyengar, J. Tomasi, M. Cossi, N. Rega, J. M. Millam, M. Klene, J. E. Knox, J. B. Cross, V. Bakken, C. Adamo, J. Jaramillo, R. Gomperts, R. E. Stratmann, O. Yazyev, A. J. Austin, R. Cammi, C. Pomelli, J. W. Ochterski, R. L. Martin, K. Morokuma, V. G. Zakrzewski, G. A. Voth, P. Salvador, J. J. Dannenberg, S. Dapprich, A. D. Daniels, O. Farkas, J. B. Foresman, J. V. Ortiz, J. Cioslowski, and D. J. Fox, Gaussian, Inc., Wallingford CT, 2009.
19. Y. Zhao, D. G. Truhlar, *Theor. Chem. Account*, **2008**, *120*, 215-241.
20. R. Ditchfield, W. J. Hehre, J. A. Pople, *J. Chem. Phys*. **1971**, *54*, 724-728.

Chapter 3: A Bisboryloxysilylene

3.1 Introduction: From N-heterocyclic Iminato (NHI) to N-heterocyclic Boryloxide (NHBO)

Nitrogen-based ligands have been widely used in organometallic and main-group chemistry owing to their strong electron donating abilities.[1a] Imines in particular, have attracted much interest among main-group chemists. Unlike amine-based nitrogen donors, imines can donate electron density to a metal centre through both σ- and π-symmetry interactions. Therefore, the electronic properties of the imine nitrogen heavily depend on the scaffold to which it is attached via the C=N double bond. For this reason, N-heterocyclic iminato (NHI) ligands, derived from N-heterocyclic carbenes (NHC), are strong 2-electron σ donors. Whatismore, the electron-rich π system of the NHC imidazole ring provides a π electron reservoir, allowing NHIs to act as 2π or even 4π electron donors (*Figure 1*).[1] In recent years, the NHI ligand family has been used to synthesize a wide range of *p*-block element complexes (*Figure 2*).[2] For group 14 elements (in which my primary research interests lie), only a small number of complexes had been reported at the beginning of my project which are stabilized by NHI ligand systems; homoleptic group 14-NHI complexes were particularly

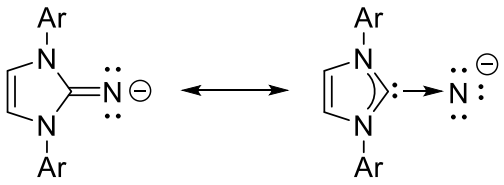


Figure 1 N-heterocyclic imine

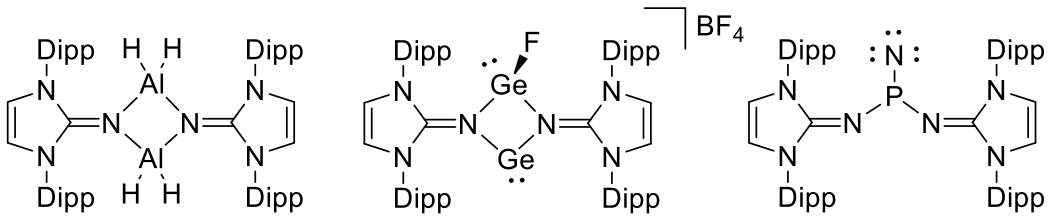
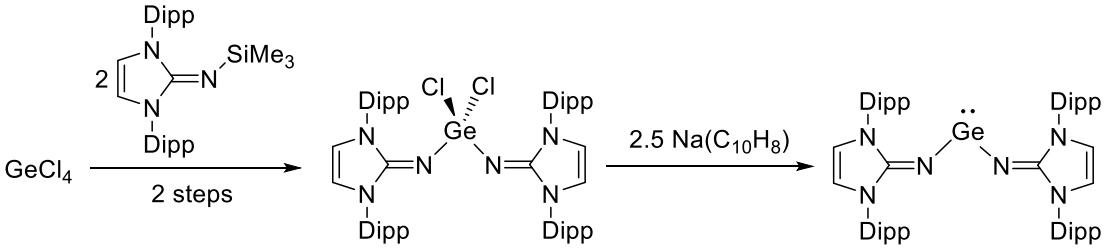
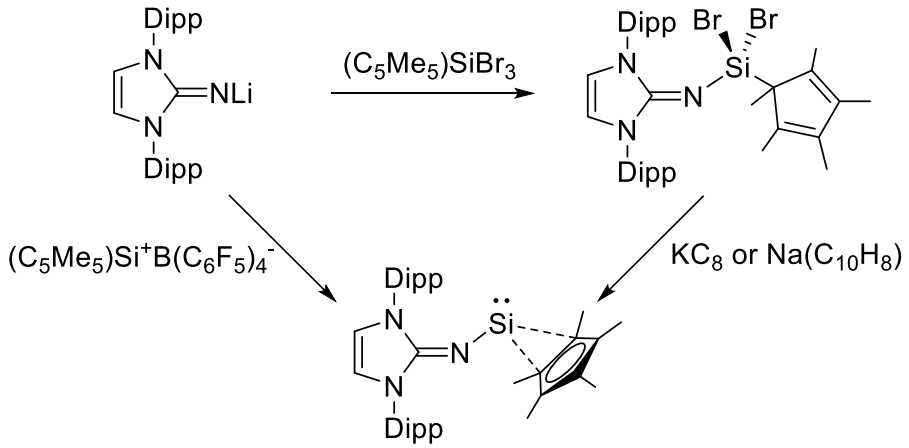


Figure 2 Selected examples of NHI stabilized main group systems

uncommon. Indeed, the only example of such a homoleptic system was reported in 2015 by Rivard. The bisiminogermylene $(IDippN)_2Ge$ was synthesized by substitution of two of the chlorine substituents in $GeCl_4$ via reaction with the trimethylsilyl derivative of IDippN to give the $(IDippN)_2GeCl_2$, followed by reduction with sodium naphthalenide (*Scheme 3*).[2k] Silicon analogues have only been seen in the form of heteroleptic systems. In 2012, Inoue reported an iminocyclopentadienylsilylene featuring a silicon(II) centre bound to an NHI and a η^2-pentamethylcyclopentadienyl ligand system. This silylene could be synthesized either by reduction of the dibromo silicon(IV) precursor by potassium graphite or sodium naphthalenide, or via metathesis between the lithium salt of IDippN and pentamethylcyclopentadienyl silyliumylidene (*Scheme 4*). The Lewis basicity of the silicon centre was confirmed by the reaction with tris(pentafluorophenyl)borane, in which the Lewis acid-base adduct of the silylene and the borane was generated and structurally characterized.[2i] Another (transient)

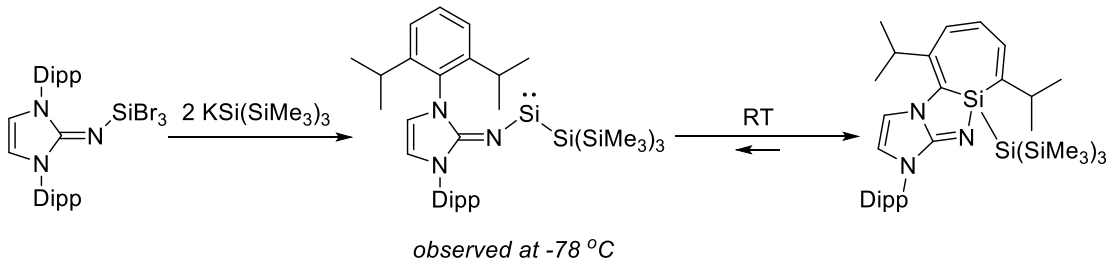


Scheme 3 Synthesis of bisiminogermylene



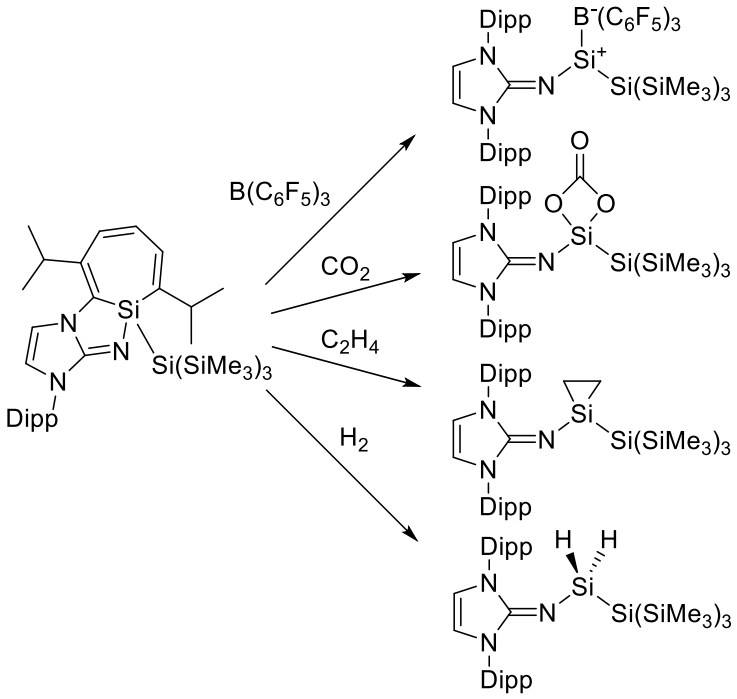
Scheme 4 Synthesis of iminocyclopentadienylsilylene

heteroleptic acyclic silylene featuring an NHI as one of the silicon-bound substituents was reported in 2017 by Inoue and Rieger in the form of an iminosilylsilylene (IDippN)($(Me_3Si)_3Si$)Si (*Scheme 5*). When a 1:2 mixture of (IDippN)$SiBr_3$ and potassium hypersilyl was dissolved in toluene, the corresponding silylene could be observed at -78 °C by multinuclear NMR and UV-vis spectroscopic measurements. At elevated temperatures (T>100 °C), the silylene was shown to be in equilibrium with a silepin, formed when the Si(II) centre inserts into the aromatic C–C bond of one of the



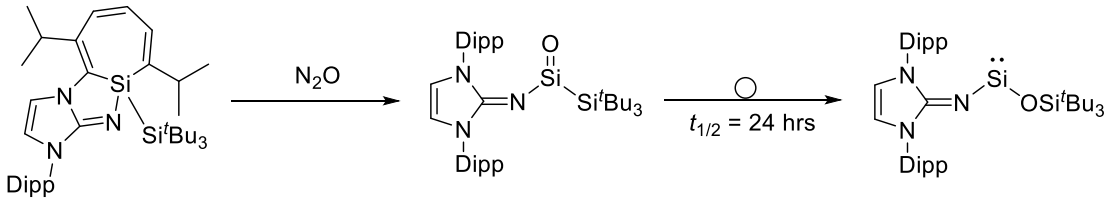
Scheme 5 Synthesis of iminosilylsilylene and its isomerization to a silepin

flanking Dipp groups (*Scheme 5*). Although the silepin is the predominant species in the equilibrium mixture at ambient temperature, the system still gives rise to “silylene like” reactivity. Thus, for example, the reaction with one equivalent of tris(pentafluorophenyl)borane leads to the formation of a Lewis adduct between the silylene and borane. Reactions with carbon dioxide, ethylene or dihydrogen also lead



Scheme 6 "Silylene-like" reactivity of silepin

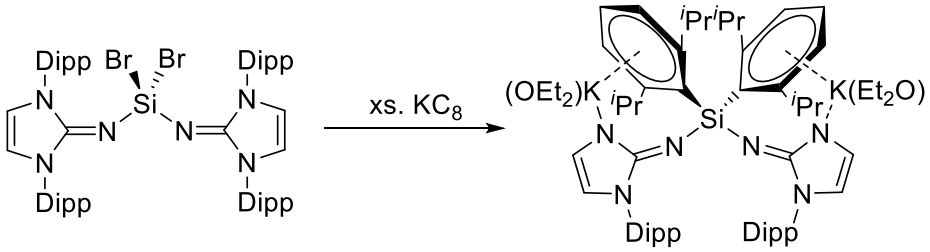
to silicon(IV) systems, corresponding to the expected products from the reactions with the free silylene itself (*Scheme 6*).[2p] The most recent example of a heteroleptic silylene system featuring an NHI substituent was again reported by Inoue and Reiger in the form of an iminosiloxysilylene (IDippN)((Me$_3$Si)$_3$SiO)Si. This compound was isolated as a formal decomposition product of a transient silanone, itself accessed by reacting nitrous oxide with an iminosilylsilylene (IDippN)(^{t}Bu$_3$Si)Si. Due to the highly polarized Si=O bond and the thermodynamically strong nature of Si–O single bonds, the supersilyl group of the silanone is observed to migrate to the oxygen atom at ambient temperatures, with a half-life of 24 hours in benzene or THF (*Scheme 7*). Reactivity-wise (IDippN)((Me$_3$Si)$_3$Si)Si irreversibly binds ethylene through 1+2 cycloaddition, which



Scheme 7 Synthesis of iminosiloxysilylene

contrasts with the reversible process reported for a dithiolatosilylene $(Ar^*S)_2Si$ (Ar* = 2,6-$Ar_2C_6H_3$, Ar = Dipp) with ethylene by Tuononen and Power in 2012.[2q]

Homoleptic bisiminosilylenes on the other hand, remain elusive. In 2015 Rivard reported an attempted synthesis of such a silylene but failed to isolate the target: the dibromo silicon(IV) precursor was unreactive towards sodium, potassium or Jones' reagent at room temperature in toluene, THF or ether; the reaction with excess sodium naphthalenide or potassium graphite, on the other hand, led to the formation of an over-reduced product (*Scheme 8*). DFT analysis suggested that the silylene was formed transiently, but that a thermodynamically favorable migration of one of the pendant Dipp substituents could then take place in the presence of excess reductant.[2k] The



Scheme 8 Attempt Synthesis of bisiminosilylene

instability of this homoleptic bisiminosilylene suggests that the NHI ligand might be too strong an electron donor to stabilize an acyclic two-coordinate silicon(II) centre. By contrast, the success in isolating heteroleptic systems indicates that silylenes with one NHI moiety can be stable in the presence of a second substituent with weaker σ donating ability.[2p,2q] With this in mind, the use of an N-heterocyclic boryloxyl (NHBO) ligand was postulated (*Figure 9*); these systems are isoelectronic with NHIs, but instead of a nitrogen-base donor, the oxygen atom in the NHBO family is more electronegative, thereby making NHBOs weaker σ-donors. In this part of the project, the focus is on

using NHBOs in order to synthesize a homoleptic acyclic silylene system. In addition, the structural and electronical properties (as well as the reactivity) of such a system are compared with related silicon and heavier group 14 systems.

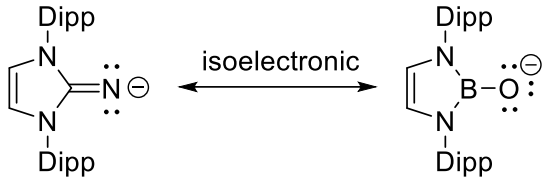


Figure 9 Structural comparison of NHI and NHBO

3.2 NHBO Ligands: A DFT Analysis

To probe the electronic properties of the anionic NHBO ligand and put them into the context of literature reported boryloxide ($(TMS_2CH)_2BO^-$)[3c] and aryloxide system (2,6-$Dipp_2PhO^-$),[3a,3b] together with $[IDippN]^-$, all four systems were subjected to quantum chemical calculations. These studies (*Figure 10*) showed that the four anionic ligands are isolobal, with the in- and out-of-plane π-donor orbitals as the highest energy occupied frontier orbitals (HOMO and HOMO-1). The energies of the σ-donor orbitals, on the other hand, vary more markedly. These were associated with the HOMO-3 (for $(TMS_2CH)_2BO^-$), HOMO-9 (for 2,6-$Dipp_2PhO^-$), HOMO-8 (for NHBO) and HOMO-4 (for NHI).

Numerically, as shown in *Figure 10*, the energies of both the in- and out-of-plane π-donor orbitals for the NHI are higher than those in the oxy ligands, indicating that the NHI is the strongest π-donor among all the ligands examined (consistent with the more electropositive nature of nitrogen compared to oxygen). Although dwarfed by NHI, the NHBO is the strongest donor among the oxygen-based ligands. Considering the

energies of the σ-donor orbitals of the four ligands, not surprisingly, the NHI also stands out with the highest orbital energy (-3.75 eV) compared to the oxy based ligands (-4.12 eV to -5.68 eV).

Overall, the computational results therefore show that the NHBO ligand is a potential [2σ+4π] donor with milder σ- and π-donor abilities compared to related NHI ligands, but stronger donor capabilities compared to other oxy ligands. This analysis therefore

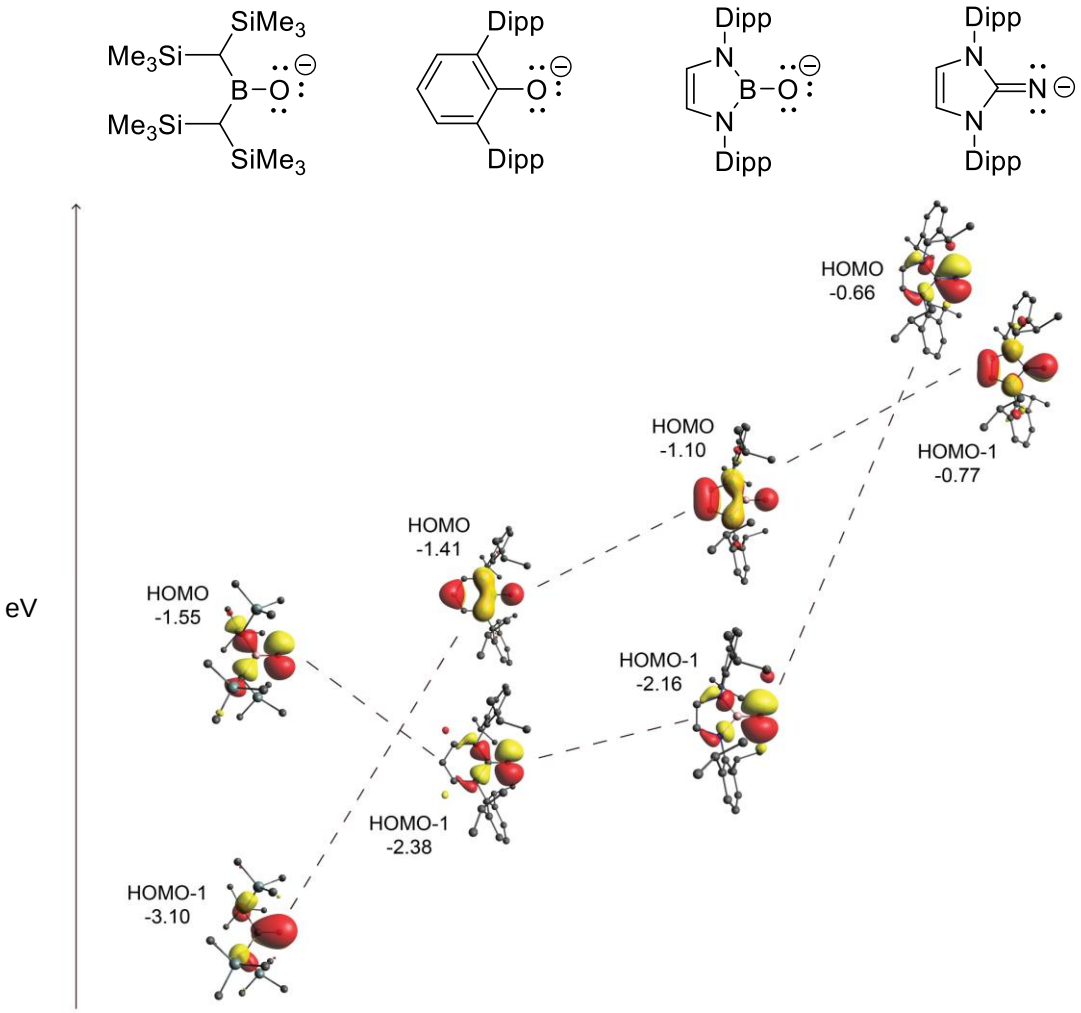
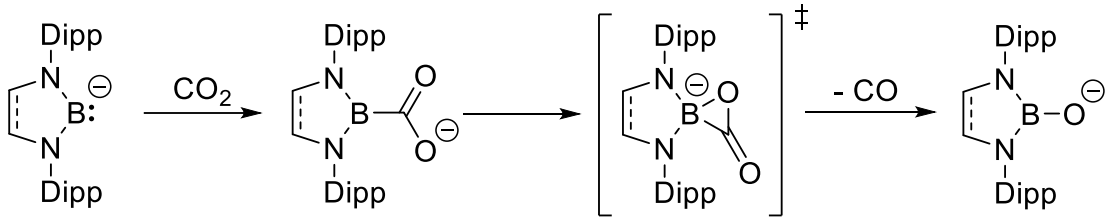


Figure 10 Frontier orbitals of selected ligands

identifies the NHBO ligand as a plausible candidate ligand for the synthesis of an homoleptic acyclic silylene – a system which has proved impossible to access for the more strongly donating NHI family.

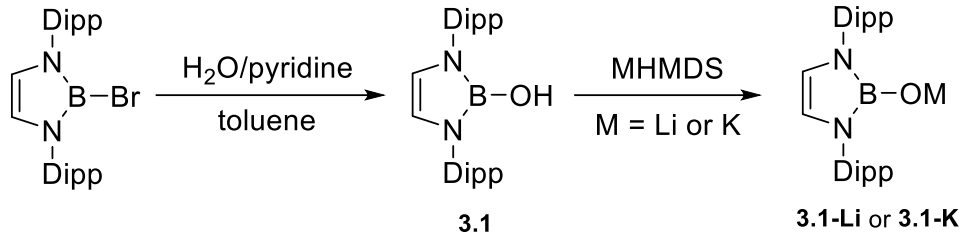
3.3 Synthesis of the NHBO Ligand and Bisboryloxysilylene

On the basis of the quantum chemical results, the NHBO ligand was targeted for investigation experimentally. The first and only reported synthesis of an NHBO system, (in this case with Dipp substituents on the endocyclic nitrogen atoms) in its protonated form, dates back to a report from 2008 by Yamashita and Nozaki. It was isolated as a



Scheme 11 Formation of NHBO as reported by Yamashita

side product from the reaction between a boryllithium reagent and carbon dioxide, followed by subsequent elimination of carbon monoxide and protonation (*Scheme 11*). The major product of the reaction is the borylcarboxylic acid.[4a] The low yield of this compound, according to Yamashita and Nozaki, can be rationalized by the high energy barrier for CO elimination from the borylcarboxylic acid with destabilization of the transition state resulting from dearomatization of the five-membered NHB ring (*Scheme 11*).[4b] Due to the challenging synthesis of boryllithium and the low yield of subsequent reaction which leads to this NHBO, an alternative synthetic route was developed. In this case, direct hydrolysis of the bromoborane $(DippNCH)_2BBr$ was achieved in a water-toluene biphasic system with pyridine as an external base to quench the hydrobromic acid generated as a co-product. As a result, protonated NHBO (**3.1**) was isolated in moderate to good yield (66%) (*Scheme 12*). Using lithium or potassium



Scheme 12 Synthesis of **1**, **1-Li** and **1-K**

bis(trimethylsilyl)amide as a base, **3.1** can then be deprotonated, resulting in the formation of the lithium (**3.1-Li**) or potassium salts (**3.1-K**) respectively, in nearly quantitative yields (97% for **3.1-Li**, 95% for **3.1-K**).

With anionic NHBO [**3.1**]$^-$ in hand, attempts to synthesize a silicon(IV) precursor were then made. In the first attempts, **3.1-K** was mixed with half an equivalent of silicon tetrachloride. The reaction generated a new species after work-up, as shown by the appearance of a set of new signals in ^{1}H-NMR (doublets at 1.14 and 1.17 ppm, *cf.* doublets at 1.16 and 1.26 ppm for **3.1-K**; septet at 3.16 ppm, *cf.* 3.62 ppm for **3.1-K**; singlet at 5.87 ppm, *cf.* singlet at 6.03 ppm for **3.1-K**). The ^{29}Si{^{1}H} NMR showed one

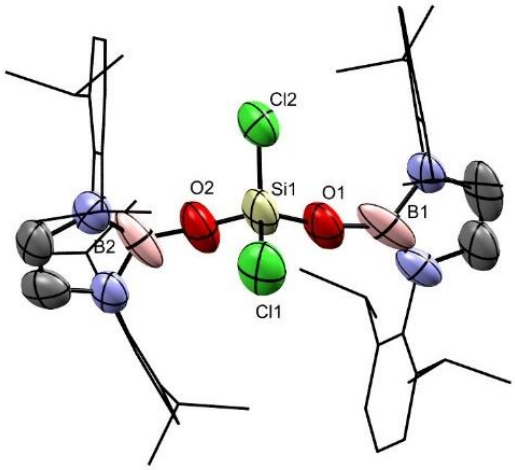
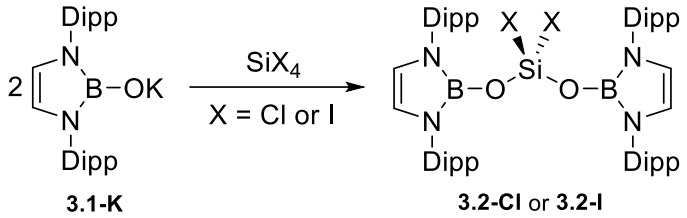


Figure 13 Molecular structure of **3.2-Cl** with ellipsoids set at the 50% probability level (one of two independent molecules in the asymmetric unit). For clarity, hydrogen atoms are omitted and the Dipp groups are simplified as wireframes. Selected bond lengths (Å) and bond angles: Si1–O1 1.64(1), Si1–O2 1.62(1), Si1–Cl1 2.018(8), Si1–Cl2 1.99(1), O1–B1 1.38(2), O2–B2 1.35(2), O1-Si1-O2 109.2(7)°, Si1-O1-B1 158(1)°, Si1-O2-B2 138(1)°, Cl1-Si1-Cl2 108.6(3)°.

singlet at -21.8 ppm, consistent with the formation of a silicon(IV) compound (*cf.* -21.9 ppm for $(IDippN)_2SiBr_2$[2k]; -21.3 ppm for $(ArS)_2SiBr_2$ (Ar = 2,6-dimesitylphenyl)[6b]). The molecular structure of the product was further confirmed by X-ray crystallography as bis(boryloxy)silicon dichloride (**3.2-Cl**) (*Figure 13*). Although the structure obtained does not meet the standards for publication, the atom connectivity could be identified unambiguously.

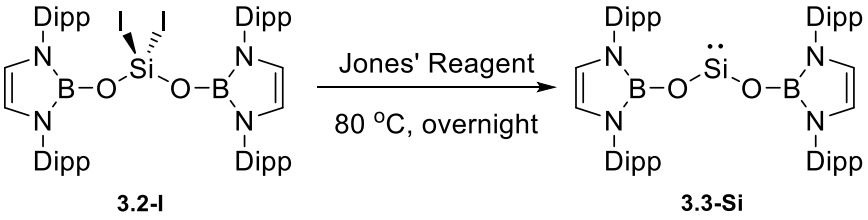
In order to obtain the target bisboryloxysilylene, **3.2-Cl** was subjected to various reductants. However, all attempts to reduce **3.2-Cl** failed. Using magnesium-based reductant such as magnesium metal or Jones' reagent ($(^{Mes}NacnacMg)_2$),[5] no reaction was observed whatsoever, either in benzene, ether or THF even at elevated temperature. The use of a stronger reductant such as potassium or potassium graphite under harsher conditions (60 °C in THF), led to cleavage of the Si–O bond(s): signals consistent with **3.1-K** were observed in ^{1}H-NMR spectrum of the product mixture. As a matter of fact, **3.2-Cl** is remarkably robust even under bench-top condition, consistent with a relatively sterically well-protected silicon centre and strong Si–Cl bonds that are apparently not prone to hydrolysis or reduction.

Owing to the unexpected stability of the chloride derivative **3.2-Cl**, the analogous diiodide was targeted. Stirring a mixture of **3.1-Li** and silicon tetraiodide in a 2:1 molar ratio in benzene generates a 1:1 mixture of the mono-substituted species $(NHBO)SiI_3$ and unreacted **3.1-Li**, even after refluxing in benzene for several days. When **3.1-K** was used, the target disubstituted species $(NHBO)_2SiI_2$ (**3.2-I**) was successfully synthesized (*Scheme 14*). In contrast to the reaction using **3.1-Li**, this synthesis is feasible at ambient



Scheme 14 Synthesis of **3.2-Cl** and **3.2-I**

temperature and is complete within a few hours. The identity of the product was confirmed by multinuclear NMR spectroscopy. The $^{29}Si\{^{1}H\}$ NMR spectrum, in particular, shows one singlet at -167.6 ppm, i.e. shifted considerably upfield compared to **3.2-Cl**, which is consistent with the fact that the signal for SiI_4 (-350 ppm) is found significantly more upfield than that for $SiCl_4$ (-18 ppm). Equipped with **3.2-I**, several different reducing agents were used in attempt to synthesize the target silylene **3.3-Si**. Similar to observations made when using **3.2-Cl**, **3.1-K** was identified in the reaction



Scheme 15 Synthesis of bis(boryloxy)silylene **3.3-Si**

mixture (by its ^{1}H NMR signature) when potassium or potassium graphite were used as the reductant. When a mild (and soluble) reductant - Jones' reagent - was employed, a new set of signals was seen in the ^{1}H NMR spectrum (doublets at 1.05 and 1.18 ppm, *cf.* overlapping doublets at 1.18 ppm for **3.2-I**; septet at 3.15 ppm, *cf.* septet at 3.22 ppm for **3.2-I**), together with the signals corresponding to $(^{Mes}NacnacMgI)_2$. The reaction went to completion when a 1:1 mixture of **3.2-I** and Jones' reagent were stirred at 80 °C in benzene overnight (*Scheme 15*). After work-up and recrystallization from pentane,

single crystals suitable for X-ray crystallography were obtained, and the product was then identified as the bis(boryloxy)silylene **3.3-Si** on the basis of its solid-state structure (*Figure 16*).

Multi-nuclear NMR and elemental analysis also support the identity of **3.3-Si**. The $^{29}Si\{^{1}H\}$ NMR spectrum of **3.3-Si** features one singlet at 35.5 ppm, i.e. significantly upfield shifted when compared to most of the other acyclic two-coordinate silylenes (*cf.* 439.7 ppm for an amidoborylsilylene (**1.34a**);[6a] 438 and 467 ppm for the two rotamers of an amidosilylsilylene (**1.34e**);[6c] 285.5, 270.4 and 270.9 ppm for bisthiolatosilylenes (**1.34b,c,d**);[6b,6d] 204.6 ppm for bisamidosilylene (**1.34f**);[6e] 432.9 ppm for vinylsilylsilylene (**1.34h**)[6f]), but somewhat similar to iminosiloxysilylene (58.9 ppm)[2q]. It has been reported that the chemical shift of the central silicon in $^{29}Si\{^{1}H\}$ NMR in acyclic two-coordinate silylenes reflects the HOMO-LUMO gap of the silylene, i.e. the bigger separation is, the higher field chemical shift.[6e] The central silicon of **3.3-Si** exhibits the most upfield shifted $^{29}Si\{^{1}H\}$ NMR signal reported for a silylene to date.

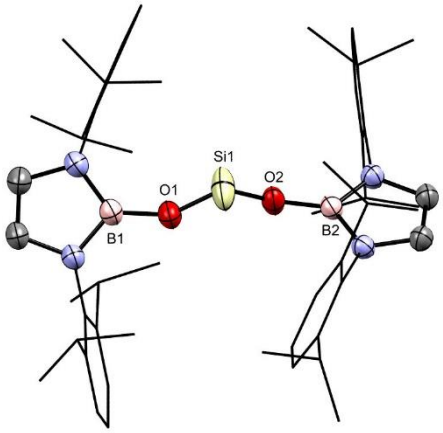


Figure 16 Molecular structure of **3.3-Si** with ellipsoids set at the 50% probability level (one out of two independent molecules in the asymmetric unit). For clarity, hydrogen atoms are omitted and the Dipp groups are simplified as wireframes. Selected bond lengths (Å) and bond angles: Si1–O1 1.607(2), Si1–O2 1.605(1), O1–B1 1.372(3), O2–B2 1.375(3), O1-Si1-O2 100.02(8)°, Si1-O1-B1 138.8(1)°, Si1-O2-B2 136.9(1)°.

This reflects a strong π donation from the NHBO ligand, which contributes to the large HOMO-LUMO gap of **3.3-Si**, consistent with the computational findings (*vide supra*).

3.4 Structural Features of Bis(boryloxy)tetrylenes

X-ray crystallography together with DFT calculations shed some light on the structural and electronic properties of **3.3-Si**. The bond angle at the central silicon atom in silylene systems is the combined outcome of the steric and electronic properties of the silicon-bound substituents. In this case the O-Si-O bond angle for **3.3-Si** is 100.02(8)°, as determined crystallographically. This angle is significantly narrower than those of amidoborylsilylene **1.34a** (109.7(1)°)[6a], amidosilylsilylene **1.34e** (116.9(1)°)[6c] and bisamidosilylene **1.34f** (110.94(5)°)[6e], but somewhat similar to iminosiloxysilylene **1.34g** (103.56(8)°)[2q]. This results from the fact that the oxygen atom of the NHBO ligand is more electronegative when compared with the boron, silicon and nitrogen donor atoms of the Si-bound substituents for the silylenes listed above. This in turn reflects Bent's rule which states that the X-Si-X angle is correlated with the electronegativity of X: the angle narrows as the electronegativity of X increases due to greater Si p-orbital participation in the Si-X bond.[7] Consistently, a natural bond orbital (NBO) analysis shows that the lone pair at silicon resides in an orbital with only 18.5% *p* character, implying that the Si–O bonds possess most of the *p*-orbital character.

The Si–O bond lengths in **3.3-Si** are 1.6074(14) Å and 1.6052(14) Å, i.e. considerably shorter than that found in the iminosiloxysilylene (1.643(1) Å)[2q], presumably because

of the π-donor nature of the NHBO substituent that increases the Si–O bond order in **3.3-Si** (while the siloxy ligand in the iminosiloxysilylene is a σ-donor only).

In order to study the structural trends on descending group 14, the heavier congeners of **3.3-Si**, namely **3.3-Ge**, **3.3-Sn** and **3.3-Pb**, were synthesized by my colleague Ying Kai Loh, and their solid-state structures were obtained. Listed in *Table 17* are key structural features of all of the bis(boryloxy)tetrylenes. It is apparent from these data that the O-E-O (E = Si, Ge, Sn or Pb) angles of **3.3-Ge**, **3.3-Sn** and **3.3-Pb** are significantly

	O–E–O (°)	E–O (Å)[a]	B–O (Å)[a]	B–O–E–O (°)[a]	E–C_{ipso} (Å)[a]
3.3-Si	100.02(8)	1.606(1)	1.374(2)	159.48(1)	3.576(2)
3.3-Ge	93.56(7)	1.778(2)	1.362(3)	144.45(1)	3.421(2)
3.3-Sn	93.25(8)	2.015(2)	1.353(3)	123.40(1)	3.123(2)
3.3-Pb	92.66(6)	2.131(2)	1.343(3)	120.37(1)	3.095(2)

Table 17 Structural features of **3-E**; [a] mean values

narrower than **3.3-Si**, progressively approaching 90° on going down the group. In addition, NBO analyses are consistent with a diminishing *p* character in the lone pair of the central E element on going down group 14 (12.3% in **3.3-Ge**, 4.4% in **3.3-Sn** and 2.4% in **3.3-Pb**). Both of these observations are consistent with relativistic effects (*s*-orbital stabilization), as well as poorer *s*/*p* mixing due to increasing difference in size between the orbitals and their increasing number of radial nodes, on going down group 14. The B–O bond lengths become increasingly shorter on descending the group, an indication of increasing π donation from oxygen to boron as the competing π donation from oxygen to E atom decreases, due to poorer overlap. DFT calculations are also consistent with the experimental data: the calculated Wiberg bond indices for the B–O

bonds in **3.3-E** show a steady increase on descending the group, being 0.89, 0.92, 1.01 and 1.06 for **3.3-Si**, **3.3-Ge**, **3.3-Sn** and **3.3-Pb**, respectively. Perhaps most interestingly, the B-O-E-O dihedral angle gets markedly narrower on descending group 14. Visualized by the superimposed structures of **3.3-E** for E = Si-Pb (*Figure 18*), the decreasing dihedral B-O-E-O angles reflect sequentially increasing interactions between the aromatic rings of the boryl backbone and the central E element. This is also manifested in the trend towards decreasing of $C_{ipso}\cdots E$ distance on descending the group (where C_{ipso} denotes the *ipso* carbon of the boryl Dipp groups). This observation is most likely the consequence of enhanced π_{arene} interactions between the aromatic π system and the vacant $p\pi$ orbital on the E elements from **3.3-Si** to **3.3-Pb**. From an alternative viewpoint, the group 14 elements become increasingly soft on descending the group, which explains the increasing importance of the (soft) arene-E interactions compared to the (hard) O-E interaction.

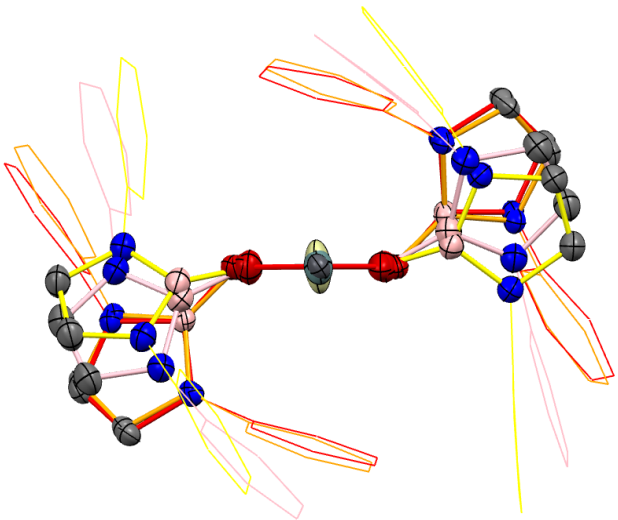
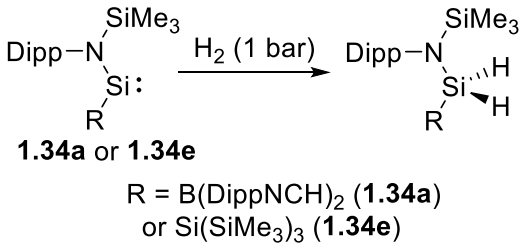


Figure 18 Superimposed structures of **3.3-Si** (yellow), **3.3-Ge** (pink), **3.3-Sn** (orange) and **3.3-Pb** (red)

3.5 Reactivity of a Bisboryloxysilylene: E–H Bond Activation (E = O or N)

Two-coordinate acyclic silylenes are known to activate E–H bonds in small molecules such as water, ammonia *etc*.[6e,5f,8] Dihydrogen activation by silylenes is, however, much rarer. To date, the only isolable silylene species that activate dihydrogen molecule are amidoborylsilylene (**1.34a**)[6a] and amidosilylsilylene (**1.34e**)[6c] (*Scheme 19*). As shown by theoretical calculations, the activation of dihydrogen by silylene likely happens in a



Scheme 19 H_2 activation by two-coordinate acyclic silylenes

concerted fashion and is therefore favored by systems having a small HOMO-LUMO gap (e.g. amidoborylsilylene 2.04 eV; amidosilylsilylene, 1.99 eV). H_2 cleavage relies on cooperative interactions between the H_2 σ bonding orbital and the formally vacant *p*π orbital at silicon, as well as 'back-bonding' from the σ lone pair at silicon to the H_2 σ* orbital.

To assess the capability for dihydrogen activation by the novel bisboryloxysilylene, a solution of **3.3-Si** was charged with 1 bar of hydrogen in a sealed NMR tube. However, no reaction was observed even at elevated temperature. DFT calculations imply that the lone pair for **3.3-Si** is actually the HOMO-2, with an energy gap between this orbital and the vacant *p*π orbital is 5.45 eV. This represents by far the largest energy gap

reported among two-coordinate acyclic silylenes, and therefore argues against the likelihood of concerted addition of dihydrogen at silicon.

Given the lack of reactivity between **3.3-Si** and dihydrogen, the activation of small molecules featuring more protic E–H bonds was investigated since previous computational and experimental studies have indicated an alternative coordination/proton shift mechanism for such substrates, which is more dependent on the LUMO energy of the silylene than the HOMO-LUMO gap.[9] Firstly, one equivalent of water was added to a solution of **3.3-Si**. Instantaneously a single new species was generated with accompanying disappearance of the ^{1}H-NMR signals due to both **3.3-Si** and water. In particular, a doublet was seen at 3.78 ppm, in the range typical of a silicon bound proton (*cf.* 3.92 ppm for (^{Me}IPrCH)Si*H*(CN){Si(SiMe$_3$)$_3$}[6f]), with a coupling constant $^{3}J_{HH}$ = 2.8 Hz, suggesting an H-H coupling with a proton three bonds away. The signal for the O–H proton was also identified as a singlet at 0.80 ppm. At the same time, ^{29}Si{^{1}H} NMR spectrum showed a new singlet at -74.5 ppm, consistent with a

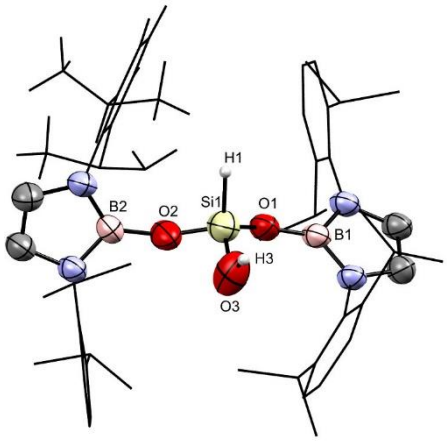
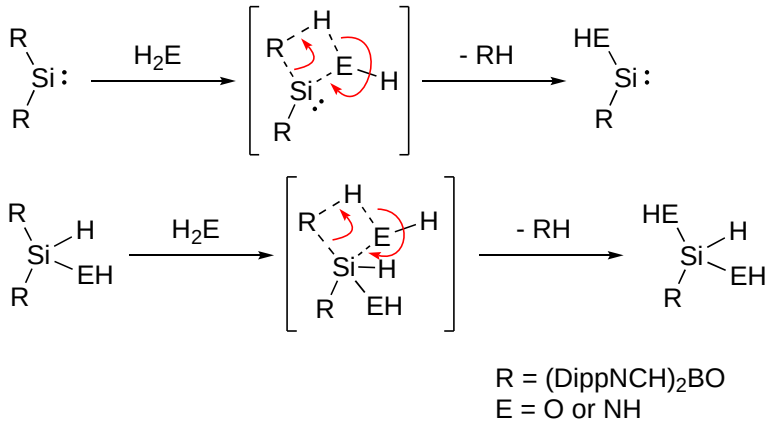


Figure 20 Molecular structure of **3.4-OH** with ellipsoids set at the 50% probability level (one out of two independent molecules in the asymmetric unit). For clarity, hydrogen atoms, except for Si–H and O–H, are omitted and the Dipp groups are simplified as wireframes. Selected bond lengths (Å) and bond angles: Si1–O1 1.609(5), Si1–O2 1.591(7), Si1–O3 1.61(1), O1–B1 1.37(1), O2–B2 1.40(1), Si1–H1 1.48(2), O3–H3 0.840, O1-Si1-O2 103.8(3)°, Si1-O1-B1 147.2(5)°, Si1-O2-B2 145.7(5)°, O3-Si1-H1 112.3(8)°, Si1-O3-H3 109°.

signal originates from a silicon(IV) centre (*cf.* -74.5 ppm for (^{Me}IPrCH)Si*H*(CN){Si(SiMe$_3$)$_3$}[6f]). Slow evaporation of solvent from a hexane solution yielded single crystals suitable for X-ray crystallography, which allowed identification of this species as the oxidative addition product **3.4-OH** on the basis of its solid-state structure (*Figure 20*). The structural features of **3.4-OH** largely resemble those of **3.3-Si**, especially around the central silicon atom. The Si–O$_B$ (mean 1.598(6) Å, *cf.* 1.6074(14) Å (mean), for **3.3-Si**) and B–O (mean 1.38(1) Å, *cf.* 1.374(2) Å (mean) for **3.3-Si**) bond lengths and O$_B$-Si-O$_B$ angle (mean 104.0(3)°, *cf.* 100.02(8)° (mean) for **3.3-Si**) are very similar to the precursor silylene **3.3-Si**. However, the Si-O-B angles (mean 139.9(1)° for **3.3-Si**, *cf.* 146.3(5)° (mean) for **3.4-OH**) differ by *ca.* 6°, presumably due to the increase of coordination number at the central silicon causing enhanced steric repulsion to the pendant boryl rings. The smaller Si(IV) center compared to Si(II) could also contribute to such an observation.

The unexpectedly high selectivity of this reaction towards **3.4-OH** and the stability of **3.4-OH** to further hydrolysis (protonated ligand is observed only when more than 10 equivalents of water are used) were further investigated using quantum chemical



Scheme 21 Possible side reactions of hydrolysis/amination of **3.3-Si**

calculations. In addition to O-H oxidative addition via a coordination/proton-shuttling pathway, the following alternatives were considered: (i) reaction of a water molecule with **3.3-Si** via a σ bond metathesis pathway, forming **3.1** and (boryloxy)hydroxysilylene, which can then undergo further reaction; (ii) after the formation of **3.4-OH**, further attack by excess water on one of the Si–O_B bonds, forming **3.1** and (boryloxy)dihydroxylsilane (*Scheme 21*). Since water molecules are known to form strong intermolecular hydrogen bonds, models including one or two molecules of water in the transition states were taken into consideration, as a transition state with a 5 or 6 membered ring (two water molecules) could potentially be energetically more favorable than those with a 3 or 4 membered ring (one water molecule). For the sake of computational efficiency, the Dipp group was simplified to phenyl.

As shown in *Figure 22*, the oxidative addition of water to **3.3-Si** forming **3.4-OH** is highly exergonic (ΔG^o = -178.7 kJ mol^{-1}), with an activation barrier of 48.6 kJ mol^{-1} (two water molecule transition state) or 137.2 kJ mol^{-1} (one water molecule transition state). Further hydrolysis is still exergonic (ΔG^o = -22.4 kJ mol^{-1}), however the activation barrier here is relatively high (115.4 kJ mol^{-1}) for a reaction occurring at ambient temperature. On the other hand, σ-bond metathesis at the Si(II) stage is essentially isogonic (ΔG^o = -7.8 kJ mol^{-1}) with a relatively flat potential energy surface along the reaction pathway ($\Delta G^{\ddagger}$ = 3.2 kJ mol^{-1}). As such, this process - although facile - could be considered reversible. The computational results are therefore consistent with experimental observations, with the observed product being formed in essentially irreversible fashion and lying at the bottom of a significant potential well.

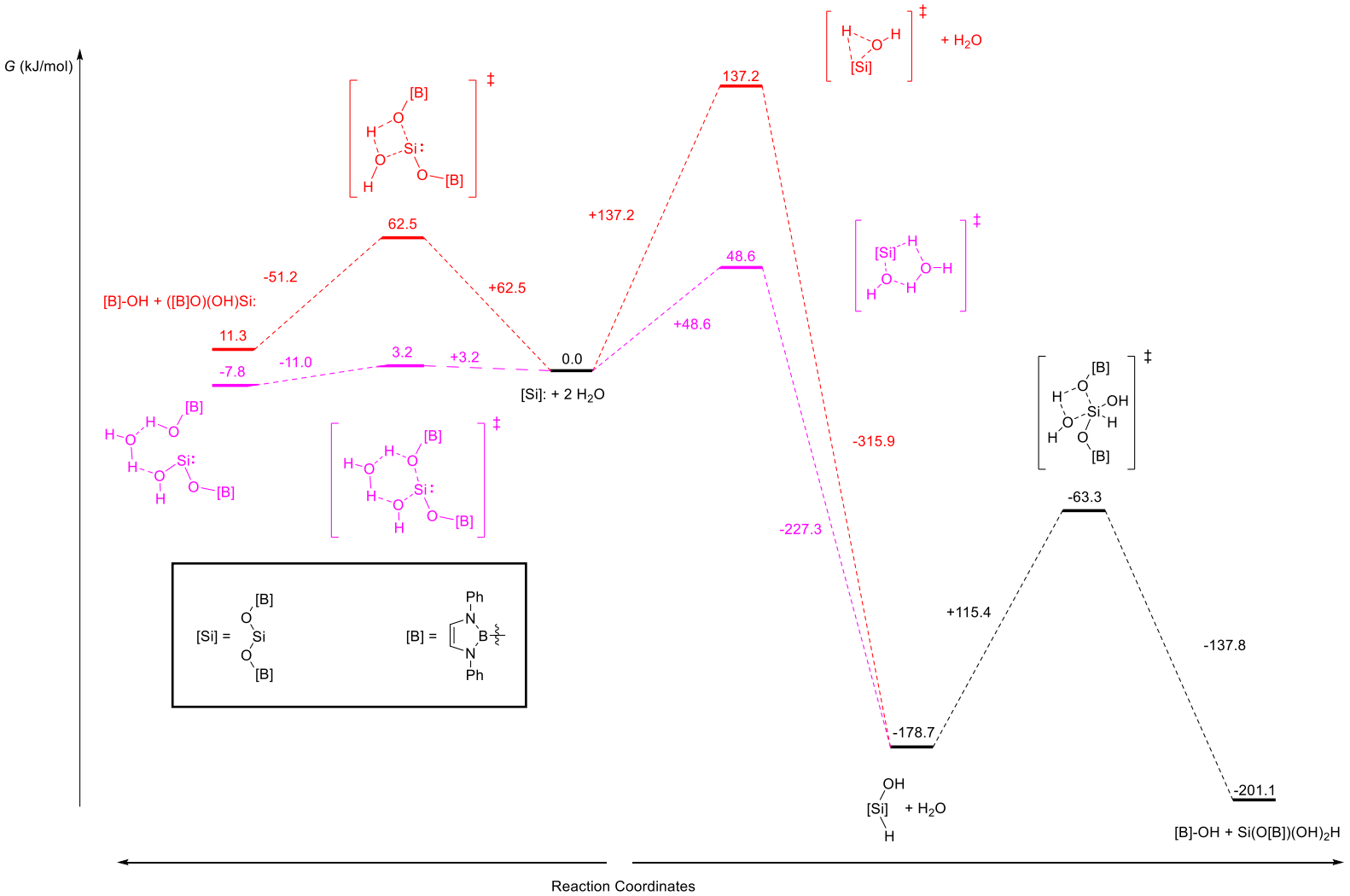
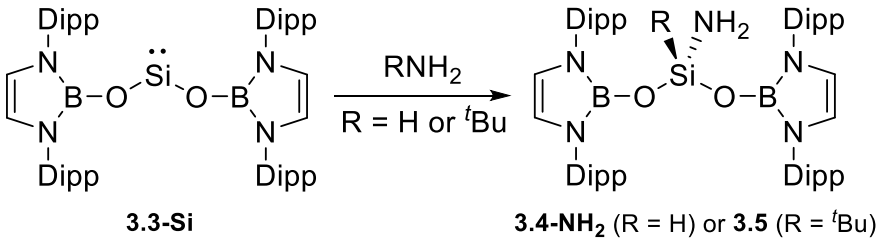


Figure 22 Energy diagram showing potential hydrolysis pathways for **3.3-Si**

In similar fashion N–H bond activation by **3.3-Si** was also investigated. A solution of **3.3-Si** was charged with either 1 bar of ammonia or one equivalent of *tert*-butyl amine. Both reactions proceeded cleanly, generating a single new product each case (**3.4-NH$_2$** and **3.5** respectively, *Scheme 23*). As with the reaction with water, the ^{1}H-NMR spectra measured in situ for the reactions with these amines showed a triplet at 4.24 ppm (**3.4-NH$_2$**) or a doublet at 4.18 ppm (**3.5**), which correspond to the Si–H proton; as well as singlets at -0.45 ppm (**3.4-NH$_2$**) or 0.24 ppm (**3.5**), which correspond to the N–H proton. The ^{29}Si{^{1}H} NMR spectra also showed singlets at -62.8 ppm (**3.4-NH$_2$**) and -67.7 ppm (**3.5**), in the range typical for a silicon(IV) centres. The formation of **3.4-NH$_2$** is further



Scheme 23 Synthesis of **3.4-NH$_2$** and **3.5**

confirmed by X-ray crystallography (*Figure 24*). When compared with the structural parameters of **3.4-OH**, the Si–O bond distances (mean 1.621(2) Å, *cf.* 1.598(6) Å (mean), for **3.4-OH**) of **3.4-NH$_2$** are elongated by *ca.* 0.02 Å while the O–B distances (mean 1.362(3) Å, *cf.* 1.38(1) Å (mean) for **3.4-OH**) shortened by ca. 0.02 Å. On the other hand, the O-Si-O angle (106.4(3)°, *cf.* 104.0(3)° (mean) for **3.3-Si**) for **3.4-NH$_2$** is ca. 2° wider than that measured for **3.4-OH**.

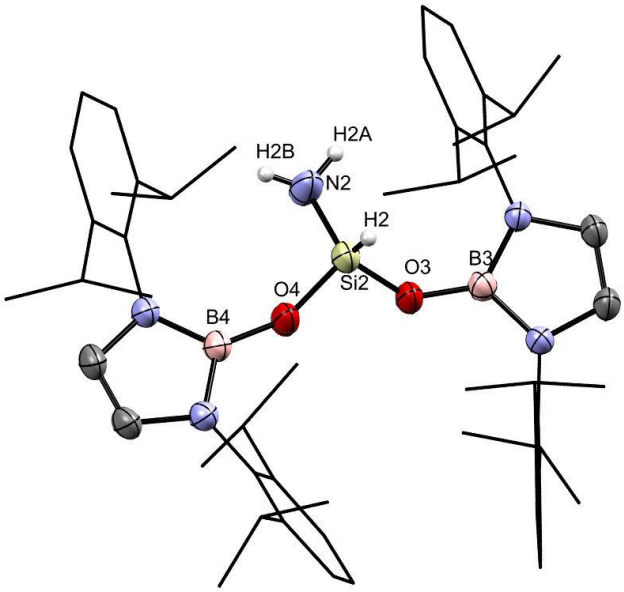


Figure 24 Molecular structure of **3.4-NH$_2$** with ellipsoids set at the 50% probability level (one out of two independent molecules in the asymmetric unit). For clarity, hydrogen atoms, except for Si–H and O–H, are omitted and the Dipp groups are simplified as wireframes. Selected bond lengths (Å) and bond angles: Si2–O3 1.652(3), Si2–O4 1.590(2), Si2–N2 1.676(3), O3–B3 1.362(3), O4–B4 1.361(3), O3-Si2-O4 106.4(1)°, Si2-O3-B3 136.1(2)°, Si2-O4-B4 156.0(2)°, N2-Si2-H2 110.7°.

Mechanistic studies of the ammonia activation process(es) were carried out using quantum chemical calculations, with similar decomposition/side reaction pathways being taken into consideration (*Scheme 21*, *Figure 25*). The formal oxidative addition process is (in similar fashion to the reaction with water) highly exergonic (ΔG^o = -109.8 kJ mol^{-1}). Comparatively speaking, the activation barrier is higher for the ammonia activation ($\Delta G^{\ddagger}$ = 75.7 kJ mol^{-1}), even using the more energetically favorable two ammonia molecules model. However, a barrier of this magnitude is still considered achievable at ambient temperature. Both metathesis processes on the other hand, are endogonic in this case. One possible explanation of this is that the metathesis processes involve the cleavage of a (strong) Si–O single bond and the formation of a (weaker) Si–N bond and are therefore not favourable. Again, the computational results are in good agreement with the experimental observations.

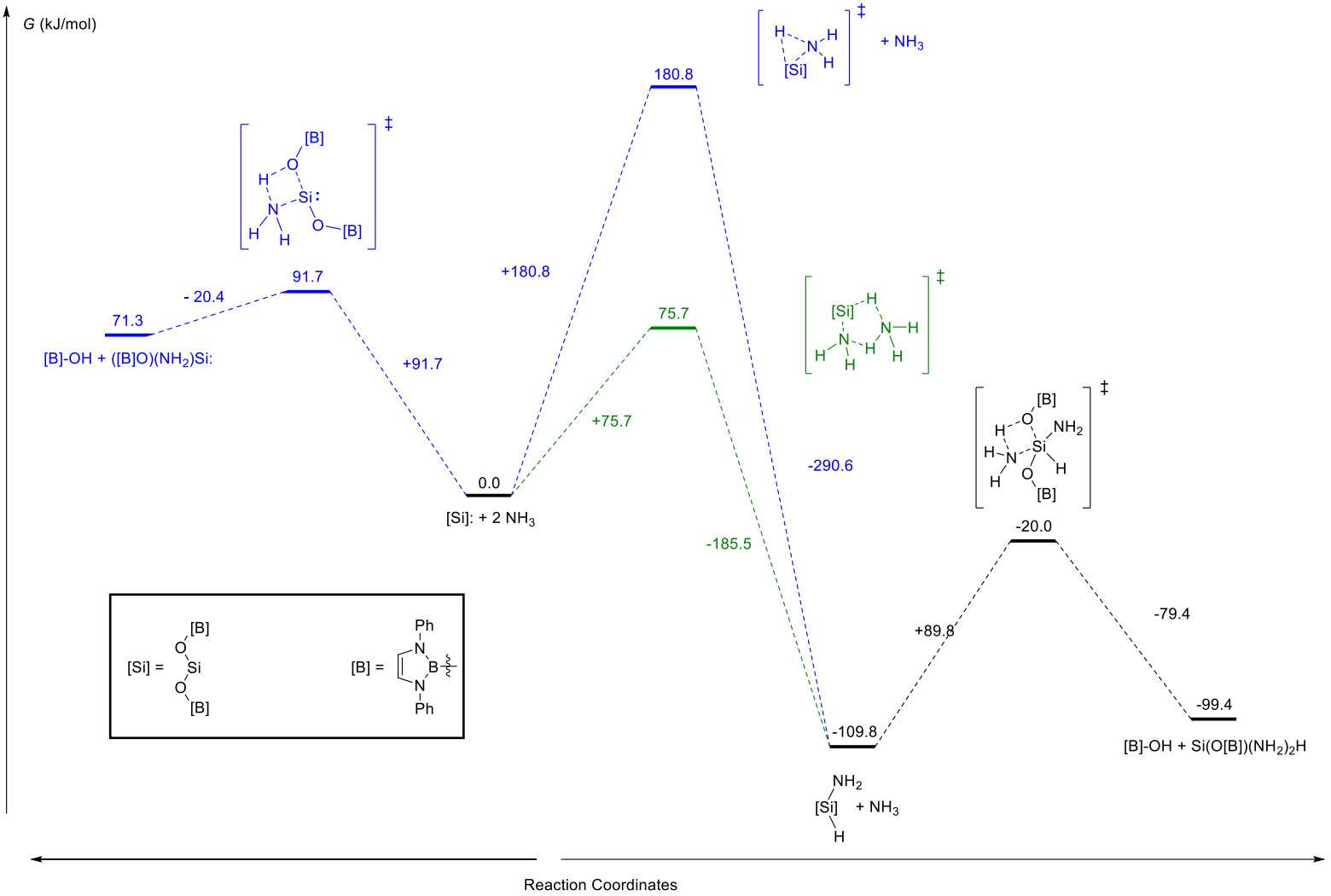


Figure 25 Energy diagram showing potential amination pathways for **3.3-Si**

3.6 Conclusions

Theoretical calculations showed in detail how the electronic properties of various oxygen-based ligands vary as a function of the ancillary substituent. Having the highest HOMO and HOMO-1 energy among boryloxy systems, the NHBO family was chosen to support a homoleptic acyclic silylene. Bis(boryloxy)silylene **3.3-Si** was successfully synthesized by reducing a silicon(IV) precursor **3.2-I** (((DippNCH)$_2$BO)$_2$SiI$_2$) using Jones' reagent. X-ray crystallography and DFT calculations enabled an in-depth study of the structural and electronic features of **3.3-Si**, as well as its heavier congeners: key bond lengths and bond angles revealed by crystallography revealed a number of systematic changes on descending group 14, consistent with periodic trends; DFT calculations shows a decrease of *p* character in the lone pair of the central E element and an increase in the of Wiberg bond indices of the B–O bonds, from **3.3-Si** to **3.3-Pb**. Preliminary reactivity studies of **3.3-Si** revealed its capabilities to activate protic E–H bonds (E = N or O). On the other hand, **3.3-Si** was not able to activate the non-polar H–H bond, due to the large energy gap between the filled σ_{nSi} and empty $p\pi_{Si}$ orbitals.

3.7 Experimental Details

General considerations

All manipulations were carried out under an inert atmosphere of argon or dinitrogen using standard Schlenk line technique or glovebox techniques. Solvents were degassed by sparging with argon and dried by passing through a column of appropriate drying

agent. NMR samples were prepared under dinitrogen in 5 mm Wilmad 507-PP tubes fitted with J-Young Teflon valve. NMR spectra were measured in benzene-d_6 which was dried over CaH_2, distilled and stored over activated 3Å molecular sieves. All NMR spectra were recorded on Bruker Avance III HD nanobay 400 MHz or Bruker Avance 500 MHz equipped with a ^{13}C detect cryoprobe at ambient temperature. ^{1}H and ^{13}C resonances were referenced internally with residual protio solvent (^{1}H) or solvent (^{13}C) resonances and were reported relative to tetramethylsilane ($\delta = 0$ ppm). ^{11}B resonances were referenced externally to $BF_3.Et_2O$. ^{29}Si resonances were referenced externally to tetramethylsilane. Assignments were confirmed using two-dimensional ^{1}H-^{1}H and ^{1}H-^{13}C correlation NMR experiments. Chemical shifts were quoted in δ (ppm) and coupling constants in Hz. Elemental analyses were carried out by Devon Microanalytical. $KN(SiMe_3)_2$ was synthesized by deprotonation of $HN(SiMe_3)_2$ with KH in toluene. $(DippNCH)_2BBr$,[10] Jones' reagent,[5b] and PPh_3CH_2[11] were synthesized by literature procedures. All other reagents were purchased from Sigma Aldrich or Alfa Aesar and stored under an inert atmosphere (argon or nitrogen) prior to use.

All calculations were performed using Density Functional Theory within the Gaussian09 (Revision A.02) program.[12] Geometry optimizations for monoanionic ligands were carried out using the PBE1PBE/SVP[13-14] level of theory; all other geometry optimizations were performed at the PBE1PBE/TZVP[13,15] level for light elements and Def2-TZVP[16] basis set with relativistic large core ECP[17] for heavy elements (Sn, Pb). Grimme's empirical dispersion correction (DFT-D3)[18] was included in all geometry optimizations. Due to the size of the system, mechanistic studies of

hydrolysis and amination of **3.3-Si** were performed on reduced systems (with Dipp groups replaced by Ph groups). Frequency calculations were performed to verify the nature of stationary points (zero imaginary frequency for minimum; one imaginary frequency for transition state). Intrinsic reaction coordinate calculations were performed on all optimized transition states to verify their nature.

Modified synthesis of $(DippNCH)_2BOH$ (**3.1**)

In a Schlenk tube $(DippNCH)_2BBr$ (3.0 g, 6.4 mmol) was dissolved in toluene (25 mL) and subsequently water (25 mL) and pyridine (3 mL) were added. The mixture was stirred at ambient temperature overnight. The layers were then separated, and the organic layer dried over anhydrous magnesium sulphate and filtered. The solvent was removed *in vacuo* yielding a pale yellow solid as $(DippNCH)_2BOH$ (1.7 g, 4.2 mmol, 66%). The spectroscopic data matched with the previously reported literature values.[4a]

Synthesis of $(DippNCH)_2BOLi$ (**3.1-Li**)

A mixture of **3.1** (1.0 g, 2.5 mmol) and $LiN(SiMe_3)_2$ (0.41 g, 2.5 mmol) was dissolved in toluene (10 mL), and the reaction mixture stirred at ambient temperature overnight. Volatiles were removed *in vacuo* resulting **3.1-Li** as a yellow solid which was used without further purification (0.98 g, 2.5 mmol, 97%). ^1H NMR (C_6D_6, 400 MHz, 298 K): δ = 1.12 (d, 12H, CHC*H*$_3$, *J* = 6.9 Hz), 1.20 (d, 12H, CHC*H*$_3$, *J* = 6.9 Hz), 3.36 (sept, 4H, C*H*CH$_3$, *J* = 6.9 Hz), 5.99 (s, 2H, C*H*=C*H*), 7.06-7.08 (m, 6H, Ar-*H*); $^{13}C\{^1H\}$ NMR (C_6D_6, 101 MHz, 298 K): δ = 23.8 (s, CH*C*H$_3$), 24.0 (s, CH*C*H$_3$), 28.1 (s, *C*HCH$_3$), 114.5 (s, *C*H=*C*H), 123.4 (s, *m*-*C*$_6$H$_3$), 126.5 (s, *p*-*C*$_6$H$_3$), 140.0 (s, *ipso*-*C*$_6$H$_3$), 147.2 (s, *o*-*C*$_6$H$_3$); $^{11}B\{^1H\}$ NMR (C_6D_6, 128 MHz, 298 K): δ = 21.6 (br, *B*-O-Li).

Synthesis of $(DippNCH)_2BOK$ (**3.1-K**)

In a Schlenk tube a mixture of **3.1** (3.0 g, 7.4 mmol) and $KN(SiMe_3)_2$ (1.5 g, 7.4 mmol) was dissolved in toluene (20 mL). The mixture was stirred at ambient temperature for 5 min. Volatiles were removed *in vacuo* resulting in **3.1-K** a pale yellow solid which was used without further purification (3.1 g, 7.0 mmol, 95%). ^{1}H NMR (C_6D_6, 400 MHz, 298 K): δ = 1.16 (d, 12H, CHC*H*$_3$, *J* = 6.9 Hz), 1.26 (d, 12H, CHC*H*$_3$, *J* = 6.9 Hz), 3.62 (sept, 4H, C*H*CH$_3$, *J* = 6.9 Hz), 6.03 (s, 2H, C*H*=C*H*), 7.04-7.10 (m, 6H, Ar-*H*); ^{13}C{^{1}H} NMR (C_6D_6, 101 MHz, 298 K): δ = 24.0 (s, CH*C*H$_3$), 24.2 (s, CH*C*H$_3$), 28.4 (s, *C*HCH$_3$), 115.0 (s, *C*H=*C*H), 123.2 (s, *m*-*C*$_6$H$_3$), 126.1 (s, *p*-*C*$_6$H$_3$), 143.4 (br, *ipso*-*C*$_6$H$_3$), 148.0 (s, *o*-*C*$_6$H$_3$); ^{11}B{^{1}H} NMR (C_6D_6, 128 MHz, 298 K): δ = 22.0 (br, *B*-O-K).

Synthesis of $((DippNCH)_2BO)_2SiCl_2$ (**3.2-Cl**)

3.1-K (1.0 g, 2.3 mmol) was dissolved in benzene (20 mL), and neat $SiCl_4$ (0.26 mL, 2.3 mmol) added dropwise. The reaction mixture was stirred at room temperature overnight, whereupon volatiles were removed *in vacuo* resulting in **3.2-Cl** an off-white solid (1.60 g, 1.8mmol, 77%). ^{1}H NMR (C_6D_6, 400 MHz, 298 K): δ = 1.14 (d, 12H, CHC*H*$_3$, *J* = 6.9 Hz), 1.17 (d, 12H, CHC*H*$_3$, *J* = 6.9 Hz), 3.16 (sept, 4H, C*H*CH$_3$, *J* = 6.9 Hz), 5.87 (s, 2H, C*H*=C*H*), 7.06-7.08 (m, 8H, Ar-*H*), 7.18-7.20 (m, 4H, Ar-*H*); ^{11}B{^{1}H} NMR (C_6D_6, 128 MHz, 298 K): δ = 18.9 (br, *B*-O-Si). ^{29}Si{^{1}H} NMR (C_6D_6, 80 MHz, 298 K): δ = -21.8 (s, central *Si*).

Synthesis of $((DippNCH)_2BO)_2SiI_2$ (**3.2-I**)

A mixture of **3.1-K** (1.0 g, 2.3 mmol) and SiI_4 (0.6 g, 1.1 mmol) was dissolved in benzene (10 mL) and the solution was stirred for 5 min. Volatiles were removed *in vacuo* and the residue was extracted into cold pentane and filtered. The solvent was removed *in vacuo* yielding **3.2-I** as an off-white solid (1.1 g, 1.0 mmol, 89%). The crude product was used without further purification. ^{1}H NMR (C_6D_6, 400 MHz, 298 K): δ = 1.18 (t, 48H, CH-C*H*$_3$, *J* = 8.1 Hz), 3.22 (sept, 8H, C*H*-CH$_3$, *J* = 6.7 Hz), 5.90 (s, 4H, C*H*=C*H*), 7.08-7.10 (m, 8H, Ar-*H*), 7.18-7.22 (m, 4H, Ar-*H*); ^{13}C{^{1}H} NMR (C_6D_6, 101 MHz, 298 K): δ = 24.2 (s, CH*C*H$_3$), 25.6 (s, CH*C*H$_3$), 28.7 (s, *C*HCH$_3$), 118.0 (s, *C*H=*C*H), 123.9 (s, *m*-*C*$_6$H$_3$), 127.9 (s, *p*-*C*$_6$H$_3$), 138.1 (s, *i*-*C*$_6$H$_3$), 146.7 (s, *o*-*C*$_6$H$_3$); ^{11}B{^{1}H} NMR (C_6D_6, 128 MHz, 298 K): δ = 19.4 (br, *B*-O-Si); ^{29}Si{^{1}H} NMR (C_6D_6, 80 MHz, 298 K): δ = -167.6 (s, central *Si*).

Synthesis of ((DippNCH)$_2$BO)$_2$Si (**3.3-Si**)

In a sealed ampoule a mixture of **3.2-I** (0.37 g, 0.34 mmol) and (^{Mes}NacnacMg)$_2$ (0.36 g, 0.51 mmol) was dissolved in benzene (10 mL) and the reaction mixture stirred at 80 °C overnight. The mixture was cooled to room temperature and volatiles removed *in vacuo*. The residue was extracted into cold pentane and filtered. Colorless crystals of **3.3-Si** were obtained by slowly evaporating pentane solvent at room temperature (0.25 g, 0.30 mmol, 87%). ^{1}H NMR (C_6D_6, 400 MHz, 298 K): δ = 1.05 (d, 24H, CH-C*H*$_3$, *J* = 6.7 Hz), 1.18 (d, 24H, CH-C*H*$_3$, *J* = 6.6 Hz), 3.15 (sept, 8H, C*H*-CH$_3$, *J* = 6.7 Hz), 5.9 (s, 4H, C*H*=C*H*), 7.08-7.10 (m, 8H, Ar-*H*), 7.18-7.23 (m, 4H, Ar-*H*); ^{13}C{^{1}H} NMR (C_6D_6, 101 MHz, 298 K): δ = 24.0 (s, CH*C*H$_3$), 24.5 (s, CH*C*H$_3$), 28.7 (s, *C*HCH$_3$), 116.6 (s, *C*H=*C*H), 123.6 (s, *m*-*C*$_6$H$_3$), 127.7 (s, *p*-*C*$_6$H$_3$), 137.5 (s, *i*-*C*$_6$H$_3$), 146.8 (s, *o*-

C_6H_3); $^{11}B\{^1H\}$ NMR (C_6D_6, 128 MHz, 298 K): δ = 20.2 (br, *B*-O-Si); $^{29}Si\{^1H\}$ NMR (C_6D_6, 80 MHz, 298 K): δ = 35.5 (s, central *Si*). Anal. calc. for $C_{52}H_{72}B_2N_4O_2Si$: C 74.81%, H 8.69%, N 6.71%, found: C 74.60%, H 8.90%, N 6.54%.

Synthesis of $((DippNCH)_2BO)_2SiH(OH)$ (**3.4-OH**)

3.3-Si (15 mg, 0.018 mmol) was dissolved in hexane (1 mL) and a saturated solution of water in benzene (0.5 mL, 0.035 M) was added. The mixture was stirred for 10 min at room temperature. Volatiles were removed *in vacuo* yielding **3.4-OH** as a white solid (10 mg, 0.012 mmol, 65%). Single crystals suitable for X-ray crystallography were obtained by slowly evaporating a hexane solution of **3.4-OH** at ambient temperature. ^1H NMR (C_6D_6, 400 MHz, 298 K): δ = 0.80 (d, 1H, Si-OH, *J* = 2.9 Hz), 1.08 (d, 12H, CH-C*H*$_3$, *J* = 7.0 Hz), 1.10 (d, 12H, CH-C*H*$_3$, *J* = 7.0 Hz), 1.17 (d, 24H, CH-C*H*$_3$, *J* = 6.9 Hz), 3.17 (two overlapping sept, 8H, C*H*-CH$_3$, *J* = 7.0 Hz), 3.78 (d, 1H, Si-*H*, *J* = 2.9 Hz), 5.86 (s, 4H, C*H*=C*H*), 7.08-7.10 (m, 8H, Ar-*H*), 7.18-7.20 (m, 4H, Ar-*H*); $^{13}C\{^1H\}$ NMR (C_6D_6, 101 MHz, 298 K): δ = 23.3 (s, CH*C*H$_3$), 23.4 (s, CH*C*H$_3$), 24.1 (s, CH*C*H$_3$), 28.3 (s, *C*HCH$_3$), 116.3 (s, *C*H=*C*H), 123.2 (s, *m*-*C*$_6$H$_3$), 127.3 (s, *p*-*C*$_6$H$_3$), 137.6 (s, *i*-*C*$_6$H$_3$), 146.4 (s, *o*-*C*$_6$H$_3$), 146.5 (s, *o*-*C*$_6$H$_3$); $^{11}B\{^1H\}$ NMR (C_6D_6, 128 MHz, 298 K): δ = 19.4 (s, *B*-O-Si); $^{29}Si\{^1H\}$ NMR (C_6D_6, 80 MHz, 298 K): δ = -74.5 (s, central *Si*).

NMR-scale synthesis of $((DippNCH)_2BO)_2SiH(NH_2)$ (**3.4-NH$_2$**)

In an NMR tube with a J-Young valve, a sample of **3.3-Si** (10 mg, 0.012 mmol) was dissolved in C_6D_6 (0.4 mL). The tube was degassed and refilled with NH_3 (~1 atm). The tube was hand shaken for 10 min, whereupon multinuclear NMR spectroscopy showed

100% conversion to **3.4-NH$_2$**. ^{1}H NMR (C_6D_6, 500 MHz, 298 K): δ = -0.45 (br, 2H, N*H*$_2$), 1.10 (two overlapping d, 24H, CH-C*H*$_3$), 1.18 (two overlapping d, 24H, CH-C*H*$_3$), 3.20 (two overlapping sept, 8H, C*H*-CH$_3$), 4.24 (t, 1H, Si-*H*, *J* = 1.6 Hz), 5.86 (s, 4H, C*H*=C*H*), 7.05-7.09 (m, 9H, Ar-*H*), 7.14-7.18 (m, 3H, Ar-*H*); ^{13}C{^{1}H} NMR (C_6D_6, 126 MHz, 298 K): δ = 23.7 (s, CH*C*H$_3$), 23.9 (s, CH*C*H$_3$), 24.5 (s, CH*C*H$_3$), 28.7 (s, *C*HCH$_3$), 116.7 (s, *C*H=*C*H), 123.5 (s, *m*-*C*$_6$H$_3$), 123.6 (s, *m*-*C*$_6$H$_3$), 127.5 (s, *p*-*C*$_6$H$_3$), 138.2 (s, *i*-*C*$_6$H$_3$), 146.9 (s, *o*-*C*$_6$H$_3$); ^{11}B{^{1}H} NMR (C_6D_6, 128 MHz, 298 K): δ = 19.4 (s, *B*-O-Si); ^{29}Si{^{1}H} NMR (C_6D_6, 80 MHz, 298 K): δ = -62.8 (s, central *Si*).

Synthesis of ((DippNCH)$_2$BO)$_2$SiH(^{t}BuNH) (**3.5**)

In a Schlenk tube a sample of **3.3-Si** (26 mg, 0.03 mmol) was dissolved in hexane (1 mL). To the solution neat *tert*-butyl amine (0.0033 ml, 0.03 mmol) was added. The solvent was then dried *in vacuo* yielding **3.5** as a white solid (10 mg, 0.014 mmol, 48%). ^{1}H NMR (C_6D_6, 400 MHz, 298 K): δ = 0.24 (s, 2H, N*H*$_2$), 0.82 (s, 9H, C(C*H*$_3$)$_3$), 1.12 (d, 12H, CH-C*H*$_3$, *J* = 6.9 Hz), 1.15 (d, 12H, CH-C*H*$_3$, *J* = 7.0 Hz), 1.18 (two overlapping d, 24H, CH-C*H*$_3$, *J* = 6.8 Hz), 3.27 (sept, 4H, C*H*-CH$_3$, *J* = 6.9 Hz), 4.18 (d, 1H, Si-*H*, *J* = 2.1 Hz), 5.90 (s, 4H, C*H*=C*H*), 7.10-7.14 (m, 4H, Ar-*H*), 7.18-7.23 (m, 8H, Ar-*H*); ^{13}C{^{1}H} NMR (C_6D_6, 101 MHz, 298 K): δ = 23.0 (s, CH*C*H$_3$), 23.4 (s, CH*C*H$_3$), 24.7 (s, CH*C*H$_3$), 25.0 (s, CH*C*H$_3$), 28.2 (s, *C*HCH$_3$), 28.2 (s, *C*HCH$_3$), 32.9 (s, C(*C*H$_3$)$_3$), 47.8 (s, *C*(CH$_3$)$_3$), 117.0 (s, *C*H=*C*H), 123.3 (s, *m*-*C*$_6$H$_3$), 123.5 (s, *m*-*C*$_6$H$_3$), 127.0 (s, *p*-*C*$_6$H$_3$), 138.4 (s, *i*-*C*$_6$H$_3$), 146.0 (s, *o*-*C*$_6$H$_3$), 146.1 (s, *o*-*C*$_6$H$_3$); ^{11}B{^{1}H} NMR (C_6D_6, 128 MHz, 298 K): δ = 19.1 (s, *B*-O-Si); ^{29}Si{^{1}H} NMR (C_6D_6, 80 MHz, 298 K): δ = -67.7 (s, central *Si*).

3.8 References

1. For reviews on NHI complexes: (a) T. Ochiai, D. Franz, S. Inoue, *Chem. Soc. Rev*. **2016**, *45*, 6327-6344; (b) X. Wu, M. Tamm, *Coord. Chem. Rev*. **2014**, *260*, 116-138.
2. For NHI stabilized main group systems: for group 13 elements: (a) N. Kuhn, R. Fawzi, M. Steinmann, J. Wiethoff, *Z. Anorg. Allg. Chem*. **1997**, *623*, 554-560; (b) D. Franz, E. Irran, S. Inoue, *Angew. Chem. Int. Ed*. **2014**, *53*, 14264-14268; (c) D. Franz, E. Irran, S. Inoue, *Dalton Trans*. **2014**, *43*, 4451-4461; (d) D. Franz, T. Szilvási, E. Irran, S. Inoue, *Nat. Commun*. **2015**, *6*, 1-6; (e) A. Todd, W. McClennan, J. Masuda, *RSC Adv*. **2016**, *6*, 69720-69726; (f) M. W. Lui, N. R. Paisley, R. McDonald, M. J. Ferguson, E. Rivard, *Chem. Eur. J*. **2016**, *22*, 2134-2145; (g) H. Liu, M. Khononov, N. Fridman, M. Tamm, M. S. Eisen, *Inorg. Chem*. **2019**, *58*, 13426-13439; (h) D. Franz, T. Szilvási, A. Pöthig, S. Inoue, *Chem. Eur. J*. **2019**, *25*, 11036-11041; for group 14 elements: (i) S. Inoue, K. Leszczyńska, *Angew. Chem. Int. Ed*. **2012**, *51*, 8589-8593; (j) T. Ochiai, D. Franz, E. Irran, S. Inoue, *Chem. Eur. J*. **2015**, *21*, 6704-6707; (k) M. W. Lui, C. Merten, M. J. Ferguson, R. McDonald, Y. Xu, E. Rivard, *Inorg. Chem*. **2015**, *54*, 2040-2049; (l) T. Ochiai, D. Franz, X. Wu, E. Irran, S. Inoue, *Angew. Chem. Int. Ed*. **2016**, *55*, 6983-6987; (m) T. Ochiai, T. Szilvási, D. Franz, E. Irran, S. Inoue, *Angew. Chem. Int. Ed*. **2016**, *55*, 11619-11624; (n) D. Wendel, T. Szilvási, C. Jandl, S. Inoue, R. Bernhard, *J. Am. Chem. Soc*. **2017**, *139*, 9156-9159; (o) T. Ochiai, S. Inoue, *RSC Adv*. **2017**, *7*, 801-804; (p) D. Wendel, A. Porzelt, F. A. D. Herz, D. Sarkar, C. Jandl, S. Inoue, B. Rieger, *J. Am. Chem. Soc*. **2017**, *139*, 8134-8137; (q) D. Wendel, D. Reiter, A. Porzelt, P. J. Altmann, S. Inoue, B. Rieger, *J. Am. Chem. Soc*. **2017**, *139*, 17193-17198; for group 15 elements: (r) R. Kinjo, B. Donnadieu, G. Bertrand, *Angew. Chem. Int. Ed*. **2010**, *49*, 5930-5933; (s) O. Back, B. Donnadieu, M. von Hopffgarten, S. Klein, R. Tonner, G. Frenking, G. Bertrand, *Chem. Sci*. **2011**, *2*, 858-861; (t) F. Dielmann, O. Black, M. Henry-Ellinger, P. Jerabek, G. Frenking, G. Bertrand, *Science*, **2012**, *337*, 1526-1528; (u) F. Dielmann, C. Moore, A. Rheingold, G. Bertrand, *J. Am. Chem. Soc*. **2013**, *135*, 14071-14073; (v) Y. Loh, C. Gurnani, R. Ganguly, D. Vidović, *Inorg. Chem*. **2015**, *54*, 3087-3089; (w) F. Buß, P. Mehlmann, C. Mück-Lichtenfeld, K. Bergander, F. Dielmann, *J. Am. Chem. Soc*. **2016**, *138*, 1840-1843; (x) P. Mehlmann, C. Mück-**Li**chtenfeld, T. T. Y. Tan, F. Dielmann, *Chem. Eur. J*. **2017**, *23*, 5929-5933; (y) M. Wünsche, T. Witteler, F. Dielmann, *Angew. Chem. Int. Ed*. **2018**, *57*, 7234-7239; (z) P. Mehlmann, T. Witteler, L. Wilm, F. Dielmann, *Nat. Chem*. **2019**, *11*, 1139-1143.
3. For selected examples: (a) A. P. Shreve, R. Mulhaupt, W. Fultz, J. Calabrese, W. Robbins, S. D. Ittel, *Organometallics*, **1988**, *7*, 409-416; (b) I. J. Casely, J. W. Ziller, M. Fang, F. Furche, W. J. Evans, *J. Am. Chem. Soc*. **2011**, *133*, 5244-5247; A. Someşan, E. L. Coz, T. Roisnel, C. Silvestru, Y. Sarazin, *Chem. Commun*, **2018**, *54*, 5299-5302.
4. For synthesis and mechanistic study of NHBO: (a) Y. Segawa, Y. Suzuki, M. Yamashita, K. Nozaki, *J. Am. Chem. Soc*. **2008**, *130*, 16069-16079; (b) H. Kisu, H. Sakaino, F. Ito, M. Yamashita, K. Nozaki, *J. Am. Chem. Soc*. **2016**, *138*, 3548-3552.

5. (a) S. Green, C. Jones, A. Starsch, *Science*, **2007**, *318*, 1754-1757; (b) S. Bonyhady, C. Jones, S. Nembenna, A. Starsch, A. J. Edwards, G. J. McIntyre, *Chem. Eur. J*. **2010**, *16*, 938-955; (c) C. Jones, *Nat. Rev. Chem*. **2017**, *1*, 1-9.
6. For structurally characterized two-coordinate acyclic silylenes: (a) A. V. Protchenko, K. H. Birjkumar, D. Dange, A. D. Schwarz, D. Vidovic, C. Jones, N. Kaltsoyannis, P. Mountford, S. Aldridge, *J. Am. Chem. Soc*. **2012**, *134*, 6500-6503; (b) B. D. Rekken, T. M. Brown, J. C. Fettinger, H. M. Tuononen, P. P. Power, *J. Am. Chem. Soc*. **2012**, *137*, 6504-6507; (c) A. V. Protchenko, A. D. Schwarz, M. P. Blake, C. Jones, N. Kaltsoyannis, P. Mountford, S. Aldridge, *Angew. Chem. Int. Ed*. **2013**, *52*, 568-571; (d) B. D. Rekken, T. M. Brown, J. C. Fettinger, F. Lips, H. M. Tuononen, R. H. Herber, P. P. Power, *J. Am. Chem. Soc*. **2013**, *135*, 10134-10148; (e) T. J. Headington, J. A. B. Abdalla, R. Tirfoin, S. Aldridge, C. Jones, *Chem. Comm*. **2016**, *52*, 1717-1720; (f) M. M. D. Roy, M. J. Ferguson, R. McDonald, Y. Zhou, E. Rivard, *Chem. Sci.* **2019**, *10*, 6476-6481.
7. H. A. Bent, *Chem. Rev*. **1961**, *61*, 275-311.
8. A. V. Protchenko, J. I. Bates, L. M. A. Saleh, M. P. Blake, A. D. Schwarz, E. L. Kolychev, A. L. Thompson, C. Jones, P. Mountford, S. Aldridge, *J. Am. Chem. Soc*. **2016**, *138*, 4555-4564.
9. M. Alberto, N. Russo, E. Sicilia, *Chem. Eur. J*. **2013**, *19*, 7835-7846.
10. D. Hermanndörfer, M. Kaaz, O. Puntigam, J. Bender, M. Nieger, D. Gudat, *Eur. J. Inorg. Chem*. **2015**, 4819-4828.
11. H. J. Bestmann, W. Stransky, O. Vostrowsky, *Chem. Ber*. **1976**, *109*, 1694-1700.
12. Gaussian 09, Revision A.02, M. J. Frisch, G. W. Trucks, H. B. Schlegel, G. E. Scuseria, M. A. Robb, J. R. Cheeseman, G. Scalmani, V. Barone, B. Mennucci, G. A. Petersson, H. Nakatsuji, M. Caricato, X. Li, H. P. Hratchian, A. F. Izmaylov, J. Bloino, G. Zheng, J. L. Sonnenberg, M. Hada, M. Ehara, K. Toyota, R. Fukuda, J. Hasegawa, M. Ishida, T. Nakajima, Y. Honda, O. Kitao, H. Nakai, T. Vreven, J. A. Montgomery, Jr., J. E. Peralta, F. Ogliaro, M. Bearpark, J. J. Heyd, E. Brothers, K. N. Kudin, V. N. Staroverov, R. Kobayashi, J. Normand, K. Raghavachari, A. Rendell, J. C. Burant, S. S. Iyengar, J. Tomasi, M. Cossi, N. Rega, J. M. Millam, M. Klene, J. E. Knox, J. B. Cross, V. Bakken, C. Adamo, J. Jaramillo, R. Gomperts, R. E. Stratmann, O. Yazyev, A. J. Austin, R. Cammi, C. Pomelli, J. W. Ochterski, R. L. Martin, K. Morokuma, V. G. Zakrzewski, G. A. Voth, P. Salvador, J. J. Dannenberg, S. Dapprich, A. D. Daniels, O. Farkas, J. B. Foresman, J. V. Ortiz, J. Cioslowski, and D. J. Fox, Gaussian, Inc., Wallingford CT, 2009.
13. (a) M. Ernzerhof, G. E. Scuseria, *J. Chem. Phys*. **1999**, *110*, 5029-5036; (b) C. Adamo, V. Barone, *J. Chem. Phys*. **1999**, *110*, 6158-6170; (c) J. P. Perdew, K. Burke, M. Ernzerhof, *Phys. Rev. Lett*. **1997**, *78*, 1396; (d) J. P. Perdew, K. burke, M. Ernzerhof, *Phys. Rev. Lett*. **1996**, *77*, 3865-3868; (e) J. P. Perdew, M. Ernzerhof, K. Burke, *J. Chem. Phys*. **1996**, *105*, 9982-9985.
14. A. Schäfer, H. Horn, R. Ahlrichs, *J. Chem. Phys*. **1992**, *97*, 2571-2577.
15. A. Schäfer, C. Huber, R. Ahlrichs, *J. Chem. Phys*. **1994**, *100*, 5829-5835.
16. F. Weigend, R. Ahlrichs, *Phys. Chem. Chem. Phys*. **2005**, *7*, 3297-3305.
17. A. Bergner, M. Dolg, W. Küchle, H. Stoll, H. Preuß, *Mol. Phys*. **1993**, *80*, 1431-

1441.
18. (a) S. Grimme, J. Antony, S. Ehrlich, H. Krieg, *J. Chem. Phys*. **2010**, *132*, 154104-154199; (b) S. Grimme, S. Erhlich, L. Goerigk, *J. Comput. Chem*. **2011**, *32*, 1456-1465.

Chapter 4: Towards Si=E Double Bonds

4.1 Chemistry of Nitrous Oxide: Beyond Sex, Drugs and Rock & Roll

Nitrous oxide (N_2O) is one of the many binary compounds involving the elements nitrogen and oxygen. First synthesized by Joseph Priestley in 1772,[1] N_2O has been used in many different areas including the food industry as a mixing and foaming agent, the motor industry as a fuel booster, and dental and clinical practices as an analgesic and anaesthetic agent.[2] More interestingly, nitrous oxide has been used in a recreational way for many years: inhalation of N_2O was a popular public activity in late 18th century Britain among the aristocracy and is now used in the same way worldwide.[2] Apart from being one the cheapest and easiest to obtain recreational drugs, N_2O also has its uses in synthetic inorganic chemistry.[3] It can be used as a weak ligand in transition metal chemistry. In theory, there are several possible binding geometries between N_2O and a single metal center: η^1-O, η^1-N, η^2-N,N and η^2-O,N (*Figure 1*). However, metal-N_2O complexes are rare due to the weak σ-donating and π-accepting abilities of N_2O.[3a] In

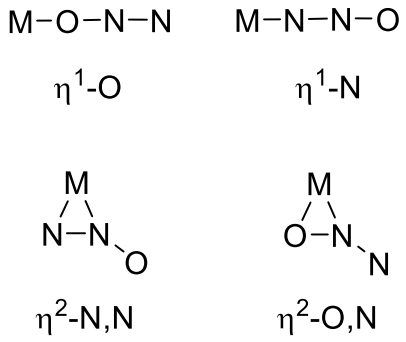


Figure 1. Different bonding geometries for metal-N_2O complexes

1969 Taube reported spectroscopic evidence of a N_2O-ruthenium complex $[(NH_3)_5Ru(N_2O)]^{2+}$.[4a] The compound can be formed *in situ* from direct ligand exchange between $[(NH_3)_5Ru(H_2O)]^{2+}$ and N_2O in aqueous solution, and the reaction itself is reversible: when the solution is degassed by sparging with argon gas, the N_2O complex disappears, only to be restored when N_2O is added a second time. Although the exact bonding mode has not been determined, the coordination of N_2O seems to weaken the N–O bond, resulting an increase in its oxidative capabilities. Normally N_2O oxidizes Cr^{2+} to Cr^{3+} over several days, whereas the same reaction happens immediately in the presence of $[(NH_3)_5Ru(H_2O)]^{2+}$ in solution.[4a] The first structurally determined N_2O-transition metal complex was reported more recently in 2011 by Chang, in the form of a vanadium compound featuring an η^1-N bonding mode (*Figure 2*).[4b] Like Taube's complex, this compound is also generated by ligand exchange, in this case between a vanadium(III) precursor and N_2O, and the bound N_2O can be removed by applying vacuum to the solution. The authors believe that the Lewis acidic V(III) center with π-donating and mild reducing character promotes the N_2O binding, and ultimately leads to a compound stable enough for a structural characterization.[4b] Another case was reported in 2018 by Malinowski, this time a N_2O-copper complex (*Figure 2*). The compound is prepared by direct coordination of N_2O to a freshly prepared sample of

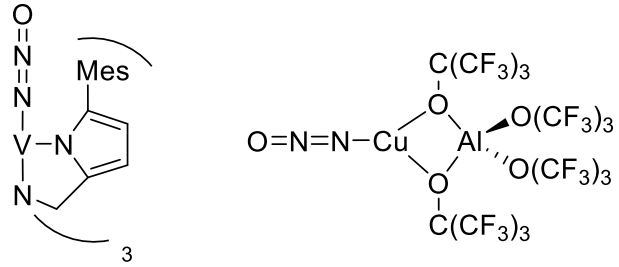
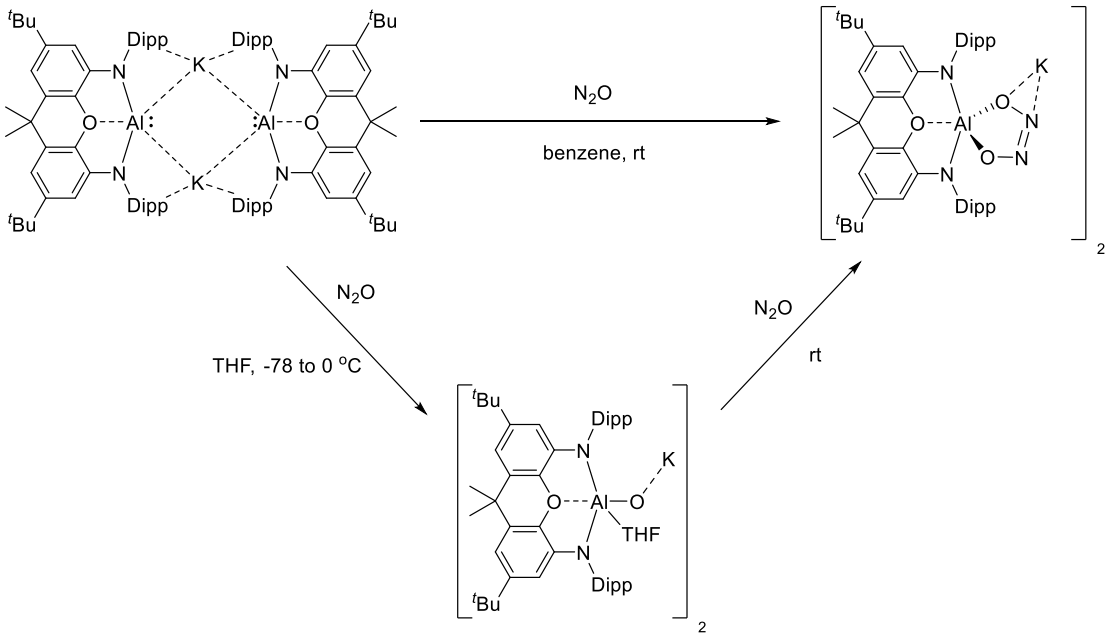


Figure 2. Structurally determined metal-N_2O complexes

$Cu(Al(OC(CF_3)_3)_4)$. Unlike previous cases, this compound does not lose its N_2O ligand even at *ca*. 10^{-4} mbar pressure.[4c]

In the realm of main group chemistry, N_2O has been used primarily as an oxygenation agent. As discussed in Chapter 1, silanones can be prepared by an oxygen-transfer reaction between N_2O and the corresponding silylene precursor.[5] The thermodynamic driving force of such reactions is the evolution of N_2 gas. On rare occasions, reactions with low valent main group compounds can lead to unexpected results. In 2018 our group reported the first example of a structurally characterized Al(I) anion, which is isoelectronic with a silylene.[6] It was hypothesized that the reaction between such an Al(I) compound and N_2O would lead to a compound featuring an Al^+–O^- unit, isoelectronic to a silanone. However, when carried out in toluene the product of the

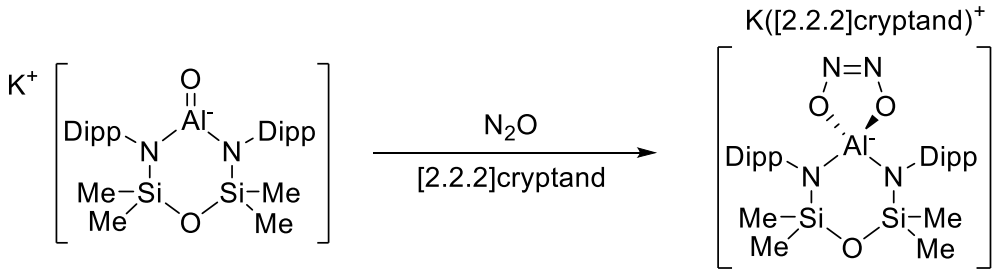


Scheme 3. Synthesis of aluminum *cis*-hyponitrite (Aldridge)

reaction was shown to be an aluminum *cis*-hyponitrite complex.[7a] Repeating the same reaction at temperatures below 0 °C in THF leads to the isolation of the desired

aluminum oxide compound with an additional coordinated THF, which suggests that the hyponitrite is generated by the reaction between the aluminum oxide anion and excess N_2O via coordination at aluminum (*Scheme 3*).[7a] Another similar aluminum *cis*-hyponitrite was reported by Coles in 2019, synthesized by reacting N_2O with a related aluminum oxide anion in the presence of [2.2.2]cryptand (*Scheme 4*).[7b] Such reactivity has never been seen between a silanone and N_2O, most likely due to the more polar nature of the Al–O bond, which increases the electrophilicity of the aluminum center and basicity at oxygen. Both aluminum hyponitrites are stable under vacuum (without losing the second equivalent of N_2O).[7b]

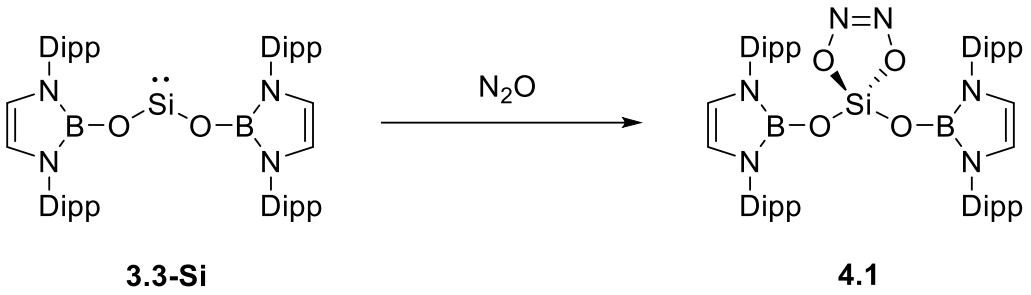
In this part of the project, the focus is on synthesizing various Si=E (E = C, N, O or Se) double-bonds using the silylene $((DippNCH)_2BO)_2Si$ (**3.3-Si**) discussed in Chapter 3 as the Si(II) precursor.



Scheme 4. Synthesis of aluminum *cis*-hyponitrite (Coles)

4.2 Synthesis of a Silahyponitrite

In attempt to synthesize the desired silanone, silylene **3.3-Si** was subjected to various oxygenation reagents. When reacting with O_2, the colorless solution of **3.3-Si** turned orange immediately. The ^{1}H NMR spectrum of the reaction mixture showed broadened



3.3-Si **4.1**

Scheme 5. Synthesis of silahyponitrite **4.1**

peaks at 1.18-1.32, 3.33 and 6.00 ppm. However, no single product could be isolated from the mixture. The reaction between **3.3-Si** and Me_3NO also resulted in a complex mixture as indicated by the *in situ* ^1H NMR spectrum. As discussed in Chapter 1, all existing three-coordinate silanones are synthesized by reacting the corresponding silylene precursor with N_2O with the elimination of one equivalent of N_2, so it made sense at this point to use N_2O as the oxygen source here.[5] When **3.3-Si** was treated with 1 bar of N_2O in C_6D_6, one single product was formed with the ^1H NMR spectrum showing a new set of signals (doublets at 1.11 and 1.14 ppm, septet at 3.05 ppm, singlet at 5.81 ppm) and the complete disappearance of the signals due to **3.3-Si**. The $^{29}Si\{^1H\}$ NMR spectrum showed one singlet at -77.6 ppm. A sample of the product was isolated by slowly evaporating a hexane or pentane solution of the reaction mixture in the form of single crystals suitable for X-ray crystallography. The crystalline samples are of good quality, but the structure suffers from periodic modulation, meaning that the structure solution is not definitive (*Figure 6*). Changing the crystallization method by using another solvent either yielded crystals prone to the same problem (with hydrocarbon or aromatic solvents) or resulted in complete decomposition or hydrolysis (with ether or THF). The preliminary structure of the product (**4.1**) is consistent with a silahyponitrite formulation with a *cis*-N_2O_2 moiety attached to the silicon center. We postulate that

compound **4.1** is formed by the reaction between a transient silanone intermediate (((DippNCH)$_2$BO)$_2$Si=O, **4.1'**) with an excess amount of N_2O, with **4.1'** itself being formed via a 1:1 reaction between **3.3-Si** and N_2O, similar to the route used to synthesize all other silanones reported to date.

To verify this theory, and to see if the reaction can be stopped at the stage of the putative silanone under certain reaction conditions, the same reaction between **3.3-Si** and N_2O was repeated in an NMR tube at low temperatures. The VT-NMR experiment was conducted in toluene-d_8 from -70 °C to 30 °C with a 10 °C increment (and a finer 5 °C increment between -30 °C and 0 °C). As illustrated by the ^{1}H NMR spectra (*Figure 7*), the reaction does not begin until the temperature reaches -25 °C, at which point the signals of **4.1** start to appear. The reaction proceeds slowly but appears to be complete by the time the temperature is raised to between -5 °C to 0 °C. However, there is no evidence to the formation of the putative silanone **4.1'**, implying that **4.1'** reacts with

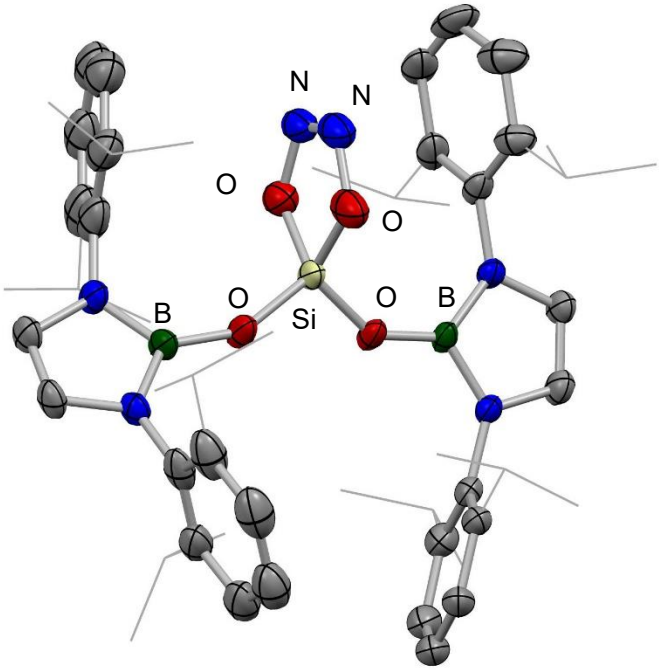


Figure 6. Preliminary X-ray crystal structure of **4.1**

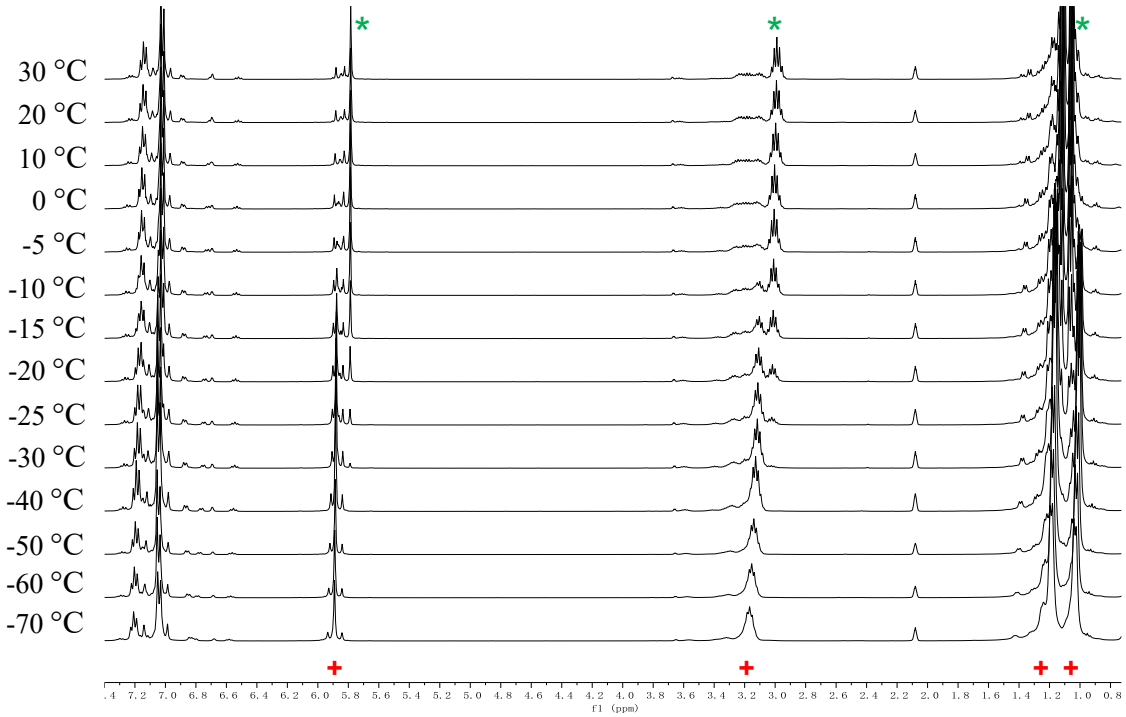


Figure 7. VT-NMR for synthesis of **4.1**. Signals for **3.3-Si** (+) and **4.1** (*)

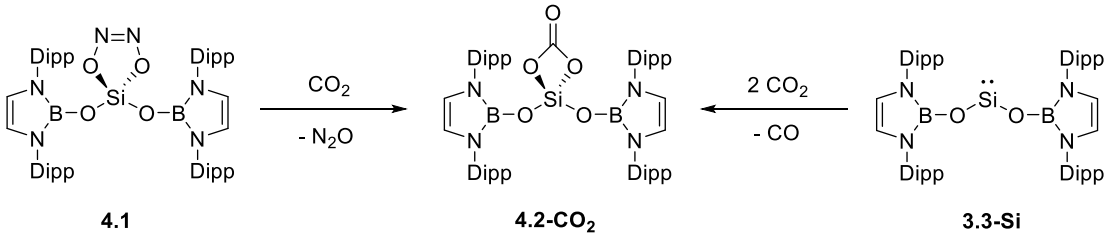
N_2O at a rate faster than **3.3-Si** does. Interestingly, when put under high vacuum in attempt to isolate a solid sample, **4.1** decomposed completely, as the ^{1}H NMR spectrum of the oily residue showed numerous new peaks with disappearance of signals of **4.1**. A reasonable explanation for this observation would be that **4.1** loses one equivalent of N_2O under high vacuum, forming **4.1'**. Due to the high reactivity of **4.1'** it quickly decomposes, for example via dimerization or C–H activation with the Dipp side group.

4.3 Reactivity of Silahyponitrite: Donor Exchange

The effects of exposing **4.1** to vacuum suggest that it can be viewed as an N_2O adduct of the silanone **4.1'**. To corroborate this hypothesis, various donors were reacted with **4.1**, in the hope of substituting the coordinated N_2O, and at the same time forming a silanone adduct that is stable enough to be isolated. Due to the instability of **4.1** under vacuum, these reactivity experiments were performed in an NMR tube equipped with a

J-Young Teflon valve, with **4.1** being generated *in situ*. The completeness of the reaction and the purity of the product **4.1** were confirmed by measuring the ^{1}H NMR spectrum of the reaction mixture *in situ*.

When back filling the NMR tube containing a solution of **4.1** in C_6D_6 with 1 bar of CO_2, a reaction occurred within 5 min. The resulting ^{1}H NMR spectrum showed the disappearance of the signals due to **4.1** and the appearance of a set of new peaks (two doublets at 1.09 and 1.14 ppm, one septet at 3.05 ppm and one singlet at 5.82 ppm).



Scheme 8. Synthesis of **4.2-CO_2**

The ^{29}Si{^{1}H} NMR spectrum also showed a new signal at -93.9 ppm. Crucially the same compound can be generated by reacting **3.3-Si** itself with CO_2 (*Scheme 8*). By concentrating a hexane solution of the product obtained by the latter method, single crystals were isolated, and the structure of the product was determined by X-ray crystallography to be the silacarbonate (**4.2-CO_2**, *Figure 9*). The formation of **4.2-CO_2** is likely through the [2+2] cycloaddition reaction between intermediate **4.1'** and CO_2, with **4.1'** being generated by eliminating one molecule of N_2O (from **4.1**) or via oxygen atom transfer from CO_2 to **3.3-Si** (with the loss of one molecule of CO). In the structure of **4.2-CO_2** the carbonate CO_3 moiety is disordered in two different positions, and, as such, it is difficult to discuss with any great certainty the structural features around the silicon center. Nevertheless, the structure confirms its connectivity as an η^2(O, O')

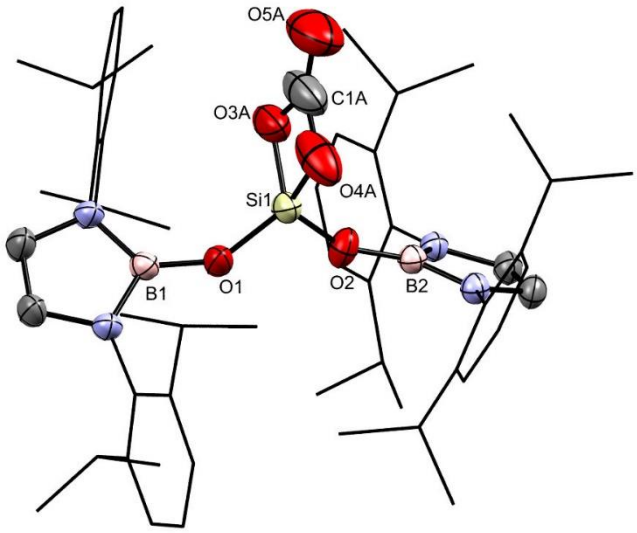
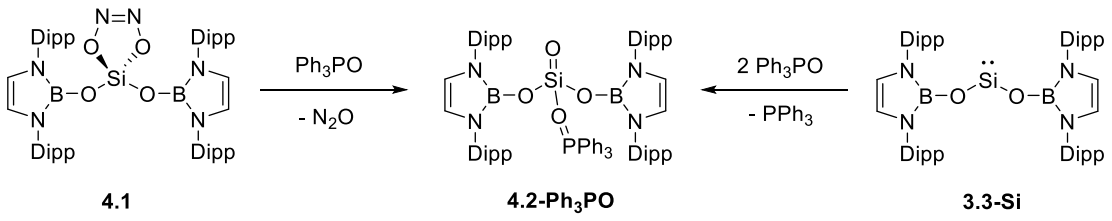


Figure 9 Molecular structure of **4.2-CO_2** with ellipsoids set at the 50% probability level. For clarity, hydrogen atoms are omitted and the Dipp groups are simplified as wireframes. Selected bond lengths (Å) and bond angles: B1–O1 1.367(3), B2–O2 1.370(3), Si1-O1-B1 146.4(2)°, Si1-O2-B2 155.0(2)°.

bound silicon carbonate complex. The B–O bond lengths of **4.2-CO_2** are 1.370(3) Å and 1.367(3) Å, which are consistent with those from **3.3-Si** (*cf.* 1.374(2) for **3.3-Si**, average of two).

To another *in situ* generated sample of **4.1**, was added one equivalent of Ph_3P=O. Here too within 5 min both starting materials had been consumed as indicated by the ^{1}H NMR spectrum, and a new set of signals was generated (two doublets at 0.94 and 1.20 ppm, one septet at 3.36 ppm and one singlet at 5.95 ppm). The $^{31}P\{^1H\}$ NMR spectrum also showed the disappearance of Ph_3P=O signal (at 24.9 ppm) and the appearance of a new singlet at 48.0 ppm. The $^{29}Si\{^1H\}$ NMR spectrum showed a new singlet at -98.1 ppm (*Scheme 10*). A sample of single crystals was obtained by concentrating the C_6D_6



Scheme 10 Synthesis of **4.2-Ph_3PO**

solution in the NMR tube and leaving it to stand overnight. X-ray crystallography determined the product to be a $Ph_3P{=}O$ adduct of the silanone (**4.2-Ph$_3$PO**, *Figure 11*). As in the case of **4.2-CO$_2$**, **4.2-Ph$_3$PO** can also be generated by a 1:2 reaction between **3.3-Si** and $Ph_3P{=}O$. The final product **4.2-Ph$_3$PO** is presumably the result of the coordination of $Ph_3P{=}O$ to **4.1'**, with **4.1'** itself being generated by oxygen atom transfer from $Ph_3P{=}O$ to **3.3-Si** with the elimination of a molecule of Ph_3P (the latter being identified by the appearance of a signal at -5.4 ppm in the *in situ* $^{31}P\{^1H\}$ NMR spectrum). In the structure of **4.2-Ph$_3$PO**, the Si=O bond distance is 1.5306(9) Å, which lies in the range of those defined by reported donor-free silanones (*cf.* 1.527(3) to 1.5432(12) Å for Kato's silanones (**1.47a-d**),[8a-b,d] 1.518(2) Å for $(Ar^*_2CCH_2)_2Si{=}O$ (**1.48c**),[8e] 1.537(3) Å for $\{(DippNCH)_2CN\}\{Si(SiMe_3)_3\}Si{=}O$ (**1.50b**)[8c]), and Lewis

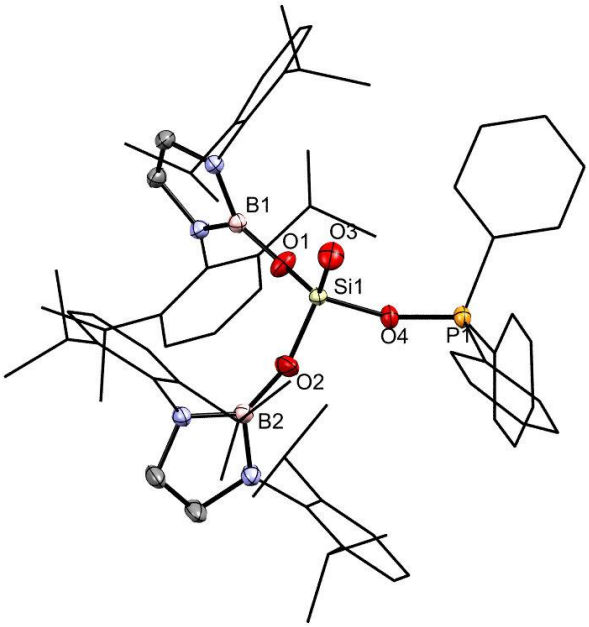


Figure 11 Molecular structure of **4.2-Ph$_3$PO** with ellipsoids set at the 50% probability level. For clarity, hydrogen atoms are omitted and the Dipp/Ph groups are simplified as wireframes. Selected bond lengths (Å) and bond angles: Si1–O1 1.628(1), Si1–O2 1.609(1), Si1–O3 1.5306(9), Si1–O4 1.7256(8), P1–O4 1.5285(9), B1–O1 1.352(2), B2–O2 1.344(2), O1-Si1-O2 107.31(5)°, O1-Si1-O3 120.23(5)°, O1-Si1-O4 98.16(5)°, O2-Si1-O3 117.33(6)°, O2-Si1-O4 100.35(5)°, O3-Si1-O4 109.95(5)°, Si1-O1-B1 144.48(8)°, Si1-O2-B2 160.0(1)°, Si1-O4-P1 143.85(6)°.

base stabilized systems (*cf*. 1.527(3) to 1.545(3) Å for base-stabilized nacnac silanones (**1.43c-e**)[9]), but shorter than that for a Lewis acid stabilized silanone (*cf*. 1.552(2) Å for ((DippNCMe)$_2$CH)Si=O{B(C$_6$F$_5$)$_3$} (**1.43a**)[10]). The Si–O$_B$ (1.628(1) Å and 1.609(1) Å, *cf*. 1.606(1) Å for **3.3-Si**, average of two) and B–O bond distances (1.352(2) Å and 1.344(2) Å, *cf*. 1.374(2) Å for **3.3-Si**, average of two) are consistent with those found in **3.3-Si**. The Si–O$_P$ distance, on the other hand, is significantly longer (1.7256(8) Å) than the Si–O$_B$ bonds, consistent with a description as a dative bond. The P–O bond distance is elongated (1.5285(9) Å) when compared to the same bond in free Ph$_3$P=O (1.462 Å[11]), indicating a decrease of P=O bond order as the result of the coordination at the silicon atom.

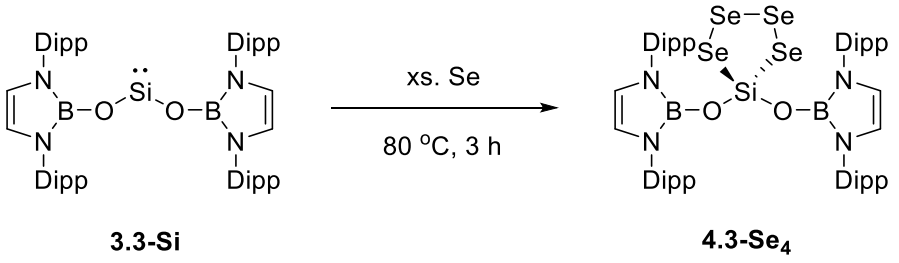
The reactivity of **4.1** demonstrated in this section supports the hypothesis that **4.1** is indeed a loosely bound N$_2$O adduct of silanone **4.1'**. Such an assumption implies that the putative silanone **4.1** has a highly electrophilic silicon center, such that even a weak donor such as N$_2$O is able to bind in a facile manner. To further probe the electrophilicity of **4.1'**, quantum chemical calculations were conducted. The index chosen here was the so-called "fluorine ion affinity (FIA)", which is essentially the calculated (negative) enthalpy change of the reaction between the electrophile and a fluoride anion. This approach has previously been reported in comparing the electrophilicity of various Lewis super acids.[12] The FIA calculated for **4.1'** is 498.8 kJ mol^{-1}, which is slightly higher even than the value calculated for B(C$_6$F$_5$)$_3$ (432.4-457.7 kJ mol^{-1}, depending on the method[12c]), a well-known Lewis acid often used as a baseline for the FIA test. These computational results give a plausible explanation for the instability of **4.1** under high

vacuum, as the resulting donor-free species **4.1'** is so electrophilic that it is able to attack even the weakest nucleophiles (*e.g.,* C–H bonds *etc*.).

4.4 Synthesis of Silaselenone

Establishing that the hypothetical silanone **4.1'** is challenging to synthesize potentially due to its high lability, attention was switched to a heavier group 16 analogue, namely a silaselenone. Selenium was selected instead of sulfur because ^{77}Se is an NMR active nucleus that can act as an NMR handle, and the chemical shift of the ^{77}Se NMR signal of the related selenone (carbon analogue) has been used to probe the π-acidity of the corresponding carbene (carbenes with high π-acidity tend to have more downfield-shifted ^{77}Se NMR signals for the corresponding selenones).[13]

As in the case of silanones, silylenes are considered to be good precursors for silaselenones.[14] In an NMR tube with J-Young Teflon cap, a C_6D_6 solution of **3.3-Si** was suspended with an excess amount of selenium powder. At ambient temperature, no change was observed over the course of 24 hours according to the *in situ* ^{1}H NMR spectrum. With heating at 80 °C, the color of the solution slowly changed from colorless to orange within one hour. After heating for three hours, the reaction was complete as the ^{1}H NMR spectrum of the reaction mixture showed a new set of signals (a doublet



3.3-Si **4.3-Se$_4$**

Scheme 12. Synthesis of **4.3-Se$_4$**

at 1.17 ppm, a septet at 3.20 ppm, a singlet at 5.89 ppm) with the complete disappearance of the signals for **3.3-Si**. The ^{29}Si NMR spectrum showed one singlet at -11.9 ppm. However, the ^{77}Se NMR spectrum at this point showed two singlets at 254.6 ppm and 797.4 ppm with 1:1 integration, which is unexpected as the silaselenone should have only one ^{77}Se signal. Leaving the reaction mixture at ambient temperature overnight yielded single crystals suitable for X-ray crystallography, and the structure of the compound was determined to be tetraselenosilolane (**4.3-Se$_4$**, *Scheme 12, Figure 13*). Similar $SiSe_4$ moieties have not yet been structurally identified in the literature. However, the $SiSe_4$ five-membered ring in **4.3-Se$_4$** is structurally similar to the reported tetrathiasilolanes, with the Se2 and Se3 atoms lying on different sides of the Si-Se1-Se4 plane.[15] On the other hand, the Si–O (1.602(3) Å and 1.603(3) Å, *cf.* 1.606(1) Å for **3.3-Si**, average of two) and B–O (1.372(4) Å and 1.374(5) Å, *cf.* 1.374(2) Å for **3.3-**

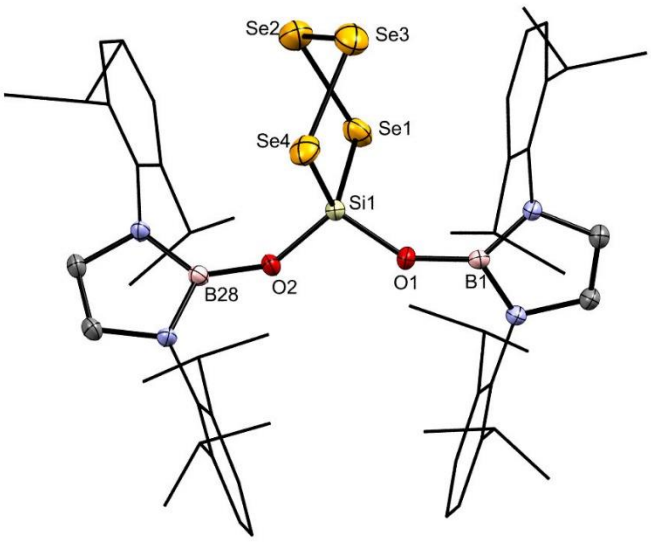
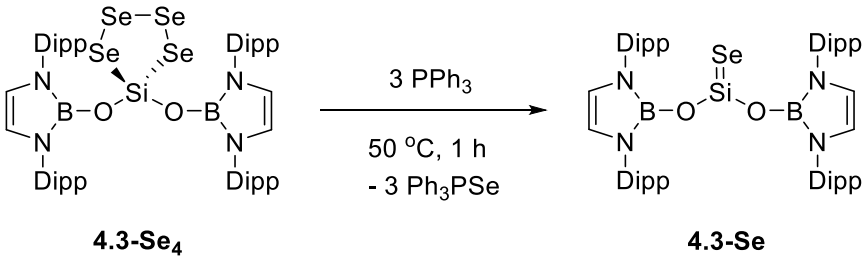


Figure 13 Molecular structure of **4.3-Se$_4$** with ellipsoids set at the 50% probability level. For clarity, hydrogen atoms are omitted and the Dipp groups are simplified as wireframes. Selected bond lengths (Å) and bond angles: Si1–O1 1.603(3), Si1–O2 1.602(3), Si1–Se1 2.305(1), Si1–Se4 2.291(1), Se1–Se2 2.3398(8), Se2–Se3 2.3161(9), Se3–Se4 2.3441(8), B1–O1 1.372(4), B28–O2 1.374(5), O1-Si1-O2 105.8(1)°, O1-Si1-Se1 104.7(1)°, O1-Si1-Se4 114.7(1)°, O2-Si1-Se1 114.4(1)°, O2-Si1-Se4 105.2(1)°, Se1-Si1-Se4 112.03(5)°, Si1-O1-B1 144.9(2)°, Si1-O2-B28 144.2(3)°.

Si, average of two) distances are consistent with those obtained from **3.3-Si**.

In attempt to obtain the corresponding mono-selenium compound, Ph_3P was used as a selenium scavenger. To a solution of **4.3-Se4** in C_6D_6 in an NMR tube was added three equivalents of Ph_3P. With mild heating at 50 °C, the solution slowly decolorized in one



4.3-Se4 **4.3-Se**

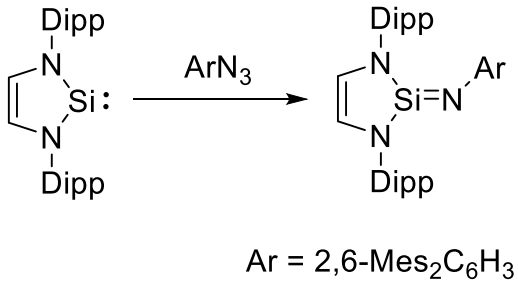
Scheme 14. Synthesis of **4.3-Se**

hour. The *in situ* ^{1}H-NMR spectrum confirmed the complete consumption of both **4.3-Se4** and Ph_3P, with the appearance of a new set of signals (two doublets at 1.08 and 1.14 ppm, a septet at 3.19 ppm, a singlet at 5.95 ppm), and the $^{31}P\{^{1}H\}$ NMR spectrum showed the appearance of the signal for Ph_3P=Se (at 35.3 ppm). The ^{29}Si NMR spectrum showed one broad signal at -11.1 ppm. Adding further Ph_3P did not generate any new signals. As such, the new compound in the reaction mixture is tentatively identified as silaselenone **4.3-Se** (*Scheme 14*). Structural authentication of this compound by X-ray crystallography has so far not been possible. The ^{77}Se NMR spectrum showed one very broad signal at -444.8 ppm. To date, the only other silaselenone with a known ^{77}Se-NMR chemical shift is {(DippNCH)$_2$B}{NDipp(SiMe$_3$)}Si=Se (262.6 ppm).[14b] Comparatively, the signal for **4.3-Se** is significantly upfield shifted, indicating a less π-acidic silylene (**3.3-Si**) when compared to {(DippNCH)$_2$B}{NDipp(SiMe$_3$)}Si (**1.34a**), if the rules for carbenes applies here. For a more rigorous quantification of this scale for silylenes, more data is

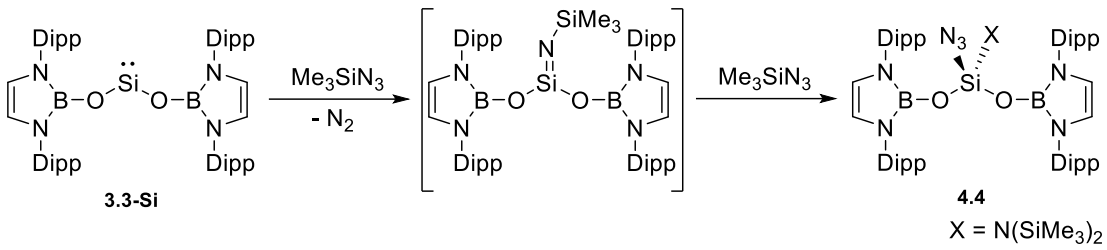
required.

4.5 Attempted Formation of a Silicon-Heteroatom Double Bonds

The dimerization of a silylene is rendered less favorable by steric bulk around the silicon centre and a large singlet-triplet energy gap. That being said, silylenes can still be regarded as synthons for silicon-heteroatom doubly bonded species. In 2010 Cui described the formation of a Si=N double bond by reacting *N*-heterocyclic silylene and aryl azide (*Scheme 15*).[16] In an analogous fashion, **3.3-Si** was treated with an excess amount of trimethylsilyl azide in hexane. The reaction was complete within minutes: *in situ* ^{1}H NMR monitoring shows full consumption of **3.3-Si** and the appearance of a new set of signals over a period of 15 minutes. Interestingly, however, a singlet at -0.1 ppm, in the region characteristic of trimethylsilyl groups, integrates to 18 protons, suggesting a 2:1 reaction between the azide and the silylene. This hypothesis was confirmed by X-ray crystallography, showing that the product is the two-fold addition product **4.4** (*Scheme 16, Figure 17*). Given the nature of the final product, a possible mechanism can be postulated, starting with the Si=N double bond formation analogous to the case reported by Cui. Due to insufficient steric protection around the Si=N bond and the



Scheme 15 Formation of Si=N double bond



Scheme 16 Synthesis of **4.4**

highly polarized nature of Si=N bond (highly electrophilic silicon centre), a second equivalent of azide adds across the Si=N bond involving breakage of the Me_3SiN_3 single bond and generation of the azide and amide functions seen in the final product. Similar two-fold addition of trimethylsilyl azide onto (cyclic) silylenes has been reported by Lappert[17a] and West[17b] (*Scheme 18*). Structural parameters of **4.4** around the silicon center largely resemble literature reported values. The N6–N7 (1.209(7) Å, cf. 1.227(4) Å for $C_6H_4(NCH_2{}^tBu)_2Si(N_3)(N(SiMe_3)_2$[17a] (**1.27a**); 1.215(4) Å for $(CH_2N{}^tBu)_2Si(N_3)(N(SiMe_3)_2$[17b]) and N7–N8 distances (1.131(8) Å, *cf*. 1.133(4) Å for **1.27a**[17a]; 1.128(4) Å for $(CH_2N{}^tBu)_2Si(N_3)(N(SiMe_3)_2$[17b]) are in the ranges observed

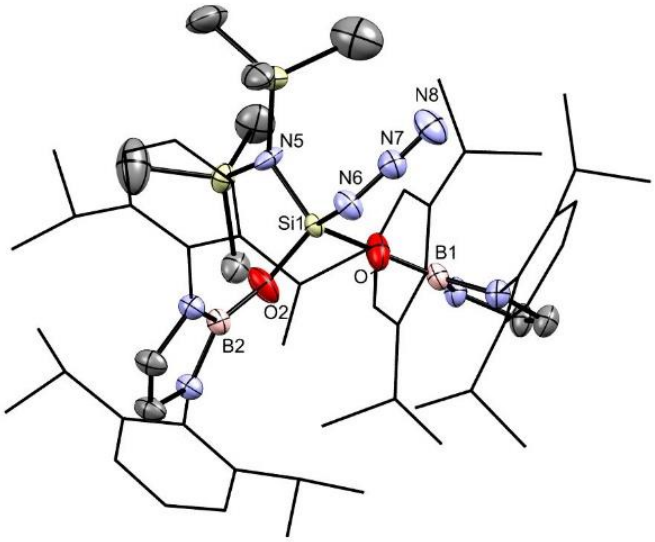
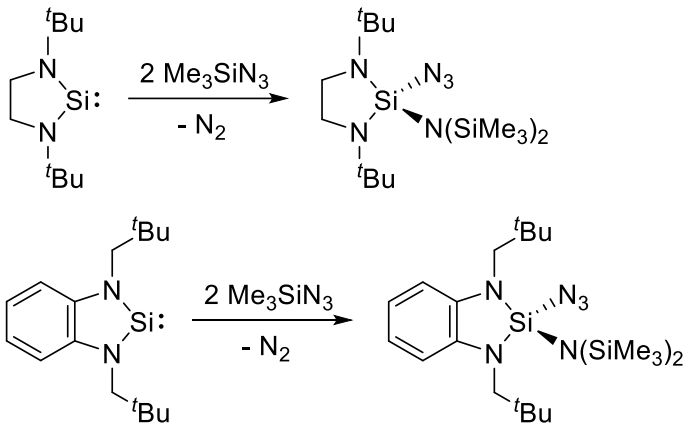


Figure 17 Molecular structure of **4.4** with ellipsoids set at the 50% probability level. For clarity, hydrogen atoms are omitted and the Dipp groups are simplified as wireframes. Selected bond lengths (Å) and bond angles: Si1–O1 1.598(2), Si1–O2 1.577(3), O1–B1 1.354(3), O2–B2 1.358(4), Si1–N5 1.73(1), Si1–N6 1.743(4), N6–N7 1.209(7), N7–N8 1.131(8), O1-Si1-O2 111.9(1)°, Si1-O1-B1 167.3(2)°, Si1-O2-B2 157.6(2)°, N5-Si1-N6 111.8(3)°.

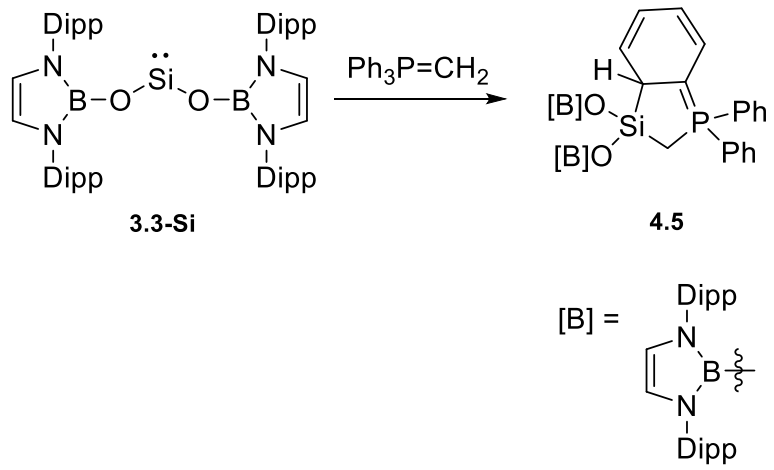
for literature compounds. The Si–N_{amide} distance for **4.4**, on the other hand, is slightly longer (1.73(1) Å, *cf.* 1.700(3) for **1.27a**[17a]; 1.720(3) for $(CH_2N^tBu)_2Si(N_3)(N(SiMe_3)_2$[17b]), while the Si–$N_3$ distance for **5** (1.743(4) Å, *cf.* 1.755(3) Å for **1.27a**[17a]; 1.773(2) Å for $(CH_2N^tBu)_2Si(N_3)(N(SiMe_3)_2$[17b]) is slightly shorter. Compared with the starting material **3.3-Si**, the Si-O-B angles in **4.4** are much wider (mean 162.4(2)°, *cf.* 137.8(1) (mean) for **3.3-Si**), presumably the outcome of the increased steric bulk around the central silicon and oxidation to Si(IV).

Attempts have also been made to construct a Si=C double bond via similar synthetic



Scheme 18 Literature examples of two-fold addition of azide onto silylenes

approaches. The "$:CR_2$" source chosen here was a phosphine ylide, due to their steric accessibility compared with available free carbenes (i.e. a free $:CR_2$ usually requires large R groups to prevent the carbene center from dimerizing or self-activation, as in NHCs). Dissolving a 1:1 mixture of **3.3-Si** and methylenetriphenylphosphine in benzene led to an immediate color change from bright yellow to dark red. The *in situ* ^{1}H NMR spectrum shows multiplets at 2.49, 3.97, 5.50, 5.57 and 6.28 ppm, all integrating to one proton, suggesting potential dearomatization of one phenyl ring of



Scheme 19 Synthesis of **4.5**

the PPh_3 unit. The $^{31}P\{^1H\}$ NMR spectrum shows only one new signal at 1.3 ppm, indicating clean conversion. Repeating the same reaction in diethyl ether resulted in the formation of dark brown blocks suitable for X-ray crystallography. This revealed the structure of the product **4.5** in the solid state (*Scheme 19, Figure 20*). As shown in *Scheme 19*, one of the phenyl rings derived from the PPh_3CH_2 starting material has been dearomatized, with the carbon-carbon bond distances between C4, C5, C6, C7 in the ring now showing an alternating pattern of double and single bonds (C4–C5: 1.351(5) Å; C5–C6: 1.440(5) Å; C6–C7: 1.346(5) Å). Moreover, the P=C2 distance is 1.705(3) Å, which lies in the typical range of P=C double bonds (*cf.* 1.713(3) Å for $Ph_3P{=}C_4F_6$[18a]; 1.709(6) Å for $Ph_3P{=}CHTiPhCp_2$[18b]). However, the sum of bond angles around C2 is 348.0(8)°, slightly deviated from planarity. The formation of a Si-C-C-P-C heterocycle hints at a plausible 1+4 cycloaddition mechanism, which had been reported in similar cases by Driess,[19a] Roesky[19b,19d] and Kira[19c] respectively (*Scheme 21*). As shown in

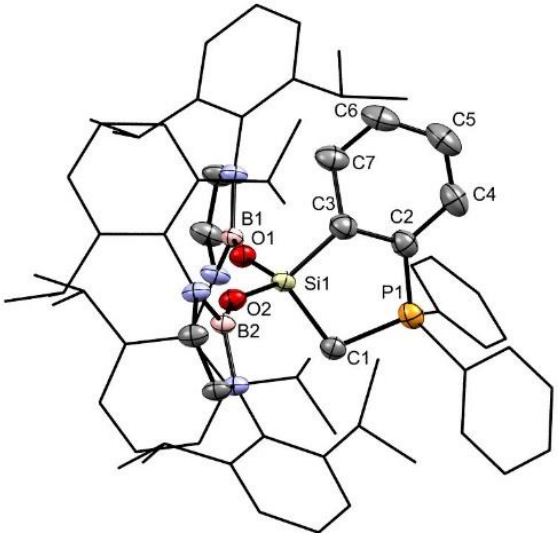
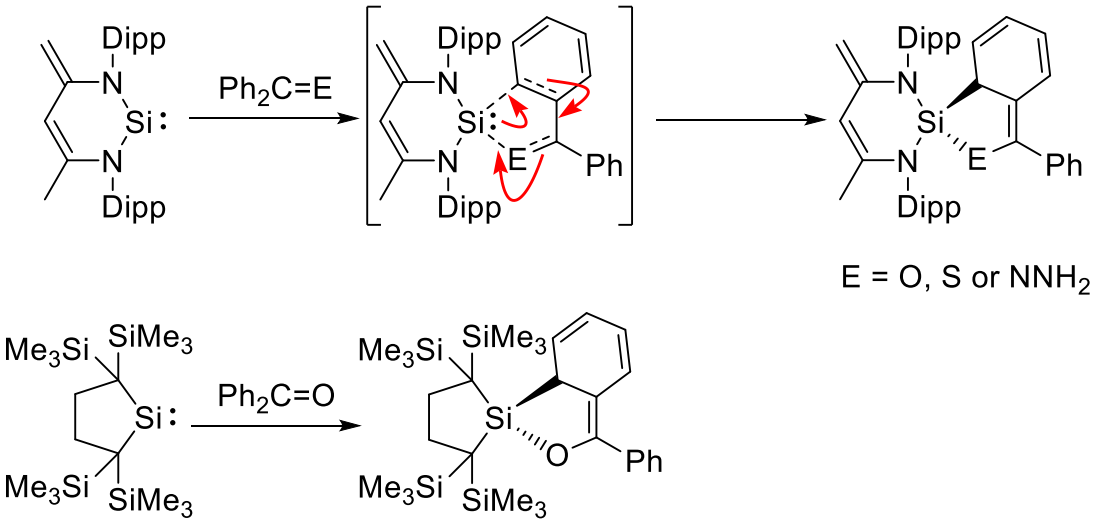


Figure 20 Molecular structure of **4.5** with ellipsoids set at the 50% probability level. For clarity, hydrogen atoms are omitted; the Dipp groups and the phenyl groups are simplified as wireframes. Selected bond lengths (Å) and bond angles: Si1–O1 1.619(2), Si1–O2 1.627(2), O1–B1 1.360(3), O2–B2 1.360(3), Si1–C1 1.885(2), Si1–C3 1.874(3), P1–C1 1.818(3), P1–C2 1.705(3), C2–C3 1.525(4), C2–C4 1.427(4), C3–C7 1.502(3), C4–C5 1.351(5), C5–C6 1.440(5), C6–C7 1.346(5), O1-Si1-O2 104.92(9)°, Si1-O1-B1 155.5(2)°, Si1-O2-B2 146.5(2)°, C1-Si1-C3 102.0(1)°.

Scheme 21, β-diketiminatosilylenes or dialkylsilylenes are able to react with benzophenone, in which [1+4] cycloaddition occurs between the silylene silicon and an O=C–C=C moiety. Whatismore, β-diketiminatosilylenes are also known to react with benzohydrazone and benzothione, forming similar cycloaddition products with nitrogen or sulfur heteroatoms.



Scheme 21 Previously reported 1+4 cycloadditions by silylenes

4.6 Conclusions

Various oxygen transfer agents has been employed in attempt to synthesize silanone **4.1'** from silylene precursor **3.3-Si**. Of all of these attempts, the most notable is the reaction with N_2O, in which a silahyponitrite (**4.1**) has been generated. **4.1** can be transformed into base-stabilized silanones (**4.2-CO_2** and **4.2-Ph_3PO**) by ligand exchange reactions with donors (CO_2 or Ph_3PO), which suggests that **4.1** itself can be regarded as a masked silanone. Reaction of **3.3-Si** with excess amount of selenium produced a tetraselenosilolane (**4.3-Se_4**) which can be used to generate silaselenone **4.3-Se** via reaction with triphenyl phosphine. Attempted syntheses of compounds with Si=E (E = N or C) double bonds resulted in a two-fold addition product **4.4** (E = N) or a [1+4] cycloaddition product **4.5** (E = C).

4.7 Experimental Details

General considerations

All manipulations were carried out under an inert atmosphere of argon or dinitrogen using standard Schlenk line technique or dry glovebox technique. Solvents were degassed by sparging with argon and dried by passing through a column of appropriate drying agent. NMR samples were prepared under dinitrogen in 5 mm Wilmad 507-PP tubes fitted with J-Young Teflon valve. NMR spectra were measured in benzene-d_6 which was dried over CaH_2, distilled and stored over activated 3Å molecular sieves. All NMR spectra were recorded on Bruker Avance III HD nanobay 400 MHz or Bruker Avance 500 MHz equipped with a ^{13}C detect cryoprobe at ambient temperature. ^{1}H and

^{13}C resonances were referenced internally with residual protio solvent (^{1}H) or solvent (^{13}C) resonances and were reported relative to tetramethylsilane (δ = 0 ppm). ^{31}P resonances were referenced externally to 85% phosphoric acid. ^{11}B resonances were referenced externally to $BF_3{\cdot}Et_2O$. ^{29}Si resonances were referenced externally to tetramethylsilane. ^{77}Se resonances were referenced externally to Me_2Se. Assignments were confirmed using two-dimensional ^{1}H-^{1}H and ^{1}H-^{13}C correlation NMR experiments. Chemical shifts were quoted in δ (ppm) and coupling constants in Hz. Elemental analyses were carried out by Elemental Microanalysis Ltd. PPh_3CH_2[20] was synthesized by literature procedures. Triphenylphosphine oxide were purchased from Sigma Aldrich and dried under high vacuum prior to use. Carbon dioxide and nitrous oxide were obtained from BOC Inc. and dried over phosphorus pentoxide prior to use. **3.3-Si** was prepared according to the preparation stated in Chapter 3.

All calculations were performed on DFT level using Gaussian09 (Revision A.02) program.[21] Geometry optimization for monoanionic ligands were performed on PBE1PBE/SVP[22-23] level of theory; all other geometry optimizations were performed on PBE1PBE/TZVP[22,24] level of theory. Grimme's empirical dispersion correction (DFT-D3)[25] was included in all geometry optimizations. Frequency calculations were performed to verify the nature of stationary points (zero imaginary frequencies for minima).

NMR-scale synthesis of $((DippNCH)_2BO)_2Si(N_2O_2)$ (**4.1**)

In an NMR tube equipped with a J-Young tap a sample of **3.3-Si** (10 mg, 0.012 mmol) was dissolved in C_6D_6. The tube was degassed and refilled with N_2O (~1 atm). The tube

was shaken for 30 min and then allowed to stand for 1 h. Multinuclear NMR experiments showed 100% conversion of **3.3-Si** to the title compound. Removing solvent under high vacuum caused complete decomposition, as shown by the measured ^{1}H NMR spectrum. Data for **4.1**: ^{1}H NMR (C_6D_6, 400 MHz, 298 K): δ = 1.11 (d, 24H, CH-C*H*$_3$, *J* = 7.0 Hz), 1.14 (d, 24H, CH-C*H*$_3$, *J* = 6.9 Hz), 3.05 (sept, 8H, C*H*-CH$_3$, *J* = 6.9 Hz), 5.81 (s, 4H, C*H*=C*H*), 7.22-7.24 (m, 8H, Ar-*H*), 7.31-7.37 (m, 4H, Ar-*H*); ^{13}C{^{1}H} NMR (C_6D_6, 126 MHz, 298 K): δ = 23.2 (s, CH*C*H$_3$), 24.2 (s, CH*C*H$_3$), 28.5 (s, *C*HCH$_3$), 116.8 (s, *C*H=*C*H), 123.5 (s, *m*-*C*$_6$H$_3$), 136.3 (s, *i*-*C*$_6$H$_3$), 145.9 (s, *i*-*C*$_6$H$_3$), the *p*-C_6H_3 signal overlaps with C_6D_6 signal; ^{1}B{^{1}H} NMR (C_6D_6, 128 MHz, 298 K): δ = 19.0 (br, *B*-O-Si); ^{29}Si{^{1}H} NMR (C_6D_6, 99 MHz, 298 K): δ = -77.6 (s, central *Si*).

Large scale synthesis of **4.1**

In a Y-shape Schlenk tube equipped with a J-Young tap a sample of **3.3-Si** (100 mg, 0.12 mmol) was dissolved in pentane. The tube was degassed and subsequently filled with N_2O (~1 atm). The tube was shaken for 30 min and allowed to stand for 1 h. The solvent was slowly evaporated inside the tube over a course of 3 d by creating a temperature difference between two ends of the Y-shape tube. Blue crystals suitable for X-ray crystallography were obtained. A minimum amount of solvent was transferred to the end of the tube containing product crystals and decanted back to the other end (3 times). The tube was then opened under a stream of argon and all liquid in the tube was decanted (out of the tube). Multinuclear NMR data obtained from the crystals is identical when compared to that obtained from NMR-scale synthesis. Due to the lability of the title compound under high vacuum, meaningful elemental analysis was

impossible to obtain.

Synthesis of ((DippNCH)$_2$BO)$_2$SiO$_2$CO (**4.2-CO$_2$**)

In a Schlenk tube equipped with a J-Young tap a sample of **3.3-Si** was dissolved in hexane. The tube was degassed and subsequently filled with N_2O (~1 atm). The tube was hand shaken for 30 min and allowed to stand for 1 h. The tube was degassed again to remove residual N_2O and refilled with CO_2 (~1 atm). The tube was shaken for a further 30 min and allowed to stand for an hour. The solvent was then removed *in vacuo*, where the title compound was obtained as a white powder. ^{1}H NMR (C_6D_6, 400 MHz, 298 K): δ = 1.09 (d, 24H, CH-C*H*$_3$, *J* = 6.7 Hz), 1.14 (d, 24H, CH-C*H*$_3$, *J* = 6.6 Hz), 3.05 (sept, 8H, C*H*-CH$_3$, *J* = 6.7 Hz), 5.82 (s, 4H, C*H*=C*H*), 7.07-7.09 (m, 4H, Ar-*H*), 7.19-7.23 (m, 8H, Ar-*H*); ^{13}C{^{1}H} NMR (C_6D_6, 126 MHz, 298 K): δ = 23.7 (s, CH*C*H$_3$), 24.6 (s, CH*C*H$_3$), 28.9 (s, *C*HCH$_3$), 117.2 (s, *C*H=*C*H), 124.0 (s, *m*-*C*$_6$H$_3$), 136.4 (s, *i*-*C*$_6$H$_3$), 146.1 (s, *i*-*C*$_6$H$_3$), 163.5 (s, O$_2$*C*=O), the *p*-C$_6$H$_3$ signal overlaps with C_6D_6 signal; ^{11}B{^{1}H} NMR (C_6D_6, 128 MHz, 298 K): δ = 19.2 (s, *B*-O-Si); ^{29}Si{^{1}H} NMR (C_6D_6, 80 MHz, 298 K): δ = -93.9 (s, central *Si*). Anal. calc. for $C_{53}H_{72}B_2N_4O_5Si$: C 71.14%, H 8.11%, N 6.26%, found: C 70.92%, H 8.36%, N 6.04%.

Alternative synthesis of **4.2-CO$_2$** from **3.3-Si**

In a Schlenk tube a sample of **3.3-Si** (50 mg, 0.06 mmol) was dissolved in hexane (1 mL). The tube was briefly degassed and then filled with CO_2 (~1 atm). The tube was then shaken for 30 min and allowed to stand for 1 h. Volatiles were removed *in vacuo* yielding **4.2-CO$_2$** as a white solid (43 mg, 0.049 mmol, 82%). Single crystals suitable for X-ray crystallography was obtained by slowly evaporating a hexane solution of **4.2-**

CO_2 at reduced pressure. Multinuclear NMR data of the product were identical when compared to those of **4.2-CO_2** obtained from **4.1**.

Synthesis of ((DippNCH)$_2$BO)$_2$SiO(Ph$_3$PO) (**4.2-Ph$_3$PO**)

In a Schlenk tube equipped with a J-Young tap, a sample of **3.3-Si** (50 mg, 0.06 mmol) was dissolved in hexane (1 mL). The tube was degassed and subsequently filled with N_2O (~1 atm). The tube was shaken for 30 min and allowed to stand for 1 h. The tube was degassed again to remove residual N_2O and refilled with argon (~1 atm). A stir bar and a sample of triphenylphosphine oxide (17 mg, 0.06 mmol) was then added to the tube and the mixture was stirred for 30 min. The solvent was then removed *in vacuo* and the residual extracted into pentane and filtered. The solvent was again removed *in vacuo*, where the title compound was obtained as a white powder (45 mg, 0.40 mmol, 66%). ^{1}H NMR (C_6D_6, 400 MHz, 298 K): δ = 0.94 (d, 24H, CH-C*H*$_3$, *J* = 6.8 Hz), 1.20 (d, 24H, CH-C*H*$_3$, *J* = 6.9 Hz), 3.36 (sept, 8H, C*H*-CH$_3$, *J* = 6.7 Hz), 5.95 (s, 4H, C*H*=C*H*), 7.00-7.12 (m, 23H, Ar-*H*), 7.22-7.26 (m, 4H, Ar-*H*); ^{13}C{^{1}H} NMR (C_6D_6, 126 MHz, 298 K): δ = 23.5 (s, CH*C*H$_3$), 25.0 (s, CH*C*H$_3$), 28.3 (s, *C*HCH$_3$), 117.3 (s, *C*H=*C*H), 123.2 (s, *m*-*C*$_6$H$_3$), 125.4 (s, C$_{Ph}$), 126.3 (s, *p*-*C*$_6$H$_3$), 128.6 (d, C$_{Ph}$) 133.2 (s, C$_{Ph}$), 133.9 (d, C$_{Ph}$), 139.2 (s, *i*-*C*$_6$H$_3$), 146.1 (s, *o*-*C*$_6$H$_3$); ^{31}P{^{1}H} NMR (C_6D_6, 162 MHz, 298 K): δ = 48.0 (s, Ph$_3$*P*=O); ^{11}B{^{1}H} NMR (C_6D_6, 128 MHz, 298 K): δ = 19.2; ^{29}Si{^{1}H} NMR (C_6D_6, 80 MHz, 298 K): δ = -98.1 (s, central *Si*).

Alternative NMR scale synthesis of **4.2-Ph$_3$PO** from **3.3-Si**

In an NMR tube equipped with a J-Young tap a sample of **3.3-Si** and triphenylphosphine was dissolved in C_6D_6 (0.4 mL). The tube was hand shaken for 5 min. ^{1}H NMR shows

100% conversion of **3.3-Si**, and a set of signals consistent with those of the title compound, together with signals from triphenylphosphine. The $^{31}P\{^{1}H\}$ NMR spectrum also showed signals for the title compound and triphenylphosphine. The solution was concentrated, and single crystals suitable for X-ray crystallography of the title compound formed overnight.

Synthesis of $[(DippNCH)_2BO]_2SiSe_4$ (**4.3-Se$_4$**)

In a Schlenk tube, a mixture of **3.3-Si** (92.5 mg, 0.11 mmol) and selenium powder (79.9 mg, 1.0 mmol) was suspended in benzene (5 mL). The mixture was heated at 80 °C for 3 h. Excess selenium powder was filtered off and the filtrate was concentrated to *ca*. 1.5 mL, and stored at a cool place (*ca*. 15 °C) overnight, yielding **4.3-Se$_4$** as orange-red crystals suitable for X-ray crystallography. The mother liquor was decanted, the crystals were washed with cold diethyl ether (2 mL) and dried in vacuo giving an analytically pure sample of **4.3-Se$_4$** (55 mg, 0.048 mmol, 43%). ^{1}H NMR (C_6D_6, 400 MHz, 298 K): δ = 1.17 (d, 48H, CHC*H*$_3$, *J* = 6.9 Hz), 3.20 (sept, 8H, C*H*CH$_3$, *J* = 7.0 Hz), 5.89 (s, 4H, C*H*=C*H*), 7.06-7.08 (m, 12H, Ar-*H*); ^{13}C NMR (C_6D_6, 126 MHz, 298 K): δ = 23.5 (s, CH*C*H$_3$), 24.7 (s, CH*C*H$_3$), 28.5 (s, *C*HCH$_3$), 117.4 (s, *C*H=*C*H), 123.6 (s, *m*-*C*$_6$H$_3$), 128.2 (s, *p*-*C*$_6$H$_3$), 138.0 (s, *i*-*C*$_6$H$_3$), 146.2 (s, *o*-*C*$_6$H$_3$); ^{11}B NMR (C_6D_6, 128 MHz, 298 K): δ = 19.0 (br, *B*-O-Si); ^{29}Si NMR (C_6D_6, 80 MHz, 298 K): δ = -11.9 (s, O-*Si*-O); ^{77}Se NMR (C_6D_6, 95 MHz, 298 K): δ = 254.6 (s), 797.4 (s).

NMR-scale synthesis of $((DippNCH)_2BO)_2SiSe$ (**4.3-Se**)

In an NMR tube equipped with a J-Young tap, a mixture of **4.3-Se$_4$** (25 mg, 0.022 mmol) and Ph_3P (17 mg, 0.065 mmol) was dissolved in C_6D_6 (0.4 ml). The reaction mixture

was heated gently at 50 °C until the solution turned colorless. The sample was then subjected to multinuclear NMR analysis (100% conversion). ^{1}H NMR (C_6D_6, 500 MHz, 298 K): δ = 1.08 (d, 24H, CHC*H*$_3$, *J* = 6.9 Hz), 1.14 (d, 24H, CHC*H*$_3$, *J* = 6.9 Hz), 3.19 (sept, 8H, C*H*CH$_3$, *J* = 6.9 Hz), 5.95 (s, 4H, C*H*=C*H*), 7.09-7.10 (m, 8H, Ar-*H*), 7.20-7.23 (m, 4H, Ar-*H*); ^{13}C NMR (C_6D_6, 126 MHz, 298 K): δ = 23.7 (s, CH*C*H$_3$), 24.9 (s, CH*C*H$_3$), 28.3 (s, *C*HCH$_3$), 117.0 (s, *C*H=*C*H), 123.5 (s, *m*-*C*$_6$H$_3$), 127.4 (s, *p*-*C*$_6$H$_3$), 136.8 (s, *i*-*C*$_6$H$_3$), 146.1 (s, *o*-*C*$_6$H$_3$); ^{11}B NMR (C_6D_6, 128 MHz, 298 K): δ = -19.1 (br, *B*-O-Si); ^{29}Si NMR (C_6D_6, 80 MHz, 298 K): δ = -11.1 (br s, central *Si*); ^{77}Se NMR (C_6D_6, 95 MHz, 298 K): δ = -444.8 (br s, Si=*Se*)

Synthesis of ((DippNCH)$_2$BO)$_2$S{N(SiMe$_3$)$_2$}(N$_3$) (**4.4**)

In a Schlenk tube, a sample of **3.3-Si** (33 mg, 0.04 mmol) was dissolved in hexane (1 mL). To the solution was added neat trimethylsilyl azide (0.011 mL, 0.08 mmol), and the mixture was stirred for 10 min. Volatiles were then removed *in vacuo* yielding **4.4** as a white solid (20 mg, 0.02 mmol, 49%). Single crystals suitable for X-ray crystallography were obtained by slowly evaporating a hexane solution of **4.4** at ambient temperature. ^{1}H NMR (C_6D_6, 400 MHz, 298 K): δ = -0.13 (s, 18H, Si-C*H*$_3$), 1.22 (two overlapping d, 24H, CH-C*H*$_3$, *J* = 6.7 Hz), 1.30 (d, 12H, CH-C*H*$_3$, *J* = 6.9 Hz), 1.37 (d, 12H, CH-C*H*$_3$, *J* = 6.9 Hz), 3.24 (sept, 4H, C*H*-CH$_3$, *J* = 6.8 Hz), 3.31 (sept, 4H, C*H*-CH$_3$, *J* = 6.8 Hz), 3.78 (d, 1H, Si-*H*, *J* = 2.9 Hz), 5.78 (s, 4H, C*H*=C*H*), 7.10-7.14 (m, 4H, Ar-*H*), 7.18-7.23 (m, 8H, Ar-*H*); ^{13}C{^{1}H} NMR (C_6D_6, 101 MHz, 298 K): δ = 4.7 (s, Si-C*H*$_3$), 23.8 (s, CH*C*H$_3$), 23.9 (s, CH*C*H$_3$), 26.6 (s, CH*C*H$_3$), 26.8 (s, CH*C*H$_3$), 28.8 (s, *C*HCH$_3$), 118.8 (s, *C*H=*C*H), 124.1 (s, *m*-*C*$_6$H$_3$), 124.3 (s, *m*-*C*$_6$H$_3$),

139.6 (s, *p*-C_6H_3), 139.6 (s, *i*-C_6H_3), 146.5 (s, *o*-C_6H_3); $^{11}B\{^1H\}$ NMR (C_6D_6, 128 MHz, 298 K): δ = 18.5 (s, *B*-O-Si); $^{29}Si\{^1H\}$ NMR (C_6D_6, 80 MHz, 298 K): δ = -92.8 (s, central *Si*) 3.8 (s, *Si*-CH_3).

Synthesis of $((DippNCH)_2BO)_2Si(PPh_3CH_2)$ (**4.5**)

In a Schlenk tube a sample of **3.3-Si** (25 mg, 0.030 mmol) and PPh_3CH_2 (8 mg, 0.030 mmol) were loaded and Et_2O (1 mL) was added. Immediately the solution turned dark red. At the same time dark red blocks suitable for X-ray crystallography precipitated from solution. The mother liquor was then decanted and the solid was dried *in vacuo*, yielding **4.5** as dark red solid (20 mg, 0.018 mmol, 60%). ^1H NMR (C_6D_6, 400 MHz, 298 K): δ = 0.88 (d, 6H, CH-C*H*$_3$, *J* = 6.9 Hz) 1.07 (d, 12H, CH-C*H*$_3$, *J* = 6.9 Hz), 1.12 (d, 12H, CH-C*H*$_3$, overlapping with Et_2O signal), 1.15 (d, 6H, CH-C*H*$_3$, overlapping with Et_2O signal), 1.22-1.25 (two overlapping d, 12H, CH-C*H*$_3$), 2.49 (dt, 1H, dearomatized, *J* = 9.0 Hz, 2.5 Hz), 3.11-3.32 (two overlapping sept, 8H, C*H*-CH_3, overlapping with Et_2O signal), 3.97 (m, 1H, dearomatized), 5.50 (m, 1H, dearomatized), 5.57 (m, 1H, dearomatized), 5.82 (s, 2H, C*H*=C*H*), 5.93 (s, 2H, C*H*=C*H*), 6.28 (t, 1H, Ar-*H*, *J* = 8.0 Hz), 6.83 (d, 1H, Ar-*H*, *J* = 2.2 Hz), 6.85 (d, 1H, Ar-*H*, *J* = 2.2 Hz), 7.02-7.10 (m, 13H, Ar-*H*), 7.32-7.43 (m, 6H, Ar-*H*); $^{31}P\{^1H\}$ NMR (C_6D_6, 162 MHz, 298 K): δ = 1.3 (s, Ph_2P); $^{11}B\{^1H\}$ NMR (C_6D_6, 128 MHz, 298 K): δ = 19.4 (*B*-O-Si); $^{29}Si\{^1H\}$ NMR (C_6D_6, 80 MHz, 298 K): δ = -24.4 (d, central *Si*, *J* = 29.3 Hz). Due to the instability of **4.5** in solution, a meaningful ^{13}C NMR spectrum cannot be obtained.

4.8 References

1. D. Zuck, P. Ellis, A. Dronsfield, *Educ. Chem*. **2012**, *26*.

2. G. Randhawa, A. Bodenham, *Br. J. Anaesth*. **2016**, *116*, 321-324.
3. For reviews on N_2O chemistry: (a) W. B. Tolman, *Angew. Chem. Int. Ed*. **2010**, *49*, 1018-1024; (b) K. Severin, *Chem. Soc. Rev*. **2015**, *44*, 6375-6386.
4. For N_2O-metal complexes: (a) J. Armor, H. Taube, *J. Am. Chem. Soc*. **1969**, *91*, 6874-6876; (b) N. A. Piro, M. F. Lichterman, W. H. Harman, C. J. Chang, *J. Am. Chem. Soc*. **2011**, *133*, 2108-2111; (c) V. Zhuravlev, P. J. Malinowski, *Angew. Chem. Int. Ed*. **2018**, *57*, 11697-11700.
5. For reviews on silanones: (a) Y. Xiong, S. Yao, M. Driess, *Angew. Chem. Int. Ed*. **2013**, *52*, 4302-4311; (b) Y. K. Loh, S. Aldridge, *Angew. Chem. Int. Ed*. **2020**. DOI: 10.1002/anie.202008174.
6. J. Hicks, P. Vasko, J. M. Goicoechea, S. Aldridge, *Nature*, **2018**, *557*, 92-95.
7. For anion aluminum hyponitrites: (a) J. Hicks, A. Heilmann, P. Vasko, J. M. Goicoechea, S. Aldridge, *Angew. Chem. Int. Ed*. **2019**, *58*, 17265-17268; (b) M. Anker, M. P. Coles, *Angew. Chem. Int. Ed*. **2019**, *58*, 18261-18265.
8. For neutral three-coordinate silanones: (a) I. Alvarado-Beltran, A. Rosas-Sánchez, A. Baceiredo, N. Saffon-Merceron, V. Branchadell, T. Kato, *Angew. Chem. Int. Ed*. **2017**, *56*, 10481-10485; (b) A. Rosas-Sánchez, I. Alvarado-Beltran, A. Baceiredo, N. Saffon-Merceron, S. Massou, D. Hashizume, V. Branchadell, T. Kato, *Angew. Chem. Int. Ed*. **2017**, *56*, 15916-15920; (c) D. Wendel, A. Porzelt, F. A. D. Herz, D. Sarkar, C. Jandl, S. Inoue, B. Rieger, *J. Am. Chem. Soc*. **2017**, *139*, 8134-8137; (d) R. Kobayashi, S. Ishida, T. Iwamoto, *Angew. Chem. Int. Ed*. **2019**, *58*, 9425-9428; (e) S. Takahashi, K. Nakaya, M. Frutos, A. Baceiredo, N. Saffon-Merceron, S. Massou, N. Nakata, D. Hashizume, V. Branchadell, T. Kato, *Angew. Chem. Int. Ed*. **2020**, *59*, 15937-15941.
9. For Lewis base stabilized silanones: (a) Y. Xiong, S. Yao, M. Driess, *J. Am. Chem. Soc*. **2009**, *131*, 7562-7563; (b) S. Yao, Y. Xiong, M. Driess, *Chem. Eur. J*. **2010**, *16*, 1281-1288; (d) Y. Xiong, S. Yao, R. Müller, M. Kaupp, M. Driess, *J. Am. Chem. Soc*. **2010**, *132*, 6912-6913; (d) Y. Xiong, S. Yao, R. Müller, M Kaupp, M. Driess, *Nat. Chem*. **2010**, *2*, 577-580.
10. S. Yao, M. Brym, C. van Wüllen, M. Driess, *Angew. Chem. Int. Ed*. **2007**, *46*, 4159-4162.
11. G. Bandoli, G. Bortolozzo, D. A. Clemente, U. Croatto, C. Panattoni, *J. Chem. Soc. A*, **1970**, 2778-2780.
12. Selected examples of uses of FIA: (a) J. C. Haartz, D. H. McDaniel, *J. Am. Chem. Soc*. **1973**, *95*, 8562-8565; (b) K. O. Christe, D. A. Dixon, D. McLemore, W. W. Wilson, J. A. Sheehy, J. A. Boatz, *J. Fluor. Chem*. **2000**, *101*, 151-153; (c) P. Erdmann, J. Leitner, J. Schwarz, L. Greb, *ChemPhysChem*, **2020**, *21*, 987-994.
13. For summaries on ^{77}Se-NMR indicator for carbenes: (a) A. Liske, K. Verlinden, H. Buhl, K. Schaper, C. Ganter, *Organometallics*, **2013**, *32*, 5269-5272; (b) H. V. Huynh, *Chem. Rev*. **2018**, *118*, 9457-9492.
14. For syntheses of silaselenones from silylenes: (a) T. Iwamoto, K. Sato, S. Ishida, C. Kabuto, M. Kira, *J. Am. Chem. Soc*. **2006**, *128*, 16914-16920; (b) A. V. Protchenko, P. Vasko, D. C. H. Do, J. Hicks, M. Á. Fuentes, C. Jones, S. Aldridge, *Angew. Chem. Int. Ed*. **2019**, *58*, 1808-1812.

15. For tetrathiasilolanes: (a) N. Tokitoh, H. Suzuki, T. Matsumoto, Y. Matsuhashi, R. Okazaki, M. Goto, *J. Am. Chem. Soc*. **1991**, *113*, 7047-7049; (b) T. Iwamoto, K. Sato, S. Ishida, C. Kabuto, M. Kira, *J. Am. Chem. Soc*. **2006**, *128*, 16914-16920.
16. L. Kong, C. Cui, *Organmetallics*, **2010**, *29*, 5738-5740.
17. (a) B. Gehrhus, P. Hitchcock, M. Lappert, *Z. Anorg. Allg. Chem*. **2001**, *627*, 1048-1054; (b) N. J. Hill, D. F. Moser, I. A. Guzei, R. West, *Organometallics*, **2005**, *24*, 3346-3349.
18. (a) M. A. Howells, R. D. Howells, N. C. Baenziger, D. J. Burton, *J. Am. Chem. Soc*. **1973**, *95*, 5366-5370; (b) H. J. R. De Boer, O. S. Akkermann, F. Bickelhaupt, G. Erker, P. Czisch, R. Mynott, J. M. Wallis, C. Krüger, *Angew. Chem. Int. Ed. Engl*. **1986**, *25*, 639-640.
19. For 1+4 cycloadditon of silylenes: (a) Y. Xiong, S. Yao, M. Driess, *Chem. Eur. J*. **2009**, *15*, 5545-5551; (b) A. Jana, H. W. Roesky, C. Schulzke, P. P. Samuel, *Organmetallics*, **2009**, *28*, 6574-6577; (c) S. Ishida, T. Iwamoto, M. Kira, *Organmetallics*, **2010**, *29*, 5526-5534; (d) R. Azhakar, R. S. Ghadwal, H. W. Roesky, R. A. Mata, H. Wolf, R. Herbst-Irmer, D. Stalke, *Chem. Eur. J*. **2013**, *19*, 3715-3720.
20. H. J. Bestmann, W. Stransky, O. Vostrowsky, *Chem. Ber*. **1976**, *109*, 1694-1700.
21. Gaussian 09, Revision A.02, M. J. Frisch, G. W. Trucks, H. B. Schlegel, G. E. Scuseria, M. A. Robb, J. R. Cheeseman, G. Scalmani, V. Barone, B. Mennucci, G. A. Petersson, H. Nakatsuji, M. Caricato, X. Li, H. P. Hratchian, A. F. Izmaylov, J. Bloino, G. Zheng, J. L. Sonnenberg, M. Hada, M. Ehara, K. Toyota, R. Fukuda, J. Hasegawa, M. Ishida, T. Nakajima, Y. Honda, O. Kitao, H. Nakai, T. Vreven, J. A. Montgomery, Jr., J. E. Peralta, F. Ogliaro, M. Bearpark, J. J. Heyd, E. Brothers, K. N. Kudin, V. N. Staroverov, R. Kobayashi, J. Normand, K. Raghavachari, A. Rendell, J. C. Burant, S. S. Iyengar, J. Tomasi, M. Cossi, N. Rega, J. M. Millam, M. Klene, J. E. Knox, J. B. Cross, V. Bakken, C. Adamo, J. Jaramillo, R. Gomperts, R. E. Stratmann, O. Yazyev, A. J. Austin, R. Cammi, C. Pomelli, J. W. Ochterski, R. L. Martin, K. Morokuma, V. G. Zakrzewski, G. A. Voth, P. Salvador, J. J. Dannenberg, S. Dapprich, A. D. Daniels, O. Farkas, J. B. Foresman, J. V. Ortiz, J. Cioslowski, and D. J. Fox, Gaussian, Inc., Wallingford CT, 2009.
22. (a) M. Ernzerhof, G. E. Scuseria, *J. Chem. Phys*. **1999**, *110*, 5029-5036; (b) C. Adamo, V. Barone, *J. Chem. Phys*. **1999**, *110*, 6158-6170; (c) J. P. Perdew, K. Burke, M. Ernzerhof, *Phys. Rev. Lett*. **1997**, *78*, 1396; (d) J. P. Perdew, K. burke, M. Ernzerhof, *Phys. Rev. Lett*. **1996**, *77*, 3865-3868; (e) J. P. Perdew, M. Ernzerhof, K. Burke, *J. Chem. Phys*. **1996**, *105*, 9982-9985.
23. A. Schäfer, H. Horn, R. Ahlrichs, *J. Chem. Phys*. **1992**, *97*, 2571-2577.
24. A. Schäfer, C. Huber, R. Ahlrichs, *J. Chem. Phys*. **1994**, *100*, 5829-5835.
25. (a) S. Grimme, J. Antony, S. Ehrlich, H. Krieg, *J. Chem. Phys*. **2010**, *132*, 154104-154199; (b) S. Grimme, S. Erhlich, L. Goerigk, *J. Comput. Chem*. **2011**, *32*, 1456-1465.

Chapter 5: Conclusions

In this thesis, syntheses of novel silylenes featuring gallyl, amido or boryloxy ligands are examined, in an attempt to investigate the possibility of accessing Si=E (E = O N, C or Se) double bonded species. The choices of ancilliary X-type ligands in silylene {(HCDippN)$_2$Ga}{Dipp(Me$_3$Si)N}Si·I^{i}PrMe (**2.4**), namely [(DippNCH)$_2$Ga]$^-$ and [DippN(SiMe$_3$)]$^-$ were inspired by the successful synthesis of a similar silylene system bearing the same amido ligand and a [(DippNCH)$_2$B]$^-$ ligand (**1.34a**). However, the reaction between **1.34a** and N_2O failed to generate the desired silanone due to a side reaction involving silyl migration. Following the literature procedures, precursors [(DippNCH)$_2$Ga]K(C$_6$H$_6$) (**2.1-K**), IDipp·SiCl$_2$ (**2.2-Cl$_2$**) and {Dipp(Me$_3$Si)N}SiCl·I^{i}PrMe (**2.2-Cl**) have been synthesized. The reaction between **2.1-K** and **2.2-Cl$_2$** affords a tri-gallyl-substituted species [IDippH][{(HCDippN)$_2$Ga}$_3$Si] (**2.3**). The anionic component of **2.3** is the first example of a tri-gallyl-substituted silyl anion. However, it is not a suitable precursor for synthesizing a Si=E double bond. The synthesis of NHC-ligated silylene **2.4** was achieved by direct salt metathesis between **2.1-K** and **2.2-Cl**. Upon reaction of **2.4** with N_2O, a silyl migrated species **2.5-O** was observed, despite calculations which indicates the existence of a potential silane-silanone equilibrium.

The boryloxyl anion [(DippNCH)$_2$BO]$^-$ first reported by Yamashita and Nozaki is also utilized in the synthesis of silylene [(DippNCH)$_2$BO]$_2$Si (**3.3-Si**). The protonated ligand (DippNCH)$_2$BOH (**3.1**) was synthesized by a modified literature procedure,

using $(DippNCH)_2BBr$ as the precursor in a biphasic water-toluene mixture, in the presence of a base (pyridine). Deprotonation of **3.1** using $KN(SiMe_3)_2$ affords anionic **3.1-K**, which was then used in the synthesis of $[(DippNCH)_2BO]_2SiI_2$ (**3.2-I**). Reduction of **3.2-I** using Jones' reagent ($(^{Mes}NacnacMg)_2$) affords the desired silylene **3.3-Si**. DFT calculations shows that the energy gap between the σ orbital and the empty *p*π orbital of **3.3-Si** is 5.45 eV, which is the largest among all reported two-coordinate acyclic silylenes to date. Reactions between **3.3-Si** and water or ammonia afford the formal oxidative addition products $((DippNCH)_2BO)_2SiH(OH)$ (**3.4-OH**) and $((DippNCH)_2BO)_2SiH(NH_2)$ (**3.4-NH_2**), respectively. However, calculations show that such reactions more likely take place *via* a two water (ammonia) molecule transition state.

Silylene **3.3-Si** was also subjected to further reactivity probes, targeting syntheses of potential Si=E containing species. The reaction between **3.3-Si** and N_2O does not produce the desired silanone, instead yielding a *cis*-silahyponitrite $((DippNCH)_2BO)_2Si(N_2O_2)$ (**4.1**), which is characterized by multinuclear NMR. Due to crystal modulation, structural determination of **4.1** is still under investigation. **4.1** is regarded as a N_2O-masked silanone as the loosely bound N_2O molecule can be eliminated upon reacting **4.1** with a donor such as CO_2 and $Ph_3P{=}O$, affording a silacarbonate $((DippNCH)_2BO)_2SiO_2CO$ (**4.2-CO_2**) and a silanone $((DippNCH)_2BO)_2SiO(Ph_3PO)$ (**4.2-$Ph_3P{=}O$**), respectively. Reaction between **3.3-Si** and an excess amount of selenium generates a tetraselenosilonane $[(DippNCH)_2BO]_2SiSe_4$ (**4.3-Se_4**). Silaselenone $((DippNCH)_2BO)_2SiSe$ (**4.3-Se**) was

then successfully synthesized via a 3:1 reaction between Ph_3P (a commonly known selenium scavenger) and **4.3-Se4**. Attempted syntheses of a potential Si=N or Si=C containing species using **3.3-Si** and Me_3SiN_3 or $Ph_3P{=}CH_2$ as starting materials do not generate the desired products, instead affording $((DippNCH)_2BO)_2S\{N(SiMe_3)_2\}(N_3)$ (**4.4**) and $((DippNCH)_2BO)_2Si(PPh_3CH_2)$ (**4.5**).